UNIVERSITA' DEGLI STUDI DI TORINO

DIPARTIMENTO DI: **SCIENZE VETERINARIE**

DOTTORATO DI RICERCA IN NEUROSCIENZE

CICLO XXIX

TITOLO DELLA TESI:

NOCICEPTORS OF DORSAL ROOT GANGLIA IN A MOUSE MODEL OF DIABETES: A MORPHOFUNCTIONAL STUDY

TESI PRESENTATA DA: **Elisa Ciglieri**

TUTOR: **Dr.ssa Chiara Salio**

COORDINATORE DEL DOTTORATO: **Prof. Marco Sassoè**

ANNI ACCADEMICI: **2013-2017**

SETTORE SCIENTIFICO-DISCIPLINARE DI AFFERENZA: **VET/01**

Grazie al Professore Adalberto Merighi, per i consigli stimolanti e l'esperta visione d'insieme.

Grazie a Chiara, tutor impagabile e paziente, sempre presente e di infinito supporto. E' stato un bellissimo viaggio, grazie per avermi accompagnata passo dopo passo.

Grazie a Francesco, mentore, guida, consigliere e correttore. Non esistono abbastanza post-it in questo Universo per esprimere la mia gratitudine.

Grazie a Carolina e Patrizia, per la tante, inifinte risate. Avete reso questo percorso unico.

Grazie a Fulvia, Susanna, Elena e Graziana, per essere state mie amiche ed una splendida cornice di questi quattro anni.

Grazie a Barbara e Livio, il cui sostegno non ha limiti e che spero di rendere orgogliosi ogni giorno. Senza paura. Sempre.

Grazie ad Amedeo, per le applicazioni topiche di coraggio.

Grazie al BB Team, che ormai mi ha sostituita con una sagoma di cartone, ma a cui vuole molto bene.

Grazie a Giuseppe e Graziella, che non hanno mai smesso di credere in me.

Grazie a Federica, Matteo, Tomas, Silvia, senza cui questo lavoro sarebbe stato terminato molto prima. Non vi ringrazierò mai abbastanza.

Grazie a Marco, sempre lì, accanto a me, silezioso e paziente. Il mondo è nostro.

"There are more things in heaven and earth, Horatio,
Than are dreamt of in your philosophy".
Hamlet, Shakespeare

SUMMARY

ABSTRACT **1**

ABBREVIATIONS **2**

1 INTRODUCTION **3**

1.1 Pain theory: historical background 3

1.2 Dorsal root ganglia and somatosensory pathways 6

1.2.1 Somatosensory pathways *6*

1.2.2 DRG structure *17*

1.3 Diabetic neuropathy: etiology, pathology and animal models 28

1.3.1 Etiology of diabetic neuropathic pain *28*

1.3.2 Animal models of diabetic neuropathy *32*

1.4 Neurotrophic factors in nociceptive transmission and pathological pain 36

1.5 Aims of the thesis 44

2 MATERIALS and METHODS **45**

2.1 Animals 45

2.2 Ethics 45

2.3 Intact dorsal root ganglion (DRG) preparation 45

2.4 Electrophysiological recording 46

2.5 Electrophysiological data analysis 48

2.6 Drugs 49

2.7 Immunofluorescence 49

2.8 Primary antibodies 50

2.9 Immunohistochemical controls 50

2.10 Software-based analysis of nociceptors distribution in mice DRGs 50

2.11 Analysis of SGCs ensheatment 54

2.12 Statistics 54

3 RESULTS **55**

3.1 Patch-clamp characterization of DRG neurons in control and diabetic mice 55

3.1.1 Active and passive membrane properties of DRG neurons in control and diabetic mice *55*

3.1.2 Voltage-clamp characterization of DRG neurons in control and diabetic mice *61*

3.1.3 Effect of glucose-enriched perfusion on DRG neurons on control and diabetic mice *67*

3.2 Physiological effect of GDNF administration on DRG neurons in control and diabetic mice 68

3.2.1 Patch-clamp characterization of DRG neurons after GDNF administration. *68*

3.2.2 Voltage-clamp analysis of GDNF administration *71*

3.2.3 GDNF effect in presence of voltage-dependent K+ channel blocker *79*

3.3 Morphological characterization of nociceptors in DRG in control and diabetic mice 81

3.3.1 Clusterization of IB4+ nociceptor sub-population in mice DRGs *81*

3.3.2 Alterations in satellite glial cell morphological organization in DRG from diabetic mice *84*

4 DISCUSSION 86

4.1 Functional alterations in sensory neurons associated with diabetes and role of GDNF 86

4.1.1 Functional alterations of sensory neurons in DRG of diabetic mice *86*

4.1.2 Functional effect of GDNF administration on DRG neurons *88*

4.1.3 Structural alterations in sensory neurons associated with diabetes *90*

4.1.4 Impact and future directions *92*

5 CONCLUSION 95

6 BIBLIOGRAPHY 98

ABSTRACT

Nociceptors in dorsal root ganglia (DRGs) encode pain information and their abnormal excitability contributes to diabetic polyneuropathy. They are classified as non-peptidergic IB4+ and peptidergic CGRP+ neurons. Neurotrophic factors, such as GDNF, are key regulators of DRG neuronal excitability and phenotype, and their altered signaling has been associated to pathological conditions.

The aim of my project was:

i) to investigate the structural and functional alterations in DRGs in a mouse model of type I diabetes, and

ii) to address the role of GDNF in perturbing cell excitability of nociceptors.

The morphology of entire DRGs was analyzed by a combination of confocal imaging and software-based analysis that automatically performs segmentation and 3D rendering of IB4+ and CGRP+ labeled neurons. While the former tend to cluster in groups of three-four, the latest do not. Albeit cluster organization is unaffected by diabetes, glial cell ensheatment of IB4+ neurons in the clusters was reduced, thus increasing the likelihood of cell-to-cell crosstalk.

Physiological alterations were investigated by patch clamp recordings from visually-identified neurons in intact DRGs before/after GDNF administration. In current clamp, GDNF induced a depolarizing shift of firing threshold in DRG neurons under control conditions and delayed firing onset, while it was less effective in diabetes. To test the involvement of voltage-dependent K^+ channels, K^+ currents were isolated in voltage clamp. GDNF potentiated K^+ conductance in control conditions, with little effect in diabetes.

My data indicate that diabetes alters morphofunctional properties of nociceptors and induces a loss of GDNF-mediated control on sensory encoding.

ABBREVIATIONS

BDNF =	brain-derived neurotrophic factor
CGRP =	calcitonin gene related peptide
C-H =	C fiber sensitive to heat
C-LTMR =	Low threshold mechanoreceptor C-fiber
C-MC =	C fiber sensitive to both mechanical stimuli and cold
C-MH =	C fiber sensitive to both mechanical stimuli and heat
C-MHi =	C fiber sensitive to mechanical stimuli and insensitive to heat
C-MiHi =	C fiber insensitive to both mechanical stimuli and heat
CNS =	central nervous system
CREB =	cAMP response element binding protein
DCML =	dorsal column – medial lemniscal
DPN	Diabetic polyneuropathy
DPN =	diabetic polyneuropathy
DRASIC =	acid-sensing ion channel
DRG =	dorsal root ganglion
DRt =	dorsal reticular nucleus
DTX =	dendrotoxin
DTX-S =	dendrotoxin sensitive
ERK =	Extracellular regulated kinase
FRAP =	fluoride-resistant acid phosphatase
FRAP =	Fluoride-resistant acid phosphatase
GABA =	Γ-aminobutyruc acid
GADPH =	glyceraldehydes 3-phosphate dehydrogenase
GFRα1, GFRα2, GFRα3, GFRα4,=	GDNF family receptor α-1/2/3/4
ICAM =	intercellular adhesion molecule
Kv =	voltage-gated potassium ion channel
LL =	large light neurons
MAPK =	Mitogen-activated protein kinase
MrgprD, MrgprB4 =	Mas-related G protein-coupled receptor D, B4
NADH =	nicotinamide adenine dinucleotide
NADPH =	nicotinamide adenine dinucleotide phosphate
Necl-1 =	nectin-like molecule 1
NF200 =	neurofilament 200
NGF =	nerve growth factor
NMDA =	N-methyl-D-aspartate
NO =	nitric oxide
NPY =	neuropeptides Y
NPY2R =	neuropeptides Y receptor Y2
NRM =	nucleus raphe magnus
NT-3, NT-4/5 =	neurotrophin-3/4/5
P2X3 =	P2X purinoceptor 3
PAG =	periaqueductal gray
PI2K =	Phosphatidylinositol-3 kinase
PKC =	protein kinase C
PLCγ =	Phospholipase C γ
PNS =	peripheral nervous system
RVM =	rostral ventromedial medulla
SD =	small dark neurons
SGC =	satellite glial cell
SP =	substance P
SST =	somatostatin
STT =	spinothalamic tract
STZ =	Streptozotocin
T1D =	type 1 diabetes mellitus
T2D =	type 2 diabetes mellitus
TG =	trigeminal ganglion
TrkA, TrkB, TrkC =	tyrosin protein kinase A, B, C
TRPV1, TRPA1, TRPM8 =	transient receptor potential vanilloid 1, ankyrin 1, member 8
TTX =	tetrodotoxin
TTX-R =	tetrodotoxin resistant
TTX-S =	tetrodotoxin sensitive
vGLUT1 =	vescicular glutamate transporter 1
VLM =	ventrolateral medulla
VPL =	ventral posterolateral nucleus
VPM =	ventral posteromedial nucleus

1 INTRODUCTION

1.1 PAIN THEORY: HISTORICAL BACKGROUND

The International Association for Study of Pain (IASP, 1986) defines pain as *"an unpleasant sensory and emotional experience associated with actual or potential tissue damage, or described in terms of tissue damage, or both"*. This description derives after centuries of works and discoveries in the pain field.

One of the first descriptions of somatosensory system belongs to René Descartes, who described in *Treatise of Man* (1664) pain as a perception located in the brain and distinguished the painful sensory transduction (or nociception) from the experience of perceiving pain. His theory also depicted nerves as hollow tubules conveying both sensory and motor information (Descartes et al., 1664). This understanding of neural function was based on Galen's postulation that three conditions are the base of perception: *1)* an organ must be able to receive a stimulus; *2)* a connection must exist between the organ and the brain; *3)* an integrating center that converts the stimulus in conscious perception must be present (Rey, 1995). Descartes considered the nerves as "connections" between organs and brain (Figure 1.1 A) and postulated that, in case of a peripheral sensory input, the activation of a "fiber" running within the nerves would have "rang a bell" in the brain, permitting to an animal spirit to flow through the nerve and elicit a motor response (Moayedi and Davis, 2013). La Forge's drawing (Figure 1.1 B) of this mechanism is one of the most famous in neuroscience.

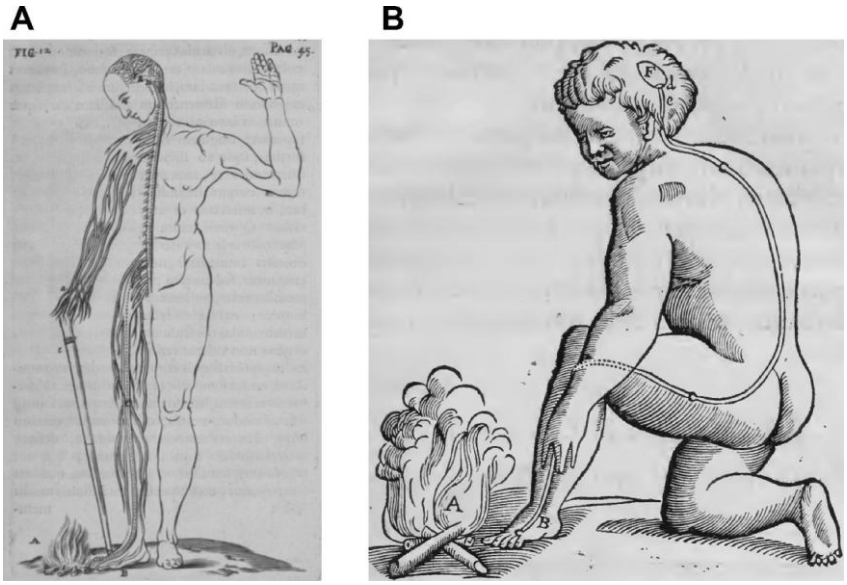

FIGURE 1.1 DESCARTES MODELS OF PAIN.
Drawings of the pain system based on Descartes' description by **A**. Florentius Schuyl and **B**. Louis La Forge. From *"Theories of pain: from specificity to gate control"*, Moayedi and Davis (2013)

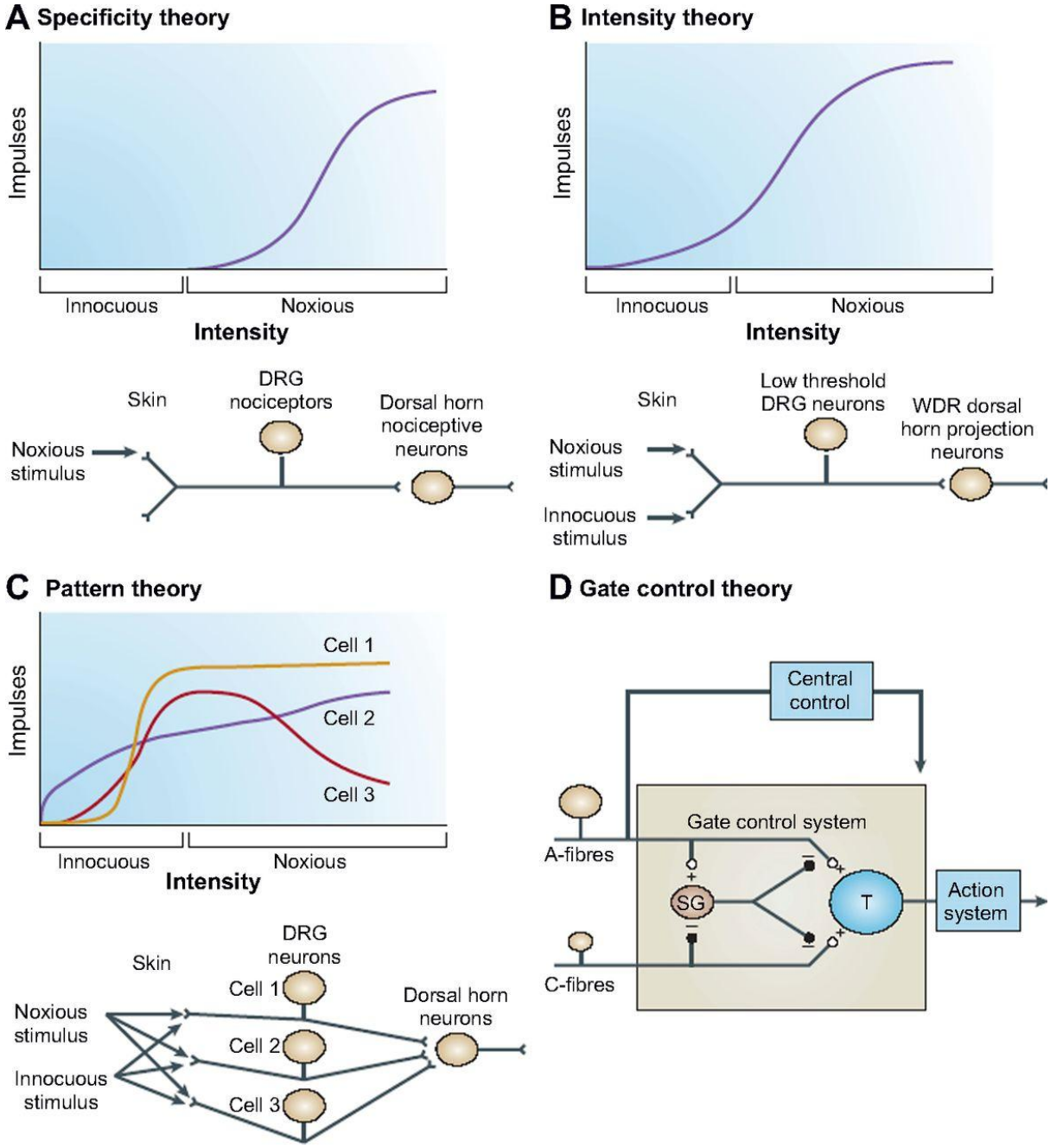

FIGURE 1.2 PAIN THEORIES .
Schematic diagrams of pain theories. **A.** Specificity theory; **B.** Intensity theory; **C.** Pattern theory; **D.** Gate theory. From *"Theories of pain: from specificity to gate control"*, Moayedi and Davis (2013).

The actual conception of a dedicated pathway for pain was developed by Charles Bell and described in *Idea of a New Anatomy of the Brain, submitted for the observation of his friends* (Bell and Shaw, 1868). He proved that brain was characterized by a heterogeneous structure and suggested that nerves were groups of neurons specialized in sensory stimulations, motor functions and "vital" sensing. Francois Magendie, based on Bells' theory of separation of sensory and motor nerves, built

his theory that nerves had different pathways entering and exiting from the spinal cord, then known as the Bell-Magendie Law of the differentiation of spinal nerves (Stahnisch, 2009). Further support of specific sensory transduction was brought in the last part of 19th century by the discoveries of specific cutaneous receptors sensitive to touch like Pacinian corpuscles (Pacini, 1835 reported in Cauna and Mannan, 1958), Meissner's corpuscles (Meissner, 1853 reported in Cauna and Ross, 1960), Merkel's disk (Merkel, 1875 cited in Iggo and Muir, 1969) and Ruffini's end organs (Ruffini, 1893). Despite this, there was not an unique opinion about the nature of pain, considering that a dedicated organ was not already discovered.

Based on the previous discoveries, Schiff and Woroschiloff, between 1854 and 1859, postulated the Specificity Theory (Figure 1.2 A) which asserted that there was a specific fiber leading pain information to the sensory modalities region of the brain (Rey, 1995). This finding was built on the discovery that tactile pathway did not decussate in the spinal cord and on observations of incisions at different spinal cord levels. Moreover, this theory was supported by the report of a patient with wounded grey matter of the spinal cord that presented impaired pain and temperature sensations but normal touch (Rey, 1995).

Alternative to the Specificity Theory, Wilhelm Erb postulated the Intensity Theory (Figure 1.2 B), which asserted that the intensity of stimulation was responsible for the pain occurrence rather than being a specific stimulus modality (Dallenbach, 1939). This theory competed with the Specific one, at least until the publication of Sherrington studies, which postulated the existence of a specific receptor for painful stimuli, that he called nociceptor (Sherrington, 1906).

In the attempt to revise and reconcile different somatosensory theories, Sinclair and Weddel (1955) suggested the Pattern Theory model (Figure 1.2 C), which postulated that any single sensation induced a specific pattern of neuronal firings, whose spatial and temporal profile encoded for the type and the intensity of the stimulation rather than specific fiber types (Sinclair, 1955; Weddell, 1955). However, this theory was unable to explain the needing of different cutaneous sensory receptors associated with peripheral fibers of different sizes (Heinbecker et al., 1933).

In 1965, Ronald Melzack and Charles Patrick Wall published a fundamental paper in which they proposed a revolutionary theory: the Gate Control Theory of Pain (Figure 1.2 D; Melzack and Wall, 1965). This model joined the Pattern and the Specificity Pain Theories, filling the gap between them. They accepted the effective subdivision in nociceptors and touch sensitive receptors and suggested that signals induced in primary afferents reached three regions of the spinal cord: the dorsal columns, the substantia gelatinosa and a bunch of cells called "transmission" cells. They

hypothesized that substantia gelatinosa hosted the gate of the sensory stimulus transmission, and that this mechanism was induced by small-sized fibers and inhibited by large-sized fibers. When a noxious stimulus overtook the gate threshold, the pathway was activated and the pain perceived. In addition, fiber descending from supraspinal sites could modulate this gate (Melzack and Wall, 1965; Moayedi and Davis, 2013). Although this theory showed soon after some anatomical inaccuracies and oversimplifications, its general framework significantly advanced our knowledge of pain.

The actual definition of pain by IASP is based on the theory published in 1968 by Melzack and Casey (Melzack and Casey, 1968) that considered pain as multidimensional and complex. The definition of multidimensionality was justified by the possibility to discriminate different features of pain, as intensity, location, quality and duration (sensory-discriminative), to induce emotional responses, as unpleasantness and fight-or-flight response (affective-motivational), and to elicit higher functions, as appraisal, ethics, context and cognitive state (cognitive-evaluative; Melzack and Casey, 1968; Moayedi and Davis, 2013). The different dimensions are not independent and can interact each others.

The debate between Specificity and Pattern Theories is not exhausted yet, and few years ago Basbaum published a paper regarding the differences between peripheral transduction of painful stimuli and central processing and perception of pain: *"This contemporary perspective on the question of specificity versus patterning relates more to the processing of nociceptive messages, and much less to the sensory experience/perception of pain. The latter is clearly influenced and in some cases dominated by emotional and cognitive factors"* (Basbaum, 2011).

1.2 DORSAL ROOT GANGLIA AND SOMATOSENSORY PATHWAYS

1.2.1 SOMATOSENSORY PATHWAYS

The somatosensory system is the part of the sensory system specialized in the conscious perception of touch, pressure, pain, temperature, position, movement and vibration, which are perceived by muscles, joints, skin and fascia.

This system is organized in a three-neuron pathway: peripheral sensory information is converted into nerve impulses by **primary sensory neurons**, which convey these stimuli via **secondary sensory neurons** to the spinal cord and brainstem to reach thalamic nuclei and, eventually, continuing in the sensory cortex in the parietal lobe through **third order neurons** (Brodal, 1969; Vallbo et al., 1979)**.**

1.2.1.1 PERIPHERAL FIBERS

Primary sensory neurons are pseudounipolar neurons with peripheral and central branches connected to the soma by a unique axon through which the electric stimulus is transmitted (Takahashi and Ninomiya, 1987). Their cell body is located in dorsal root ganglia (DRGs; Figure 1.3 A) or in trigeminal ganglia (TGs, for sensory inputs from head and neck; Figure 1.3 B). The system relaying somatic sensitivity is one of the most heterogeneous within the sensory system, transducing a broad range of stimuli such as touch, pressure, vibration, position, temperature, stretch and nociception**.**

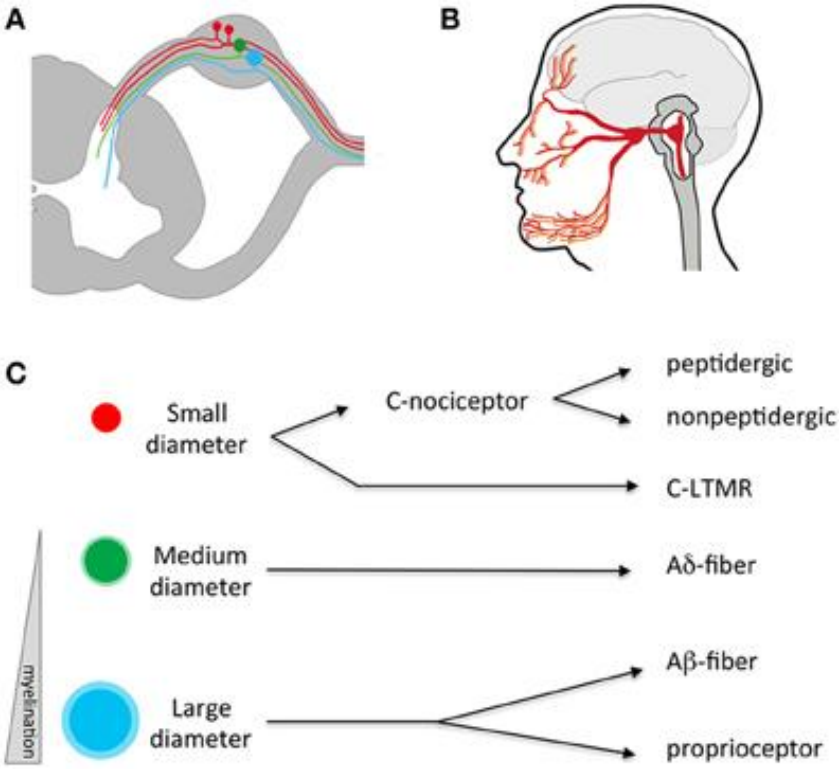

FIGURE 1.3 ANATOMY OF THE SOMATOSENSORY SYSTEM.
A. Somatosensory neuron cell bodies in a dorsal root ganglion; **B.** Territory of innervation of somatosensory neurons residing in the trigeminal ganglion; **C.** Categorization of primary sensory neurons based on soma size and degree of myelination.
From *"The functional and anatomical dissection of somatosensory subpopulations using mouse genetics"*, Le Pichon and Chesler (2014).

In simplistic terms, the peripheral somatosensory system can be organized in sensory fibers specialized in encoding low-threshold innocuous stimuli (non-nociceptive pathways) or high-threshold noxious stimuli (nociceptive pathways). **Nociception** is thus defined as the neural process of encoding noxious stimuli (IASP taxonomy, 1994).

Peripheral afferents are classified based on 1) the conduction velocity or 2) the sensory modality or 3) the morphology.

1- The **conduction velocity** of action potentials is proportionally correlated with the fiber diameter (Figure 1.3 C) and on the degree of myelination and it is associated with its functional role (Harper and Lawson, 1985). Thus, fibers can be classified as Aα, Aβ, Aδ and C fibers according to their diameter. **Aα** (or group Ia, Ib and II) are the faster and heavily myelinated

fibers, characterized by a large diameter and associated with receptors localized in muscles and tendons. **Aβ** fibers are slightly smaller and slower myelinated fibers conveying most of the tactile inputs. **Aδ** thinly-myelinated or **C** unmyelinated fibers (which correspond respectively to group III and IV in muscles) mostly convey nociceptive and thermal stimuli.

2- According to the **sensory modality**, receptors can be classified in nociceptors, thermoreceptors, chemoreceptors and mechanoreceptors.

Nociceptors are receptors that respond to noxious stimuli and are characterized by free nerve endings with Aδ (group III) fine-myelinated or C (group IV) unmyelinated fibers (Basbaum et al., 2009; Besson and Chaouch, 1987; Millan, 1999). They are typically activated by an intense mechanical stimulation (mechanosensitive nociceptors), by an exposition to intense cold/heat (thermosensitive nociceptors) or by all the stimuli just described (polymodal nociceptors). Aδ fibers and unmyelinated C fibers, respectively, convey the first rapid "sharp" phase of pain and the second wave of "dull" pain (Landau and Bishop, 1953; Treede et al., 1992).

Thermoreceptors are slowly adapting Aδ or C fibers receptors characterized by free nerve endings and activated by increase or decrease in temperature (Barbacid, 1994). A thermal stimulus can be either noxious or innocuous, warm or cold. Different specializations in Aδ-C fibers encode these different stimuli.

A *heat* stimulus typically evokes a fast sharp and the slower dull components. The first component is mediated by the fast conducing Aδ fibers, while the longer component suggests that it is conveyed by slow C fibers. Consistent with these observations, a block of Aδ fiber, as pressure, inhibits first pain (Price et al., 1977).

Experiments conducted by Treede et al. (1998) allowed a further subdivision of Aδ fibers in two categories:

- *Type I* afferents with high heat threshold (>53°C) to short lasting stimuli and delayed response. These fibers are hosted in glabrous and hairy skin and sensitize after burning injury, mediating thermal hyperalgesia (Meyer and Campbell, 1981b).
- *Type II* afferents have a lower heat threshold (47°C) with a faster short lasting response and their lack in the glabrous skin can explain the lack of the first heat pain in this region. These fibers also show a high mechanical threshold (Treede et al., 1998).

C fibers are found depth in the epidermis and dermis and their activating threshold (37-49°C) is below the heat nociceptive threshold (45°C). C fibers can be further subdivided in two categories (Meyer and Campbell, 1981a):

- *quickly adapting* fibers, which respond to a suprathreshold stimulus with short lasting high peak discharge;
- *slowly adapting* fibers which respond with a pretty uniform discharge during the ongoing stimulus.

Interestingly, C fibers innervating hairy skin tend to sensitize after a burn injury while afferents innervating glabrous skin do not (Campbell and Meyer, 1983).

Cold temperatures can variably activate nociceptors according to the type of skin (<10-15°C in glabrous skin, <18°C in hairy skin; Chéry-Croze, 1983) and the speed of the temperature change. Interestingly, cold-activated C fibers are considered responsible for the perception of a burning or heat pain (Davis, 1998), while the "cool" sensation is supposed to be mediated by Aδ fibers.

Chemoreceptors are exogenous and endogenous chemical signals receptors, mostly encoded by C fibers; this receptors may alter pain threshold to noxious stimuli by activating mechano-insensitive "silent nociceptors" (Schmidt et al., 2000) and sensitizing non-nociceptive fibers, thus causing them to convey noxious information (i.e. Aαβ fibers in the case of mechanical allodynia; Ma and Woolf, 1996). After a damage, tissues release a large amount of algogenic and sensitizing chemicals, such as protons, potassium ions, phospholipids, purine, etc. that, in turn, stimulate the inflammatory process with the consequent release of several inflammatory mediators (bradikinin, prostaglandins, prostacyclines, ATP, serotonin, cathecolamines, histamine, etc.; Millan, 1999). This "inflammatory soup" contributes to the activation of nociceptors (primary hyperalgesia) and facilitates the onset of neurogenic inflammation due to the antidromic depolarization of sensory terminations. This activation causes the release of tachykinins, calcitonin gene related peptide (CGRP) and other peptides from peripheral peptidergic sensory neurons, that prolongs and extends the inflammatory process to intact tissue (secondary hyperalgesia; Barnes et al., 1990; Levine et al., 1993). Some neurotrophins, and namely neurotrophic growth factor (NGF), also play an important role in this process by regulating the sensitivity of nociceptors to thermal and chemical stimuli and by controlling peptides release (Koltzenburg et al., 1999; Malcangio, 1997).

Mechanoreceptors (Figure 1.4) are activated by physical deformation of the tissue in which they reside (Ingber, 1997; Johansson and Vallbo, 1979) and can be further subdivided, depending on the terminal ends structure, in two categories:

Encapsulated if they are enclosed in a cellular or connective capsule as:

- Meissner's corpuscles (Aβ fiber/group II) which are rapidly adapting and sensitive to fine tactile discrimination;
- Pacinian corpuscles (Aβ fiber/group II), which are rapidly adapting and respond to pressure and vibration;

- Ruffini's corpuscles (Aβ fiber/group II), which are slowly adapting and provide proprioceptive information;

Non-encapsulated as:

- free nerve endings (Aδ/group III and C/group IV fiber), which are slowly adapting, and are sensitive to painful and non-painful (thermal, pressure, touch) stimuli;
- peritrichial nerve endings (Aβ fiber /group II), which are rapidly adapting and are sensitive to the bending of hair follicles;
- Merkel's discs (Aβ fiber/group II), which are slowly adapting and respond to discriminative touch.

A particular type of mechanoreceptors is represented by stretch receptors that convey information from skeletal muscle and tendons:

- Muscle spindles are dynamic stretch receptors mechanically jointed with muscle fibers. All intrafusal fibers are innervated by Aα fibers, which collect information about the muscle contraction speed, while just some intrafusal fibers (called nuclear chain fibers) are innervated by Aβ fibers, which collect information on the intensity of the stretch;
- Golgi tendon organs are fusiform-shaped stretch receptors located at myotendineal junction and convey information through Aα fibers.

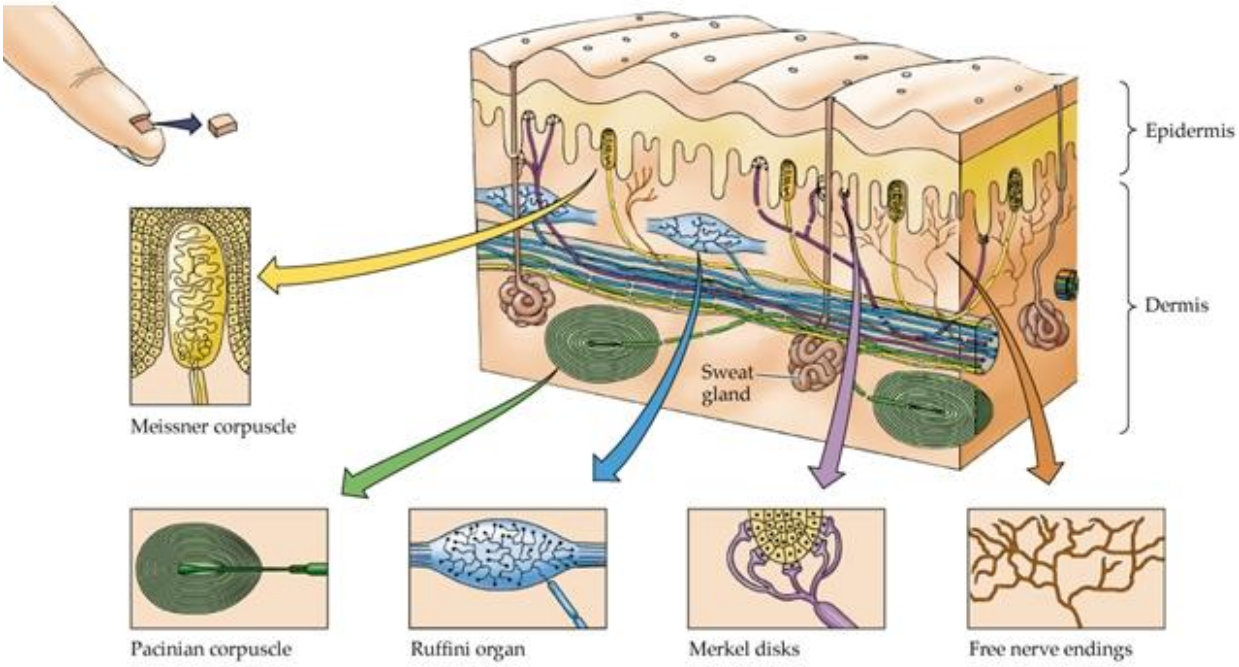

FIGURE 1.4 SENSORY RECEPTORS.
From *"Neuroscience. 2nd edition"*, Purves et al.(2001a)

Polymodal receptors are mostly C fibers and are so defined as they can be activated by stimuli of different nature (heat, as mechanical or chemical). For instance, in an experiment on human

peroneal nerves, Schmidt et al.(1995) recorded 15% of C fibers sensitive to mechanical stimuli and insensitive to heat (C-MHi), 10% only-heat sensitive (C-H), 25% insensitive to heat and mechanical stimuli (C-MiHi) and 50% sensitive to both heat and mechanical stimuli (C-MH).

1.2.1.2 SPINAL DORSAL HORN

The central processes of DRG primary sensory neurons enter the spinal cord via the dorsal roots of the spinal nerves.

The anatomy of the spinal cord comprises the central grey matter, formed by cells somata, and the surrounding white matter, formed by ascending and descending fibers. The grey matter can be subdivided in three main columns: the **dorsal horn**, that receives somatosensory information, the **ventral horn,** that contains motor neurons, and the **lateral horn**, that innervates visceral and pelvis organs. In *"The cytoarchitectonic organization of the spinal cord in the cat"*(Rexed, 1952), Bror Rexed divided the **dorsal horn** of the spinal cord in six regions or laminae, depending on the cell sizes and shapes included, on the orientations of axons and dendrites and on the thickness of the axons' myelin sheath. Even if the first descriptions were based on anatomical features of cats, following studies supported the model also in other species, e.g. in humans and in rodents (Milosevic et al., 2005).

Primary afferent fibers in the dorsal root are subdivided in two groups: the medial and the lateral divisions.

The **medial division** consists in **medium/large-sized** afferents bifurcating in ascending and descending branches that reach laminae II, III and IV. Large ascending fibers rise omolaterally, in respect to the dorsal root entry zone, forming the gracilis and cuneatus fasciculi of the dorsal column which travel to the respective nuclei in the medulla where make synapse with **secondary sensory neurons** (Light and Perl, 1979b).

The **lateral division** collects **small-sized** fibers (Aδ and C) and ramificates into short ascending and descending collaterals, forming the dorsolateral tract of Lissauer. Afferents of Lissauer's tract ascend or descend across one to three spinal levels, before penetrating the grey matter of the dorsal horn and forming synapses with **secondary sensory neurons** in lamina I, II (*substantia gelatinosa*) or in laminae III-V. Second order neurons then send fibers that decussate in the controlateral side of the spinal cord and ascend along the spinothalamic tract (Light and Perl, 1979b).

Different types of primary afferent fibers terminate with specific synaptic patterns within the spinal dorsal horn (Todd, 2002), as follows:

- **C fibers** mainly terminates in the superficial laminae I and II (Light and Perl, 1979a);
- **Aδ fibers** in laminae I, II, V and VI (Nagy and Hunt, 1983; Swett and Woolf, 1985);
- **Aβ fibers** in laminae III and V (Woolf, 1987).

Considering the projections on the base of the sensory modality:

- **Mechanoreceptors** mainly terminate in laminae II (inner), III and VI;
- **Nociceptors** mainly terminate in laminae I, II (outer) and V (Light and Perl, 1979a).

1.2.1.3 ASCENDING PATHWAYS

The general somatic afferent system, which transmits sensory stimuli from **somatic** structures to the higher centers, is anatomically divided, according to the sensory modalities transmitted, in two main different pathways: the **spinothalamic tract** (STT) and the **dorsal column-medial lemniscal** (DCML) **tract** (Poggio and Mountcastle, 1960)**.**

Spinothalamic tract. STT (Figure 1.5) transmits painful, tactile, chemical and thermal stimuli. It is composed by second order neurons projecting from laminae I, III, IV and V or from the spinal nucleus of the trigeminal to the controlateral thalamus. The STT axons decussate at the level of the anterior white commissure as they ascend, dividing in the ventral and lateral pathways, which covey different sensory information (Giesler et al., 1979; Poggio and Mountcastle, 1960). **Ventral STT**, located in the anterior funiculus of the spinal cord white matter, conveys crude non-discriminative touch and pressure, while **lateral STT**, located in the lateral funiculus, conveys pain and temperature (Martin et al., 1990). Ventral and lateral STT (Figure 1.5 A) rise separately along the spinal cord until they merge in the medulla, forming spinal lemniscus. The same type of sensory inputs from the head are collected by trigeminal afferents (Figure 1.5 B) which contact second order neurons in the spinal trigeminal nucleus, originating the trigeminal thalamic tract and the trigeminal leminscus (Cozzi et al., 2009).
While spinal lemniscus terminates in the ventral posterolateral nucleus (VPL) of the thalamus, the trigeminal lemniscus ends in the ventral posteromedial (VPM) nucleus of the thalamus. From the thalamus, **third order neurons** project to the somatosensory cortex via thalamocortical pathways.
These pathways collectively play a key role in transmitting discriminative aspects of nociceptive information.

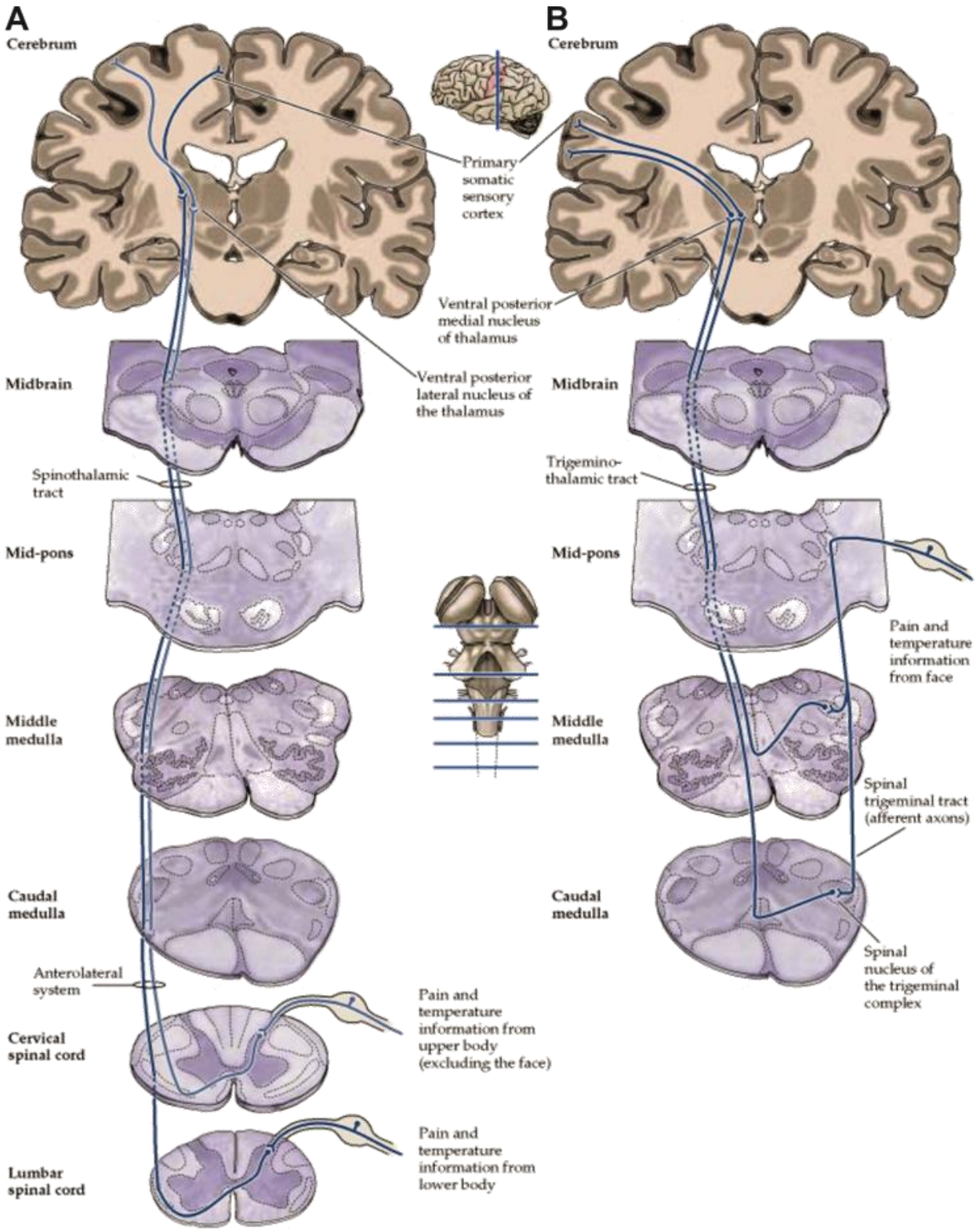

FIGURE 1.5 ASCENDING PATHWAYS.
A. Spinothalamic tract (STT) and **B.** trigeminal thalamic tract. From *"Neuroscience. 2nd edition"*, Purves et al. (2001b).

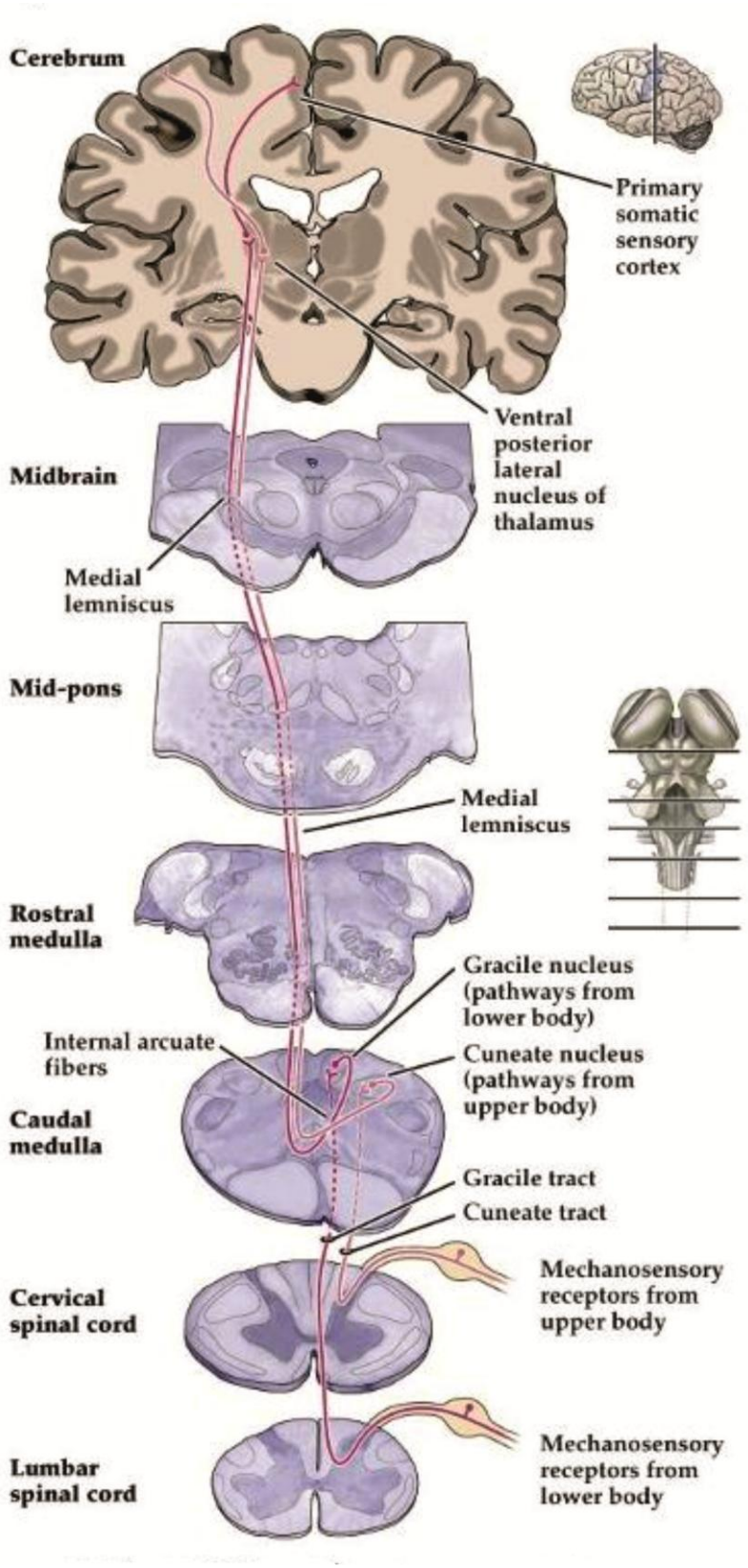

FIGURE 1.6 ASCENDING PATHWAYS.
Dorsal column-medial lemniscus (DCML) tract. From *"Neuroscience. 2nd edition"*, Purves et al. (2001b).

Dorsal column-medial lemniscal. DCML (Figure 1.6) transmits discriminative tactile and proprioceptive stimuli to the cortex. It is mainly composed by mechano- and propioreceptor A fibers conveying sensory input from the skin, muscles and joints. Central branches from lower limbs ascend in the dorsal column **fasciculus gracilis**, while the branches from upper limbs form the **fasciculus cuneatus**. Both these tracts reach the medulla and form synapses with second order neurons resident in the nucleus gracilis and the nucleus cuneatus, respectively. Within the medulla, the axons of the second order neurons decussate and ascend to the VPL nucleus of the thalamus along the **medial lemniscus**. Regarding mechanosensory afferents innervating the head, the first order trigeminal neurons form synapses in the pontine nucleus of the trigeminal and converge in the trigeminal lemniscus, which ends in the VPM nucleus of the thalamus. From the thalamus, **third order neurons** project again to the somatosensory cortex via thalamocortical pathways (FitzGerald and Folan-Curran, 2002).

Other ascending pathways include:

Spinoreticular tract. In addition to STT and DCLM tracts, which are phylogenetically recent (**neospinothalamic tract**), another important sensory pathway is represented by the spinoreticular tract. This pathway comprises neurons from laminae V and VII (this in the lateral horn) and, together with the trigeminoreticular, forms the most phylogenetically ancient somatosensory pathway, also known as **paleospinothalamic tract**. The spinoreticular tract ascends ispilaterally and forms synapses with the reticular formation of the brainstem, and its role is to maintain the arousal through the activation of the cortex and to inform the limbic system on the nature of the incoming stimuli, eliciting emotional responses (FitzGerald and Folan-Curran, 2002).

Spinotectal tract. Spinotectal tract is formed by afferents from laminae III-V and VII-VIII (ventral and lateral horns) which ascend via lateral funiculus. This tract ends in the lateral geniculate nucleus of the thalamus, that is a relay center for the visual pathway. Here, somatosensory information and visual information are integrated, in order to control head movements (Cozzi et al., 2009).

Spinomesencephalic tract. This tract mainly terminates in the periacqueductal grey and the raphe nuclei, that are involved in descending modulation of pain.

Spinohypothalamic tract. This pathway regulates most of the autonomic responses to nociception. In addition, some collaterals reach the limbic system, mediating the emotional component of pain perception.

Spinocerebellar tracts. Spinocerebellar tracts are four (**spinocerebellar dorsal, spinocerebellar ventral, cuneocerebellar** and **rostral spinocerebellar).** Spinocerebellar pathways convey unconscious proprioceptive information from muscles and joints and also receive collaterals from cutaneous sensory neurons.

Spino-olivary tract. Spino-olivary tract is constituted by axons of second order neurons projecting tactile information from laminae III and IV to the olivary bodies in the medulla. From these nuclei, third order neurons convey the information to the cerebellum, which use them to modulate motor coordination (FitzGerald and Folan-Curran, 2002).

1.2.1.4 DESCENDING PATHWAYS

Descending pathways of spinal nociception originate from many brain regions and play a critical role in the modulation and integration of both acute and chronic pain. For many years, the attention was focused on their inhibitory control of pain, however recent evidences show that descending control can be facilitatory and inhibitory (Zhuo and Gebhart, 1997). Descending control arises from a number of supraspinal sites, such as the midbrain periaqueductal gray (PAG), the nucleus raphe magnus (NRM) and the rostral ventromedial medulla (RVM; Fields et al., 2006; Heinricher et al., 2009). Minor sources of descending modulation include pontine noradrenergic nuclei (Pertovaara, 2006) and two areas of the caudal medulla, the dorsal reticular nucleus (DRt) and ventrolateral medulla (VLM; Tavares and Lima, 2002).

The PAG-RVM system. The PAG is strongly interconnected with the hypothalamus and limbic forebrain structures including the amygdala, and also receives direct spinomesencephalic input. The PAG projects to the RVM and NMR neurons, which in turn send their output to the spinal dorsal horn. NRM neurons are primarily activated by inputs from the PAG that, in turn, is activated when the tonic inhibition of local enkephalinergic neurons is removed. This inhibition of inhibitors is mediated by the intervention of hypothalamic afferents that release opioid peptides (β -endorphin) in response to specific sensory inputs from the spinoreticular tract (Zhuo and Gebhart, 1997; Ren and Dubner, 2002). In the spinal cord they release serotonin to excite inhibitory interneurons and stimulate the local release of opioid peptides, such as dynorphin or enkephalin, to block the noxious stimulus from the first order neuron central processes (D. Purves et al., 2009; Patestas and Gartner, 2016).

1.2.2 DRG STRUCTURE

DRGs are bilaterally located to the spine (31 pairs in human, 34 in rodents; Figure 1.7; Hofstetter et al., 2006; Sengul and Watson, 2012) and are primarily constituted by the cell body of primary sensory neurons which are individually enveloped by satellite glial cells (SGCs). The whole structure is enclosed in a firm connective capsule.

1.2.2.1 PRIMARY SENSORY NEURONS

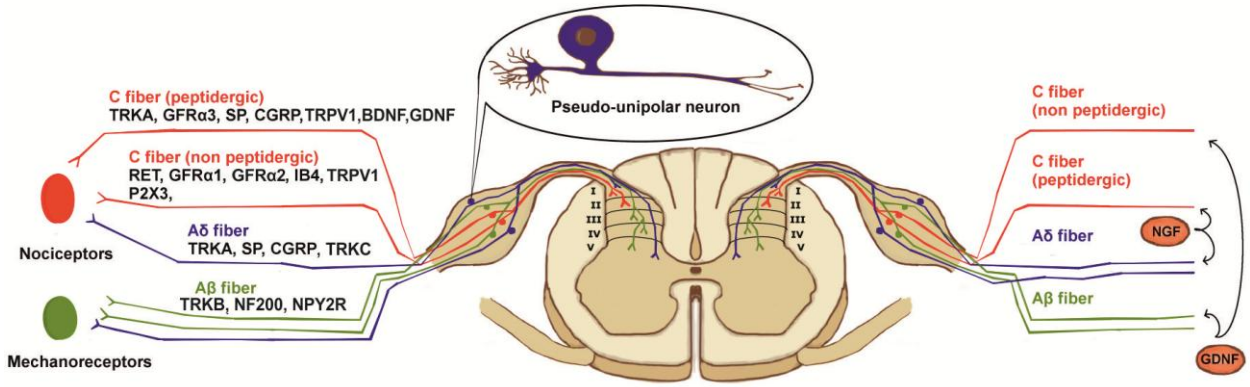

FIGURE 1.7 PRIMARY SENSORY NEURONS FROM PERIPHERY TO SPINAL CORD.
On the left side, neurochemical markers of the different populations of primary sensory neurons. On the right side, dependency of sensory neurons from different neurotrophic factors. *trkA-trkB-trkC*, tyrosin kinase A/B/C; *GFRα1/2/3*, GDNF family receptor 1/2/3; *SP*, substance P; *CGRP*, calcitonin gene related peptide; *TRPV1*, transient receptor potential vanilloid 1; *BDNF*, brain-derived neurotrophic factor; *GDNF*, glial cell line-derived neurotrophic factor; IB4, isolectin B4; *P2X3*, ATP-gated ion channel; *NF200*, neurofilament 200; *NPY2R*, neuropeptide Y receptor Y2; *NGF*, nerve growth factor.

DRG sensory neurons have been classified following morphological, electrophysiological and neurochemical criteria:

Considering the morphology only, DRG neurons can be simply divided according to the size of the somata (Barabas et al., 2014; Kestell et al., 2015), in:

- **Large-sized** neurons (associated with Aβ and Aα fibers) with large diameter (>50 µm). These neurons are involved in low-threshold mechanical sensations and proprioception;
- **Medium-sized** neurons (mostly associated with Aδ fibers and some C fibers) with a shorter diameter (30-50 µm);
- **Small-sized** neurons (associated with C fibers) that have a small diameter (10-30 µm) and are sensitive to different stimuli such as heat, pruritogens, irritants, tissue damage and mechanical stress.

The different sizes were also found to correlate with the staining to basic aniline dyes which reflected the neuronal content of neurofilaments (Lieberman, 1976; Lawson, 1979; Rambourg et al., 1983). Thus, according to an old histological classification, DRG neurons can be subdivided into:

- **Small dark** (SD) **neurons**
    - ~ 70%;
    - mainly thermo- and mechanoreceptors (small part as nociceptors);
    - slow conducting C fibers;
    - containing substance P (SP) and calcitonin gene related peptide (CGRP).
- **Large light** (LL) **neurons**
    - ~ 30%;
    - low threshold mechanoreceptors;
    - fast conducting A type fibers.

These old morphological classifications have been more recently substituted by classifications based on the neurochemical profile, which increased the number of subpopulations within each morphological category (see for example Averill et al. 1995).

Large-sized DRG neurons (>50 μm, 40%) can be identified by the following neurochemical markers:

- **NF200** (heavy neurofilament subunit, 200 kDa) occurs in 73% of DRG neurons (Kestell et al., 2015) and is one of the subunit recognized by the antibody RT97 and characterizing large light neuronal population (Lawson et al., 1984). mRNA level is found to be 20-fold higher in the large neurons than in the small one (Ho and O'Leary, 2011).
- **Necl-1** is a member of the Necls family of cell adhesion molecules, which mediate axonal-glial interactions (Maurel et al., 2007). Heterophilic binding between Necl-1 and Schwann cells promotes the myelin ensheatment. Also in this case, mRNA expression of this molecule is preferential in large-sized neurons and the combination with NF200 suggests their cooperation in giving rise to axons myelin ensheatment.
- **Parvalbumin** is a calcium binding protein that acts as a calcium buffer to modulate intracellular calcium homeostasis (Neher and Augustine, 1992), thus affecting synaptic transmission (Müller et al., 2007). The presence or the absence of parvalbumin in NF200+ neurons allows to recognize proprioceptive medium-to-large neurons to mechanosensitive cells, respectively (Le Pichon and Chesler, 2014);

- **NPY2R** is the neuropeptide Y (NPY) Y2 receptor and characterizes a small population of large-sized neurons that co-express CGRP (Zhang et al., 1997). The expression of this receptor is up-regulated after injury. YR2 is then transported centrally to the dorsal horn, where may act as presynaptic receptor and autoreceptor for the local release of NPY. The NPY-NPY2R binding inhibits Ca^{2+} influx via voltage-sensitive calcium channel (Bleakman et al., 1991) and inhibits the release of SP from the terminals, exerting an inhibitory effect (Shi et al., 2006; Zhang et al., 1997);
- **TrkB** is a tyrosine protein kinase receptor bound by the brain-derived neurotrophic factor (BDNF; Merighi et al., 2008b) and also (but not exclusively) expressed by medium-large-sized neurons, that are mainly proprioceptors.
- **TrkC** is a tyrosine protein kinase receptor bound by the neurotrophic factor neurotrophin-3 (NT-3) that is essential for the survival during the development of large-sized mechanoreceptors (Ernfors et al., 1994; Fariñas et al., 1994).
- In addition, large-sized DRG neurons present the vescicular glutamate transporter 1 (vGLUT1; Brumovsky et al., 2007), a small amount of T-type low threshold Ca^{2+} current (Scroggs and Fox, 1992), the acid-sensing ion channel DRASIC (Xie et al., 2002) and the low affinity neurotrophins receptor p75 (Zhou et al., 1996).

Small-sized neurons (10-30 μm, 60%; Figure 1.8) are divided in two main categories based on the peptide content: the peptidergic and the non-peptidergic neurons (Hunt and Rossi, 1985).

Peptidergic neurons (30-45%) are small-to-medium neurons, mainly characterized by the expression of calcitonin gene-related peptide (CGRP) and substance P (SP; Merighi et al., 1991; Salio et al., 2005). Peptidergic neurons differentiate under the control of the nerve growth factor (NGF, Crowley et al., 1994) and can be identified with the following markers:

- **CGRP** occurs in virtually all peptidergic neurons, which may represent up to 47% of all DRG neurons (Kestell et al., 2015). CGRP is the gold standard for labelling peptidergic primary sensory neurons (Basbaum et al., 2009). Its expression is not restricted to small-sized neurons but is also present on DRG neurons with somata larger than those of nociceptors, whose fibers are Aδ (33%) or Aα/β (17%; McCarthy and Lawson, 1990). CGRP is co-expressed with SP (60%) and with the capsaicin receptor TRPV1 (Kestell et al., 2015). Recurring to genetic ablation, McCoy et al. (2013) demonstrated that CGRP is mainly involved in the regulation of noxious heat, capsaicin sensitivity and itch, but has a secondary role also on thermoregulation.

- **Substance P** (**SP**) occurs in up to 33% of DRG neurons (Kestell et al., 2015). SP released at spinal cord level enhances nociceptive transmission and leads to central sensitization in chronic pain, while at the periphery, plays a crucial role in cutaneous antidromic events, such as extravasation, vasodilatation and regulation of sympathetic ganglia activity (Cuello, 1987). Virtually, all SP-containing neurons express CGRP, while less than half also express the neurotrophic factor BDNF (Salio and Ferrini, 2016).
- **Somatostatin** (**SST**) occurs in 12% of DRG neurons (Shi et al., 2014) as a regulatory peptide that acts exerting an inhibitory effect both on dorsal horn and DRG neurons. Almost all SST neurons are CGRP+ , but SP negative, thus constituting a different subpopulation of peptidergic neurons (Salio and Ferrini, 2016);
- **BDNF** (brain-derived neurotrophic factor) is expressed in about 25% of CGRP+ neurons, that also express SP (Salio and Ferrini, 2016).
- **GDNF** (glial cell line-derived neurotrophic factor) is expressed in about 20%of CGRP+ neurons, that also express STT (Salio and Ferrini, 2016).
- **Transient receptor potential vanilloid 1** (**TRPV1**) occurs in 49% of DRG neurons (Kestell et al., 2015) and results activated by noxious heat (>42°C) or chemical substances mimicking heat (e.g. capsaicin). Experiments performed on TRPV1-knockout mice confirm a reduction of thermal hyperalgesia in inflammatory condition (Caterina et al., 2000). Almost all CGRP+ and SP+ are also TRPV1+ (94%). Interestingly, around 20% of TRPV1+ neurons are negative for both CGRP and IB4 staining, revealing that this two categories are not totally comprehensive of small diameter neurons (Cavanaugh et al., 2011);
- **TRPA1**, a channel expressed in a subset of TRPV1+ neurons, is activated after direct exposition to chemical irritants (e.g. mustard oil) or indirectly, through the activation of cellular mechanisms linked to calcium or to G protein-coupled receptors (Guimaraes and Jordt, 2007);
- **TRPM8** occurs in 10% of DRG neurons, in a subset of TRPV1- and TRPA1- negative peptidergic neurons. TRPM8 neurons are associated with both C or Aδ fibers and encode cold pain (<18°C) stimuli (McKemy, 2007);
- **TrkA** is the high affinity receptor for the nerve growth factor NGF and is responsible for mediating NGF effects on neurons survival and differentiation during the development (White et al., 1996).
- **NP1YR** is the receptor for NPY expressed on CGRP+ neurons. The binding NPY-receptor inhibits Ca^{2+} influx via voltage-sensitive calcium channel (Bleakman et al., 1991) and inhibits the release of SP and CGRP from the terminals, exerting an inhibitory effect (Shi et

al., 2006; Zhang et al., 1997); controversially, experiments in which NPY were injected in the hindpaw of rats with a partial transaction of sciatic nerve showed that this peptide worsen mechanical hyperalgesia, while improving thermal hyperalgesia (Tracey et al., 1995).

Non-peptidergic neurons (30-40%) are small nociceptive and non-nociceptive neurons associated with C fibers. Although they are under the control of NGF at the early developmental stages, they differentiate in the mature form under the control of GDNF (Molliver and Snider, 1997). Non-peptidergic neurons can be identified with the following markers:

- **IB4** is the classical marker for non-peptidergic neurons, so called for the presence, on the membrane surface, of glycoproteins which are bound by the vegetal marker isolectin B4 (IB4; McCoy et al., 2013; Stucky and Lewin, 1999);
- **GFRα1**, the GDNF family receptor 1, is the receptor preferentially bound by **GDNF**. Interestingly, GFRα1 can transduce both in a Ret dependent and in a Ret independent way: in the former, many intracellular pathway are activated, such as extracellular regulated kinase (ERK), mitogen-activated protein kinase (MAPK) and phosphatidylinositol-3 kinase (PI2K) (Creedon et al., 1997), while Ret-independent signaling activates Src-like kinase activity, that induces a rapid phosphorylation of cAMP response element binding protein (CREB) and upregulation of *c-fos* mRNA**,** involved in cell survival (Trupp, 1999);
- **Ret** is a tyrosine kinase receptor responsible for the correct phenotyping during embryogenesis and neuronal activity modulator in adulthood. Ret is up-regulated while trkA is down-regulated in a subset of small-sized neurons during the first weeks after birth, passing from NGF-dependence to GDNF-dependence (Molliver et al., 1997a). Interestingly, a study suggested that the glycoproteins bound by the marker IB4 are the one of the glycosilated extracellular domain of Ret (Boscia et al., 2013). Usually, intracellular signaling enhanced by the neurotrophic factor **GDNF** is mediated by the aggregation of the receptor complex GFRα1-2/Ret, where the former acts as a binding site for the neurotrophic factor and the latter as internal signal inducer (Trupp, 1999);
- **P2X2/3** are the ATP-gated ion channels preferentially expressed by non-peptidergic afferents. Neurons labeled with IB4 are found in around 50% of P2X2+ neurons and 58% of P2X3+ (Kobayashi et al., 2005);
- **LA4** antibody, which recognizes a membrane oligosaccharide different from RT97 (Dodd and Jessell, 1985);
- **FRAP**, the fluoride-resistant acid phosphatase (FRAP, Nagy and Hunt, 1983);

- **MrgprD (Mas-related G protein-coupled receptor D)** occurs in around 75% IB4+ neurons and is involved in mechanical nociceptive stimulation. Many experiments performed with double knockout MrgprD/TRPV1 showed that a partial sensing of mechanical sensitivity was however retained, while temperature-related sensitivity was almost completely impaired. This participation of MrgprD to temperature-sensing is probably mediated by factors released in extreme-temperature condition and activating these receptors (Pogorzala et al., 2013).

Not all the small-sized neurons can be precisely categorized in the peptidergic or non-peptidergic subsets (Figure 1.8; Le Pichon and Chesler, 2014). Example of outsider neurons are the low threshold mechanoreceptor C fiber (C-LTMR; Bourane et al., 2009), even if some authors consider them as non-peptidergic subclasses for the markers they express (such as TH, VGLUT3, TAFA4, ret in Delfini et al., 2013; or GINIP in Gaillard et al., 2014) and MrgprB4+ neurons, that respond to innocuous gentle mechanical stimuli, combining to the physical stimulus a positive affective valence (Vrontou et al., 2013).

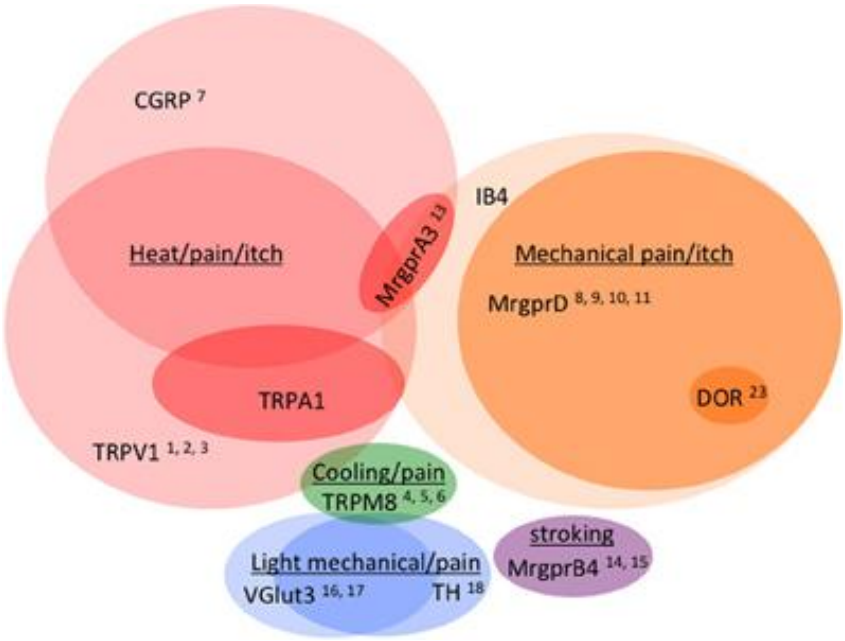

FIGURE 1.8 VENN DIAGRAM ILLUSTRATING THE DISTRIBUTION OF MARKERS OF DIFFERENT CLASSES OF SMALL-SIZED NEURONS.
From *"The functional and anatomical dissection of somatosensory subpopulations using mouse genetics"*,Le Pichon and Chesler (2014).

Electrophysiological properties. DRG neuron populations are also heterogeneous regarding their functional features, including, conduction velocities (CVs), their receptive properties and somatic action potential (AP) configuration (Harper and Lawson, 1985; Yoshida et al., 1978).

In the work "*Electrophysiological differences between nociceptive and non-nociceptive dorsal root ganglion neurons in the rat in vivo"* Fang et al. (2005) analyzed *in vivo* different electrophysiological parameters of rat DRG neurons:

- **CV.** Within C fiber subset, non-nociceptive low threshold mechanoreceptor (C-LTM) and the nociceptive mechano-cold receptor (C-MC) show the fastest CVs, while nociceptive neurons for mechano-heat (C-MH) sensation the slower. Within Aδ fiber subset, the faster are the HTM while, within Aα/β subset, the non-nociceptive LTM and the nociceptive MC;
- **AP kinetics.** Non-nociceptive LTM show faster AP kinetics than nociceptors in all CV subsets. In addition, many works reported an inverse relationship between somatic AP duration and CV (Harper and Lawson, 1985; Rose et al., 1986). AP rise time and fall time analysis reveal, as expected, that these components are both shorter in non-nociceptive LTM neurons than in nociceptors;
- **AP overshoot.** Nociceptors show larger AP overshoot than non-nociceptive LTM neurons. Within the single subsets, a difference is found only in C fiber group, whose MC has the smallest overshoot;
- **AP frequency.** Nociceptors show the lower level of electrotonic response to trains of electrical stimuli and, between subsets, the C fiber group has the lower frequency in absolute;
- **AHP duration.** Nociceptors show larger AHP duration than non-nociceptive LTM neurons.

Cell-specific AP configurations are determined by Na^+, Ca^{2+} and K^+ voltage-dependent ion channels:

- **Na^+channels** influence AP rise time and, subsequently, AP duration and CV. An example is the greater AP overshoot of nociceptors, which can be the result of voltage-gated Na^+channel Nav1.8, one of the main responsible for inward Na^+ current in small-sized DRG neurons (Herzog et al., 2001). The others Na^+ channels most expressed by nociceptors are Nav1.7 and Nav1.9 and, together with Nav1.8, contributing to their AP profile (Djouhri et al., 2003a; Fang et al., 2002);
- **K^+currents** resulting from voltage-gated and Ca^{2+} -activated K^+ channels modulate the duration of AHPs in nociceptors, while other K^+ currents (e.g. I_A fast transient or I_H hyperpolarization-activated) may influence AP frequency differences between the subsets (Vogalis et al., 2002).

Large-sized and small-sized neurons are also characterized by the pattern of Na^+ and K^+ channels they express:

Large-sized neurons

- **Na^+ channels** that characterize large-sized DRG neurons are tetrodotoxin sensitive (TTX-S), namely Nav1.1, Nav1.6 and Nav1.7 (Ho and O'Leary, 2011). Nav1.1 and Nav1.6 are preferentially expressed in medium to large DRG neurons (Black et al., 2004) while Nav1.7 is broadly expressed in all DRG neurons (Black et al., 1996). 10-30% of large-sized DRG neurons express TTX resistant (TTX-R) Nav1.8 (Djouhri et al., 2003b) and, in addition, present high levels of NF200 and Necl-1 mRNA, typically associated to fast conducting myelinated neurons (Lawson et al., 1993; Maurel et al., 2007);
- **K^+ channels** are the most numerous and broad class of ion channels in neurons. Large-sized DRG neurons are mainly characterized by dendrotoxin sensitive (DTX-S) sustained and delayed rectifier-type channels Kv1.1/Kv1.2 (Figure 1.9; Pearce and Duchen, 1994; for details

  Tsantoulas and McMahon, 2014).

Small-sized neurons:

- **Na^+ channels** that characterize small-sized peptidergic neurons are the TTX-R Nav1.8 and Nav1.9. The former encodes for a slowly-gating current responsible for the majority of depolarizing inward current during AP (Blair and Bean, 2002), while the latter encodes for a slowly-gating channel that underlies a persistent current (Dib-Hajj et al., 2002). These channels are the predominant Na^+ channels expressed in small neurons. In non-peptidergic IB4+ neurons, Na^+ channels account for one half as TTX-R Nav1.8, while over 70% are Nav1.9 (Fjell et al., 1999). Studies revealed that Nav1.9 has a more negative midpoint inactivation than Nav1.8 and a lower threshold for activation (Tate et al., 1998), and this difference could justify the more hyperpolarized activation and inactivation of TTX-R voltage-dependent steady state currents in IB4+ neurons. The TTX-S Nav1.7 is also present in both small-sized neurons populations, being the most broadly expressed Na^+ channel in DRG neurons (Black et al., 1996);
- **K^+ channels** mainly express a DTX resistant transient or A-type K^+ current, whose feature well-fit with the involvement of Kv4.2 and Kv1.4 (Figure 1.9; Tsantoulas and McMahon, 2014; for details).

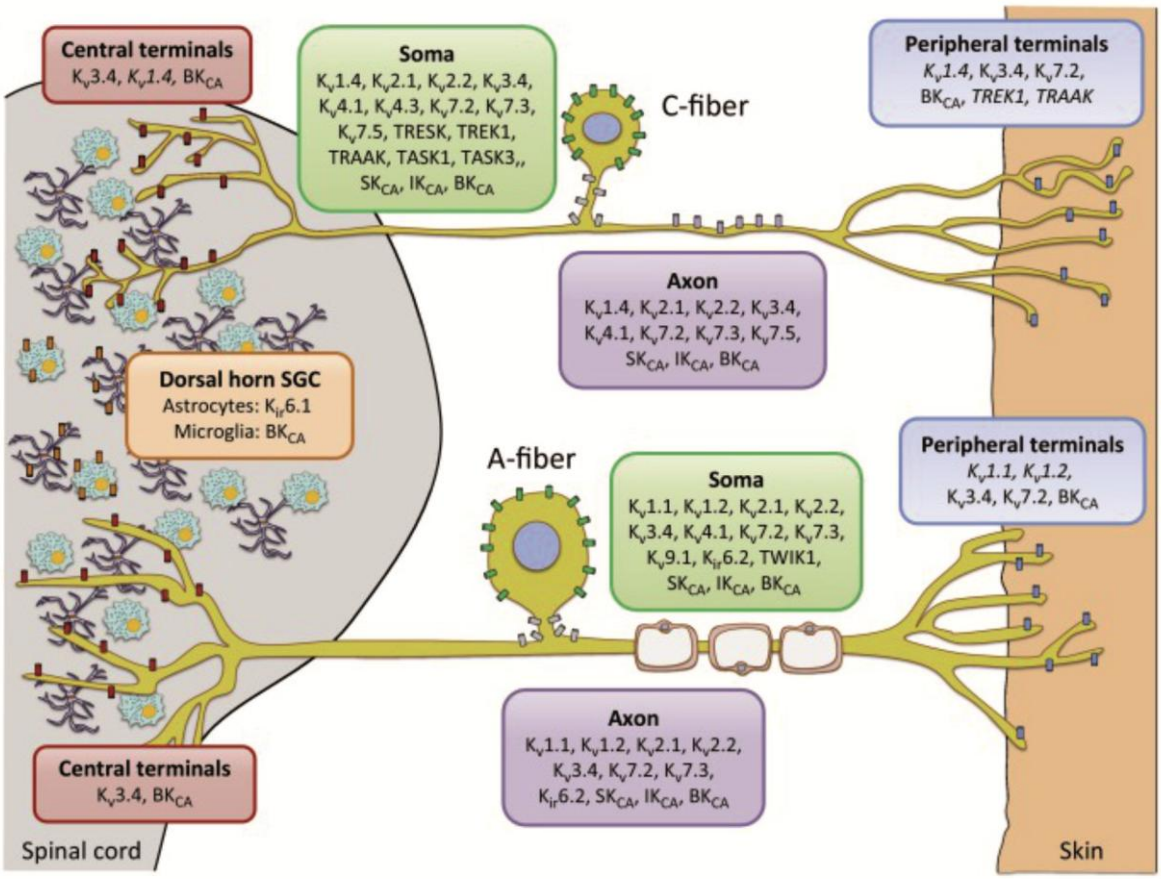

FIGURE 1.9 EXPRESSION OF K^+ CHANNELS IN PRIMARY SENSORY NEURONS.
From *"Opening path to novel analgesics: the role of potassium channels in chronic pain"* (Tsantoulas and McMahon, 2014).

1.2.2.2 SATELLITE GLIAL CELLS (SGCS)

Satellite glial cells (SGCs) are glial cells that cover the surface of nerve cell bodies in sensory, sympathetic and parasympathetic ganglia. The soma of sensory DRG neurons in adult animals is typically enwrapped, together with its initial axonal segment, by an individual satellite cell sheath and sharply separated from the adjacent neurons (Figure 1.10). Each soma, together with its glial ensheatment, forms a discrete unit which is electrically insulate from neighboring neurons (Pannese, 1981). However, sensory neurons sharing the same satellite cell ensheatment, with their cytoplasmic membrane in direct contact, are occasionally found. The organization assumed by SGCs can be distinguished in monolayer and flattened pattern or multilayer overlapping pattern, and this arrangement can change within a single discrete unit, passing from 4-6 µm to 40-50 µm. Instead, the distance between glial cells and neurons is around 20 nm. SGCs exhibit a laminar structure, lacking long, branching processes but presenting lamellar expansions and microvilli, mostly on the inner surface of the sheath. This organization greatly increases the surface of SGCs

and, as a result, the ratio between surface and volume. Microvilli are also present on neurons, fitting the invagination of glial cells and increasing in turn their surface to have a higher chance of chemical exchange (Hanani, 2005). The complete ensheatment characteristic of each discrete unit is unique and not detected in other areas of the CNS. Different studies showed that there is a direct relationship between the number of SGCs forming the envelope and the size of the enwrapped neuron. The need of more SGCs to sustain bigger cells is consistent with the hypothesis that these cells play a role in metabolically supporting sensory neurons (Ledda et al., 2004; Pannese, 1981). SGCs do not form a complete barrier allowing the passage of ions, micro and macromolecules and macrophages, but are able to slow down this diffusion, probably having an important role in the control of molecule trafficking (Pannese, 1981).

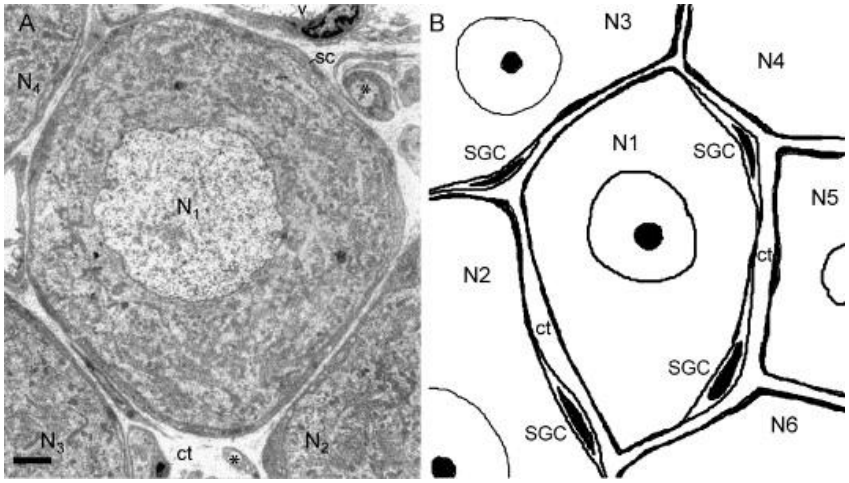

FIGURE 1.10 THE SENSORY NEURON-SGC UNIT.
From *"Satellite glial cells in sensory ganglia: from form to function"*, Hanani (2005). *sc* SGCs, *ct* connective tissue, $N_{1\text{-}6}$ neurons. Calibration bar 2 µm.

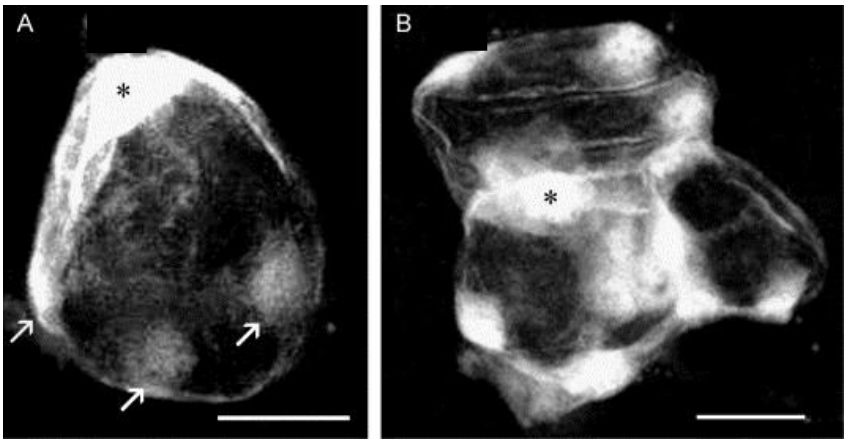

FIGURE 1.11 DYE-COUPLING OF SGCS.
From *"Satellite glial cells in sensory ganglia: from form to function"*, Hanani (2005). Dye injected cell indicated with the asterisks, arrows for the dye-coupled cells. Calibration bars 20 µm.

SGCs are in communication each other through gap junctions, that permit the passage of ions and molecules up to 1 kDa (Spray, 1996). SGCs were identified as "dye-coupled" (Figure 1.11) by injecting low-molecular weight tracer molecules in their cytoplasm (Hanani et al., 2002). In particular, 21% of the SGCs injected were dye-coupled and around 3% of SGCs tend to dye-coupled with SGCs that were enveloping adjacent neurons (Hanani et al., 2002). Moreover, the degree of coupling seems to be sensitive to the extracellular pH,

increasing with slightly basic pH (around pH 8.0) and decreasing with more acidic pH (pH 6.8) (Huang et al., 2005).

Among the different SGCs functions there is the control of the microenvironment surrounding sensory neurons. SGCs are able to uptake substances as glutamate, then converted through vary enzymes in glutamine, malate and lactate which are essential for neurons (Miller et al., 2002). SGCs can control the level of external K^+, acting as spatial buffering system. SGCs are sensitive to chemical stimuli, inflammatory substances and pain mediators: the nitric oxide (NO) synthase is contained in 5% of DRG neurons, while SGCs express guanylate cyclase, which synthesizes cyclic GMP after activation via NO stimulation. It was hypothesized that neurons release NO to communicate with SGCs, which in turn reply releasing arginine, a fundamental precursor of NO (Aoki and Semba, 1992). Cyclic GMP can influence both membrane properties and synaptic transmission, while NO has a protective role at low-dose, inhibiting enzymes associated with apoptosis, and a toxic effect at high-dose (Zhang and Snyder, 1995).

SGCs express both the specific receptor for the peptide endothelin, involved in the transmission of pain signals (Pomonis et al., 2001), and bradykinin, which acts inducing an inward current in SGCs that can contribute to the sensitization in pathological condition (England et al., 2001). SGCs also express ATP receptors P2Y, whose activation induces an increase of intracellular Ca^{2+} (Weick et al., 2003). Interestingly, Rozanski et al. (2013) have highlighted how this receptor is important for SGCs-neurons communication, being part of the so called "sandwich synapses": different neurons can communicate through SGCs using a transglial transmission model, where the first neuron releases ATP to activate P2Y receptors on the SGC interposed and in turn this glial cell releases Ca^{2+} from intracellular stores, triggering the release of a second transmitter to activate the first neuron itself or another neuron (Figure 1.12).

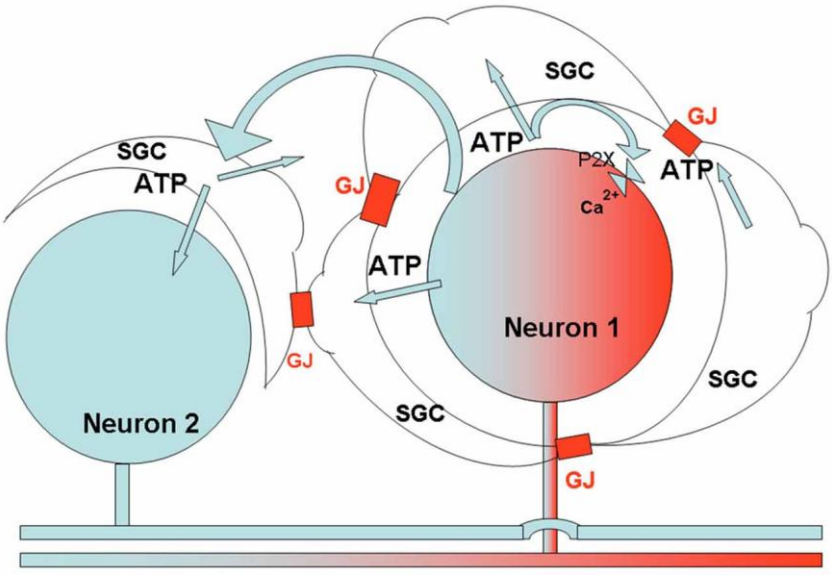

FIGURE 1.12 RELATIONSHIP BETWEEN SGCS AND DRG NEURONS.
From *"Role of satellite cells in gastrointestinal pain"*, Hanani (2015).

Finally, SGCs can take up neurotrophins, such as NGF and BDNF, from the external environment to reduce the accumulation and the neural activation induced by these molecules or to compensate their lacking, by releasing them from the storage sites (Aoki and Semba, 1992).
All together these findings evidence different main roles for SGCs: a mechanical support for neurons, considering the tight association with neurons and between different SGCs and the presence of a high content of microtubules and filaments in SGCs cytoplasm; a control of micro and macromolecules trafficking to and from neurons; a metabolic support; a buffering regulation of extracellular environment regarding ions and peptides; a regulatory control of neuronal communication. All these mechanisms may play an important role in the development of altered neuronal excitability under pathological conditions (Dublin and Hanani, 2007).

1.3 DIABETIC NEUROPATHY: ETIOLOGY, PATHOLOGY AND ANIMAL MODELS

1.3.1 ETIOLOGY OF DIABETIC NEUROPATHIC PAIN

In accordance with data from World Health Organization, the number of people with diabetes mellitus (DM) has risen from 108 million in 1980 to 422 million in 2014. The global incidence of DM among adults has risen from 4.7% in 1980 to 8.5% in 2014. In 2015, an estimated 4.6 million deaths were directly caused by DM and other 2.2 million deaths were already attributed to high blood glucose in 2012. DM is a group of metabolic diseases that share the occurrence of hyperglycemia, which is consequent to defects in insulin secretion, action or both (Ventura-Sobrevilla et al., 2011). Type 1 diabetes mellitus (T1D, insulin-dependent) recurs in 5% of diabetic population and is characterized by a progressive autoimmune impairment of insulin-producing pancreatic β cells, that causes insulinopenia and systemic hyperglycemia. Microangiopathy complications are common, while macroangiopathy and metabolic syndrome are exceptional. Type 2 diabetes mellitus (T2D, non insulin-dependent) is the most common form and recurs in 95% of the total diabetic population. Generally, it is the result of the combination of genetic background, diet and sedentary lifestyle, which develops in insulin resistance and prediabetes, precursor of hyperglycemia and diabetes (O'Brien et al., 2014). Prediabetes is a condition characterized by impaired glucose tolerance, which implies a non-diabetic high blood glucose level and an increased risk of cardiovascular pathology. Prediabetes is recognized as contributor factor of the development of idiopathic neuropathy in non-diabetic patients and the precursor stage of diabetes mellitus. The high blood glucose level that characterizes diabetes is also the leading factor of micro and macrovascular complications, resulting from cellular dysregulation and damage. Macrovascular

alterations underlie conditions as dilated cardiomyopathy and atherosclerosis, while microvascular alterations are involved in the development of nephropathy, retinopathy and neuropathy (Sullivan et al., 2008). The most common complication is diabetic neuropathy, which occur in approximately 50% of all diabetic patients (for in-depth analysis see Figure 1.13 and Singh et al. 2014).

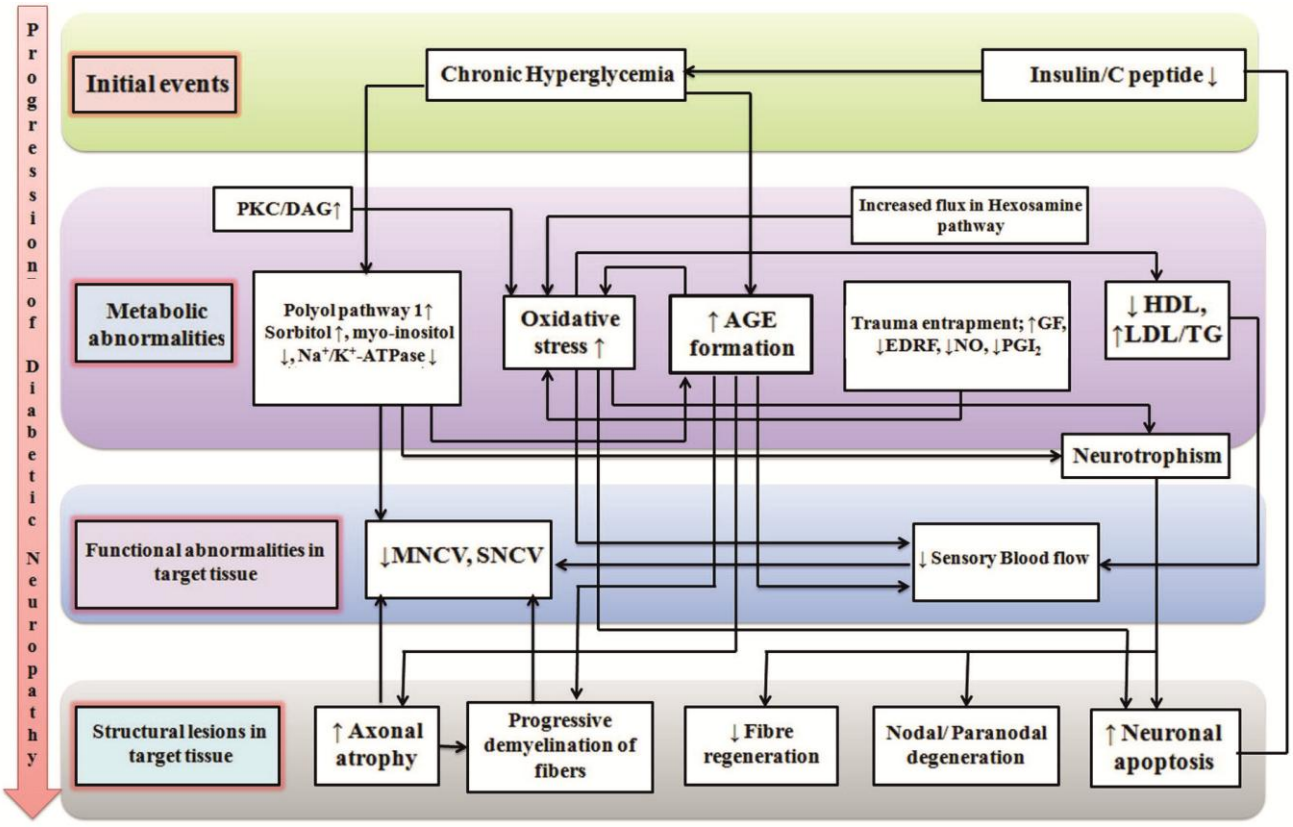

FIGURE 1.13 SEQUENTIAL EVENTS LEADING TO DIABETIC NEUROPATHY.
Modified from *"Diabetic peripheral neuropathy: current perspective and future direction"*, Singh et al. (2014).

Diabetic neuropathy includes a number of distinct syndromes: peripheral neuropathy, which is the most common and causes pain or loss of sensation in the limbs extremities; autonomic neuropathy, which causes altered functions of internal organs as bowel, bladder, lungs and hearth; proximal neuropathy, which affects the top part of the lower limbs, as thighs, hips and buttocks; focal neuropathy, which can affects any single of group of nerves in the body, causing pain or muscle weakness (NIH, 2009).

Symmetric sensory polyneuropathy, referred to as diabetic polyneuropathy (DPN), is the most common complication of patients affected by type 1 and type 2 diabetes. Symptoms of DPN are considered manifestations of dysfunction of the somatosensory system, so their clinical features vary according to the type and the length of nerve fibers involved. Complications against small-sized thinly myelinated Aδ fibers and unmyelinated C fibers, responsible for temperature and pain stimuli transduction, can cause hyperalgesia and allodynia (increased sensitivity to painful and

innocuous stimuli, respectively). Dysfunction of myelinated Aβ fibers, normally transducing mechanosensation, can result in sensory ataxia and decreased proprioception (O'Brien et al., 2014).

Patients with DPN present pain symptoms in 10-20% of the cases, with a prevalence of type 2 diabetes on type 1 (35% vs. 22%), of females on males (38% vs. 31%) and with variability between ethnic groups (Lawson and Backonja, 2013). Thus, pain is not a universal feature of patients with clinically assessed DPN and this discrepancy highlights the lack of a consistent pathogenic mechanism that link diabetes to neuropathies and neuropathies to pain. In fact, although neuropathic pain is a common manifestation of altered function of the nervous system in patients affected by DPN, a frequent sign is also represented by sensory loss. Occasionally, pain symptoms and sensory loss can be both present at the same time (Lawson and Backonja, 2013). Indeed, loss-of-function signs associated with peripheral lesions may results in spontaneous pain due to ectopic activity (Maier et al., 2010). DPN is characterized by a progressive nerve degeneration from distal to proximal areas and this mechanism was considered responsible for both neuropathic pain and disappearance of pain over the time. The mechanisms that bring to a painful or a painless DPN are still poorly understood, but some studies had highlighted a link between cutaneous reinnervation by epidermal small-sized fiber terminations and a reduction of the neuropathic pain (Smith et al., 2006). These findings, which are focused on the distal region of sensory axons, reawakened the theories that peripheral nerve alterations have a main role on pain rise. Aside from nerve degenerations, also an increased level of inflammatory molecules as ICAM, a marker of endothelial dysfunction, and C-reactive protein were found in patients with painful diabetic neuropathy and not in the painless one (Doupis et al., 2009). However, many other inflammatory markers did not vary between diabetic patients with and without pain symptoms, and currently there are no direct evidences linking chemical or physical alterations related to diabetes or neuropathies and the presence of pain (Lawson and Backonja, 2013). Interestingly, rat model of type 1 and type 2 diabetes can present in a stable fashion an early thermal hyperalgesia that can possibly progress in hypoalgesia. The persistence of a hyperalgesic state seems to be linked to the presence of residual endogenous or exogenous insulin, whereas the passage to an hypoalgesic state seems to follow the depletion of heat-activated epidermal fibers. Moreover, the block of glucose metabolism prevents the thermal hyperalgesia and the following hypoalgesia (Calcutt et al., 2004), while insulin therapy reverse hypoalgesia only (Chu et al., 2008). These findings suggest that the main feature of hyperalgesia is hyperglycemia, while hypoalgesia depends on both hyperglycemia and marked insulin deficiency (Lawson and Backonja, 2013). On the other hand, different studies in rat models of type 1 diabetes provided contrasting evidence concerning the role of hyperglycemia in altering pain behavior, supporting a main role of insulinopenia (Romanovsky et al., 2010).

Chronic hyperglycemia and elevated blood glucose level are responsible for metabolic aberration and contribute to nerve damage by altering several biochemical mechanisms. Even if currently none have been found critical, they provide the rational for developing different type of therapeutic approaches. Different hypotheses have been formulated to explain the insurgence of neuropathic pain:

- *spontaneous discharge of injured and uninjured afferent neurons* (Yoon et al., 1996): pro-nociceptive factors released during the wallerian degeneration of nerves damaged act sensitizing the adjacent nerve terminals on uninjured fibers. The activity increase last for few days, while neuropathic pain can endure longer, suggesting the contribute of other mechanisms (Han et al., 2000);
- *spinal sensitization*: hyperactive primary sensory neurons increase the release of amino acids on secondary neurons, causing an enhanced response to noxious stimuli (Woolf, 1993). The administration of NMDA antagonists normalize the enhanced pain because its receptor has a role in increasing the excitability of spinal neurons via a mechanism including SGCs and glutamate (Ferrari et al., 2014);
- *upregulation of spinal dynorphin*: the release of this peptide expressed in spinal interneurons of lamina I and II is enhanced in inflammatory condition via descending facilitatory mechanism. The pronociceptive role of dynorphin was highlighted also by the potentiation of CGRP-evoked release, mechanism linked to the enhancement of afferent nociceptive input (Gardell et al., 2003a).

At the cellular level, diabetes induces the disruption of several important metabolic and intracellular pathways (Giacco and Brownlee, 2010). For example, the alteration of the polyol pathway, which reduces glucose into sorbitol and, then, in fructose, oxidizing NADPH and NADH. In diabetic condition, the decrease levels of NADH and NADPH prevent the synthesis of many protective substances, such as myo-inositol, required for nerve activity, and of scavengers of reactive oxygen species (Giacco and Brownlee, 2010). Moreover, glucose reduction products can bind in a non-enzymatic way proteins and lipids, producing advanced glycation end-products. Glycation can alter the function of involved proteins, as laminin, collagenase and fibronectin, essential for nerve regeneration. The result of this aberrant mechanism is the induction of oxidative stress, cytokines secretion, extracellular matrix degradation and inflammatory pathway activation (Nascimento et al., 2016). In addition, high blood glucose level promotes a dramatic activation of protein kinase C (PKC), which increases radical oxygen species, apoptosis, accumulation of matrix and inhibition of NO production (Giacco and Brownlee, 2010). A common point of the previous alterations is the

mitochondrial reactive oxygen species production: intracellular hyperglycemia increases the voltage across the mitochondrial membrane, preventing the formation of superoxide and causing the accumulation of oxygen radicals. Upstream, there is the inhibition of the key glycolytic enzyme glycerldehyde 3-phosphate dehydrogenase (GAPDH), which catalyzes the glycolysis steps and breaks down glucose for energy and carbon molecules. If GAPDH is impaired, all the intermediates levels of glycolysis increase, causing the impairment described above in this paragraph (Giacco and Brownlee, 2010).

1.3.2 ANIMAL MODELS OF DIABETIC NEUROPATHY

As endocrine disorders, T1D and T2D outline quite a complex disease, involving several bodily systems. Considering that, animal models should be chosen carefully, depending on which aspects of the disease is going to be investigated. Most of the experiments are performed on rodents, even if some studies still recur to larger animals. In most of the cases, diabetes is chemically- or nutritionally-induced to allow reproducible laboratory conditions and unambiguous diabetic phenotype. In other studies, diabetic-induced alterations are studied in spontaneous occurring animal models of T1D and T2D, which may more accurately mimics some aspects of human pathology (see Table 1.1 and Table 1.2 modified from Rees and Alcolado, 2005; King, 2012). In the last years, molecular biological techniques have helped to develop a large number of new models for the study of diabetes as knock-in, generalized knock-out and tissue-specific knock-out (Rees and Alcolado, 2005).

TABLE 1.1 Animal models of type 1 diabetes (T1D).

Induction mechanism	Model	Main features
Chemical Induction	High dose STZ	Simple model of hyperglycemia
	Alloxan	
	Multiple low dose STZ	Model of induced insulitis
Spontaneous autoimmune	NOD mice	B cells depletion
	BB rats	
	LETL (Long Evans Tokushima lean) rat	
Other animal species	New Zealand white rabbit	
	Keeshond dog	
	Celebes black ape	

TABLE 1.2 Animal models of type 2 diabetes (T2D).

Induction mechanism	Model	Main features
Obese models (monogenic)	Ob / Ob mouse— (leptin deficient) db / db mouse— (leptin resistant) Zucker (fa / fa) rat— (leptin resistant) NSY mouse AKITA mice	Obesity-induced hyperglycemia
Obese models (polygenic)	KK mouse OLETF rat NZO mice TallyHo/Jng mice NoncNZO10/LtJ mice	Obesity-induced hyperglycemia
Induced obesity	High fat feeding Israeli sand rat Fat-fed streptozotocin-treated rat	Obesity-induced hyperglycemia
Non-obese model	Goto Kakizaki rat	Hyperglycemia induced by insufficient β cell function/mass
Spontaneous model	CBA/Ca mouse Diabetic Torri rat New Zealand obese mouse	Obesity-induced hyperglycemia

Mouse models provide fundamental tool to study pathogenesis, prevention and treatment of diabetes-related complications, as DPN. Their main advantages are the lower cost, the ease of genetic manipulation and the simple breeding. To minimize inter-investigator variability, standardize phenotyping and diabetic-assessment protocols, but also identify novel animal models,

NIH formed the Diabetic Complications Consortium (DiaComp). DPN phenotyping protocols check behavioral responses, nerve conduction velocity (NCV) and anatomical alterations. The analysis of behavioral responses to thermal or mechanical stimuli allows to assess allodynia, hyperalgesia or hypoalgesia: regarding thermal alterated sensitivity, tail-flick and thermal hindpaw withdrawal tests are recommended, while for mechanosensory alterations the Von Frey filaments and the mechanical hindpaw withdrawal. The analysis of NCVs allows to assess the nerve function and represents the gold standard for identifying electrophysiological neuronal impairments. Instead, analysis of anatomical alterations may concern the intraepidermal nerve fiber densities (IENFD), which is a marker of small-sized fibers alterations. In addition, it is important to assess the metabolic phenotype through body weight, fasting blood glucose level and impaired glucose tolerance (O'Brien et al., 2014). Of course, the analysis could be deeper and also consider glycated hemoglobin, plasma insulin, cholesterol and triglycerides levels.

1.3.2.1 MURINE MODELS OF T1D

Streptozotocin-induced diabetes. STZ is a broad-spectrum antibiotic produced by *Streptomyces achromogenes*, it has a structural similarity with glucose and is taken up by pancreatic β cells via glucose transporter 2, causing the death of the cells by DNA fragmentation and impairment of glucose transport (Ventura-Sobrevilla et al., 2011). DiaComp recommends to induce hyperglycemia with a single high dose of STZ (SHD; approximately 150 mg/kg) or multiple low doses (MLD; 50 mg/kg/day for 5 days). Both protocols cause diabetes and the development of neuropathic phenotype, but some crucial differences exist:

i) the SHD-STZ model induces a severe neuropathy lasting until 12 weeks after injection and is characterized by variable alterations of sensory profiles including increased thermal latency and decreased mechanosensitivity, NCV and IENFD (Ventura-Sobrevilla et al., 2011). However, a high toxicity and in some cases mortality escorts this approach;

ii) the MLD-STZ model is less toxic, with a gradual death of β cells, increase of glycemia and lymphocytic pancreatic infiltration, which mimic the human pathology. However, this model shows moderate or absent neuropathy (McEvoy et al., 1984).

Spontaneous nonobese diabetic mice (NOD mice). NOD mice present an heritable polygenic immunodeficiency against β cells, mediated by CD4+ and CD8+ T cells, that causes a diabetes similar to the human one at around 4 weeks of age (Pearson et al., 2016). Given the polygenic basis of this model, the development of diabetes is susceptible of variations. Thus, some studies showed

that hyperalgesia developed around 8 weeks of age and hypoalgesia at 12 weeks (Gabra and Sirois, 2005).

Akita (B6Ins2^{Akita}) mice. Akita mice model is characterized by a point mutation of *Ins2* insulin gene, which causes an impaired insulin secretion and a subsequent hyperalgesia. The diabetic phenotype starts to develop at 7 weeks of age with a reduction of the NCV around 16 weeks of age, even if the DPN faces a slow progression (Sullivan et al., 2008).

"Humanized mouse" model. New models have been recently developed to mimic the human pathologies more accurately. An example for type 1 DM is the development of a "humanized mouse": immunodeficient mice were engrafted with human β cells and components of immune system, in order to reproduce the environment of type 1 diabetic patients (Brehm et al., 2012).

1.3.2.2 MURINE MODELS OF T2D

Monogenic obesity models. Spontaneous models of type 2 DM are often based on monogenic modifications that impaired leptin signaling and produce a severe nerve deficit. Leptin is a hormone secretes by adipocytes after meals and influences appetite by hypothalamic signaling. Monogenic modifications can be against leptin itself (ob/ob mice) or against its receptor (db/db mice), causing an impairment of leptin action and the induction of a diabetic metabolic profile after the development of hyperphagia and consequent obesity, hyperglycemia and hyperinsulinemia. Db/db mice develop diabetes at 4 weeks of age, bypassing prediabetic stage, and develop hyperalgesia and allodynia between 8 and 12 weeks of age, with severe sensory and motor NCV deficits and morphological alterations (Sullivan et al., 2007). Ob/ob mice are a mild type of type 2 DM and are considered a typical model of obesity and hypoalgesia. They develop impairments of motor and sensor NCV around 11 weeks of age, showing chronic hyperglycemia, thermal hypoalgesia and tactil allodynia (Drel et al., 2006).,

Polygenic obesity models. KKmice, NZO mice, TallyHo/Jng mice, NoncNZO10/LtJ mice are a variety of different polygenic models for obesity, glucose intolerance and diabetes. Unlike the monogenic models, there are no wild-type controls (Leiter, 2009)

Diet-induced models. Mice develop obesity after a high-fat diet and show a gradual onset of metabolic alterations, mimicking human pathology. They exhibit prediabetes features as weight gain, increased adiposity, mild hyperinsulinemia, impaired glucose tolerance and normoglycemia. Although the lacking of frank hyperglycemia, these mice display increased sorbitol pathway activity in the peripheral nerve, as well as oxidative stress, accumulation of DNA damage and a

prolonged inflammatory response in peripheral nerve and DRG neurons. Notably, a 6-weeks feeding with normal fat diet after 16 weeks on high fat diet reduced tactile allodynia and essentially corrected thermal hypoalgesia and sensory nerve NCV deficit (Obrosova et al., 2007). Diet-induced mice are employed as model for neurologic pathophysiology related to prediabetes (O'Brien et al., 2014).

See Table 1.1 and Table 1.2 for a summary of the main advantage and disadvantages of the above models.

1.4 NEUROTROPHIC FACTORS IN NOCICEPTIVE TRANSMISSION AND PATHOLOGICAL PAIN

Neurotrophic factors are a group of molecules supporting growth, survival, and differentiation of both developing and mature neurons. They are classified into three main families: the neurotrophin family, the GDNF family and the CNTF family (Connor and Dragunow, 1998). Here will be discussed more in detail the first two families (Figure 1.14; Boucher and McMahon, 2001), being strictly implicated in the survival of sensory neurons during the development (Fariñas et al., 1994; White et al., 1996; Molliver et al., 1997a; Marmigère and Ernfors, 2007), in the regulation of physiological properties during adulthood as well as in pathological conditions (Bardoni and Merighi, 2009; Bardoni et al., 2007; Ernfors et al., 1994; Lewin et al., 1994; Trupp, 1999).

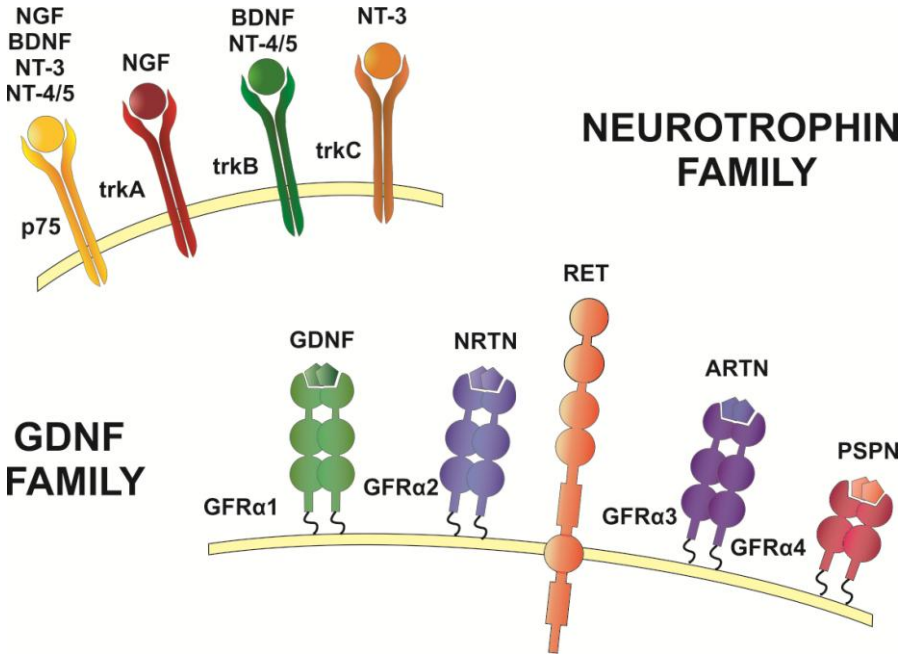

FIGURE 1.14 NEUROTROPHIN AND GDNF FAMILIES OF NEUROTROPHIC FACTORS.
Top Neurotrophin family ligands bind to specific Trk receptors, while all bind p75 receptor, resulting in their dimerization. Each receptor can activate different signaling pathways. **Bottom** Glial cell line-derived neurotrophic factor (GDNF) ligands activate several intracellular pathways via the signal transducer Ret after binding the specific GDNF-family receptors-α (GFRα). NGF, nerve growth factor; BDNF, brain-derived neurotrophic factor; NT-3/4/5, neurotrophin 3/4/5; NRTN, neurturin; ARTN, artemin; PSPN, persephin.

The **Neurotrophin family** is composed by nerve growth factor (NGF), brain-derived neurotrophic factor (BDNF), neurotrophin-3 (NT-3) and neurotrophin-4/5 (NT-4/5).

NGF. NGF promotes the survival of DRG neurons during both development and adulthood, by binding the high-affinity receptor trkA and/or the low-affinity receptor p75. The binding of trkA by NGF induces the dimerization and the phosphorylation of the receptor, with the consequent activation of the PI3K/Akt and the MEK/MAP enzymatic cascades, controlling neural survival and neurites growth. Experiments performed on NGF-null and trkA-null mice showed a critical reduction of different neurons, among which the sensory neurons, as well as an impaired phenotypic differentiation and a defective cutaneous innervations, proving the absolute need of NGF during development (Barde et al., 1982).

Although NGF appears to be fundamental for DRG neuron development, many studies proved its functional role in nociception and in the development of chronic pain. Specifically, *in vivo* injections of NGF are directly responsible for the induction of thermal and mechanical hyperalgesia both in rats and mice (Lewin et al., 1993; Malin et al., 2006). NGF causes sensitization of TRPV1 cation channel (Shu and Mendell, 2001), that under normal condition tends to desensitize after repeated activation. This sensitization is due to different mechanisms: trkA activation by NGF activates numerous kinases, such as tyrosin kinase Src via PI3 kinase, serine/threonine kinases PKC (Bhave et al., 2003), PKA (Shu and Mendell, 2001) and calcium/calmodulin-dependent kinase II (Shu and Mendell, 2001), inducing the phosphorylation and the consequent induction of TRPV1 Ca^{2+} transients (Zhang et al., 2005). In addition, trkA activation causes the depletion of phosphatidylinositol-4,5-biphosphate (PIP_2) via phospholipase Cγ (PLCγ) which is an inhibitor of TRPV1, determining the loss of an endogenous regulatory mechanism (Prescott and Julius, 2003). NGF administration also increases expression of TRPV1 (Donnerer et al., 2005) and its insertion to the plasma membrane (Zhang et al., 2005). Eventually, NGF also recurs to bradykinin intracellular pathway, a mediator of sensitization able to reduce the heat threshold of TRPV1 (Cesare et al., 1999). The partial denervation of peripheral tissue causes the increased availability of NGF in the target site for remaining uninjured afferents, producing an ectopic activity generation (Ali et al., 1999). All together these mechanisms cause an increased activity of TRPV1 in sensory neurons, with the additional release of excitatory mediators such as SP and CGRP, that potentially contribute to hyperalgesia (Lewin et al., 1994).

BDNF. BDNF exerts its trophic and neuromodulatory effects by acting on the high-affinity specific receptor trkB (Middlemas et al., 1991; Kaplan and Stephens, 1994). Under physiological

conditions, it is mainly synthesized in primary sensory neurons and released in an activity-dependent manner at the spinal cord level through anterograde transport (Michael et al., 1997). The modality of transport and release are similar to those observed for conventional neurotransmitters, thus suggesting a role for BDNF as neuromodulator (Merighi et al., 2008a; Merighi, 2016). In small and medium size peptidergic neurons this neurotrophin co-localizes with CGRP (41%; Salio and Ferrini, 2016) and trkA (21%; Merighi et al., 2008), while just 10% of DRG neurons are BDNF+/trkB+ and trkA- (Salio et al., 2005). To verify the precise peptidergic expression of BDNF, Salio and Ferrini (2016) characterized the relationship of this neurotrophic factor with peptidergic markers SP and STT (Salio and Ferrini, 2016): around 40% of BDNF+ neurons also express SP and, considering that SP+ population is a subset of CGRP expressing neurons, this 40% should be BDNF/SP/CGRP+ (Salio et al., 2005). Conversely, no co-expression was found between BDNF and STT (Salio and Ferrini, 2016). A significant number of BDNF+ neurons appear in neither peptidergic nor non-peptidergic, suggesting the expression of this neurotrophic factor in non-nociceptive populations too (Salio and Ferrini, 2016). In physiological conditions, BDNF is stored with SP and CGRP in the central primary afferent terminals in the spinal dorsal horn (Salio et al., 2005), and once released, induces an increase of glutamatergic NMDA-mediated EPSCs in spinal neurons (Merighi et al., 2008b). In presence of thermal, mechanical or chemical noxious stimulation, BDNF receptor trkB phosphorylation is increased, activating intracellular signals transduction as MAP kinase pathway, which may induce long-term plasticity (Pezet et al., 2002). TrkB receptor is expressed both on post- and pre-synaptic terminals in lamina II (Salio et al., 2005), where it induces channel properties modifications, as increasing opening time or enhancing transmitters release (Merighi et al., 2008a). Moreover, BDNF may also have indirect inhibitory effects, being trkB expressed on GABAergic terminals of some inhibitory interneurons in lamina II, where its activation increases the spontaneous release of GABA and glycine (Bardoni et al., 2007)
However, the role of BDNF in neuropathic pain has been debated in past studies, due to its multiple mechanisms of action (Merighi et al., 2008a).

By using conditional knock-out mice to block the expression of BDNF in nociceptive sensory neurons, Zhao et al. (2006) assessed that BDNF play a key role in the development of inflammatory pain and secondary hyperalgesia, rather than chronic neuropathic pain. On the other hand, BDNF released from spinal microglia in neuropathic pain was found to cause pain hypersensitivity by disrupting synaptic inhibition onto lamina I neurons (Coull et al., 2005).

NT-3. NT-3 has a fundamental role in promoting survival of sensory neurons during development and neurites sprouting (Wang et al., 2015), by acting through its high-affinity receptor trkC. TrkC is mainly expressed in large-sized myelinated neurons (Wang et al., 2015) and the bound with NT-3 elicits mechanical hypoalgesia and inhibits SP release (Malcangio, 1997), which is not induced in neuropathic condition (Boucher et al., 2000). NT-3 seems to exert an anti-nociceptive effect in neuropathic pain processing, reducing the expression of pain-related channels as Nav1.8, Nav1.9 (Wilson-Gerwing et al., 2008) and TRPV1 in small-sized neurons (Wilson-Gerwing et al., 2005). The mechanism underlying this inhibition is not fully understood, because small-sized neurons usually do not express NT-3 receptor trkC. An hypothesis is that, under inflammatory condition, low affinity binding of NT-3 with trkA exerts a major effect on these neurons (Kullander and Ebendal, 1994).

NT 4/5. NT4/5 is a member of neurotrophin family, which preferentially binds trkB and regulates survival and differentiation of neurons (Berkemeier et al., 1991). It has a role in supporting a subclass of cutaneous sensory afferents, D-hair receptors, which are the terminal ending of Aδ fibers surrounding the base of hair (Stucky et al., 1998). These neurons account for just 5% of the total DRG neurons (Airaksinen et al., 1996). In mice NT-4/5 $^{-/-}$, a selective loss of small-sized neurons, electrophysiologically identified as D-hair receptors, was observed, suggesting that this neurotrophic factor and BDNF, even sharing the same receptor, act on different neuronal populations (Carroll et al., 1998). In addition, it seems that NT-4/5 (unlike other neurotrophins), requires the binding of the low affinity receptor p75 for a correct signaling via trkB (Rydén et al., 1995). Repeated injections of a specific antibody against NT-4/5 failed to reverse the thermal hyperalgesia in a model of sciatic nerve ligation, effect contrary compared to the abolition obtained with BDNF, demonstrating that the bound of NT4/5 to trkB activates a different signal transduction pathway, Shc/ERK in turn of Ras/MAPK, which is not involved in nociceptive transmission (Minichiello et al., 1998).

The **GDNF family** is part of the transforming growth factor β (TGF-β) superfamily and comprises GDNF, neurturin, persephin and artemin. These growth factors share the mechanism of signaling by binding a receptor complex composed by the tyrosine kinase transmembrane receptor Ret and the glycosylphosphatidylinositol (GPI)-anchored co-receptors that, depending on the ligand, are known as GFRα1 (GDNF), GFRα2 (neurturin), GFRα3 (artemin) and GFRα4 (persephin).

GDNF. Since the identification in 1993 (Lin et al., 1993), GDNF has shown to be responsible of an impressive number of effects on the nervous system. GDNF has survival effects on

dopaminergic (Lin et al., 1993) and motor neurons (Henderson et al., 1994), as well as on IB4+ sensory neurons in DRGs (Fjell et al., 1999). *In vivo*, GDNF has a neuroprotective role and normalizes nociceptors physiology after injury, as ameliorating the reduction in conduction velocity of C type fibers (Bennett et al., 1998) and restoring the expression of specific markers and receptors (IB4 binding, expression of STT, CGRP and P2X3; Figure 1.15 B; Bennett et al., 1998).
GDNF, as BDNF, is synthesized and anterogradely transported to the dorsal horn by peptidergic sensory neurons (Ohta et al., 2001). GDNF and BDNF are expressed by distinct DRG neuronal populations (Figure 1.15 A), with the one expressing GDNF smaller than that expressing BDNF (Salio and Ferrini, 2016). In particular, almost all GDNF+ neurons also co-express CGRP, around 68% are also STT+, while no one co-express SP. Thus, GDNF, CGRP and SST are expressed in a subpopulation of peptidergic neurons, phenotipically distinct from that containing BDNF/SP/CGRP. Interestingly, IB4+ neurons did not co-localize with BDNF or GDNF but express the complex receptor for GDNF GFRα1/Ret, which inhibits the release of glutamate on lamina II neurons, exerting a inhibitory effect of nociceptive signaling transmission (Bencivinni et al., 2011; Salio et al., 2014). Functionally, GDNF preferentially binds GFRα1 (even if it also shows a weak affinity to GFRα2) increasing the affinity of this co-receptor for Ret and inducing its dimerization. Ret is thus activated via autophosphorylation of tyrosine residues, inducing the activation of different signaling pathways as MAPK (ERK1/2), PI3K and PLCγ (Figure 1.15 B; Carnicella and Ron, 2009). These pathways are the same activated by the trk family, confirming a commonality of mechanisms among neurotrophic factors.

The role of GDNF in modulating pain mechanisms is still controversial as both pronociceptive and antinociceptive roles were described, depending on the type of pain condition (inflammatory vs neuropathic), the stimulus induced (mechanical, thermal, and noxious) and the peripheral area innervated (skin, muscle; Fang et al., 2003; Wang et al., 2003a; Malin et al., 2006; Boucher et al., 2000; Malcangio et al., 2000; Salio et al., 2014; Merighi, 2016).

Depending on the nature of the animal model, some investigations have shown a decreased GDNF expression in the delayed arthritis model (Fang et al., 2003) while others an increase in the sciatic nerve injury (Hammarberg et al., 1996). It is important to notice that, in the latter case, the upregulation is in the proximal and in the distal trunk nerve, but not in DRG neurons, suggesting a role of Schwann cells in the GDNF enhanced expression (Höke et al., 2000). Conversely, other studies on neuropathic pain highlighted both a decrease (Nagano et al., 2003) or an increase

(Amaya et al., 2004) of GDNF expression. An hypothesis is that the downregulation of GDNF acts as a compensatory mechanism to reduce the inflammation pain (Fang et al., 2003).

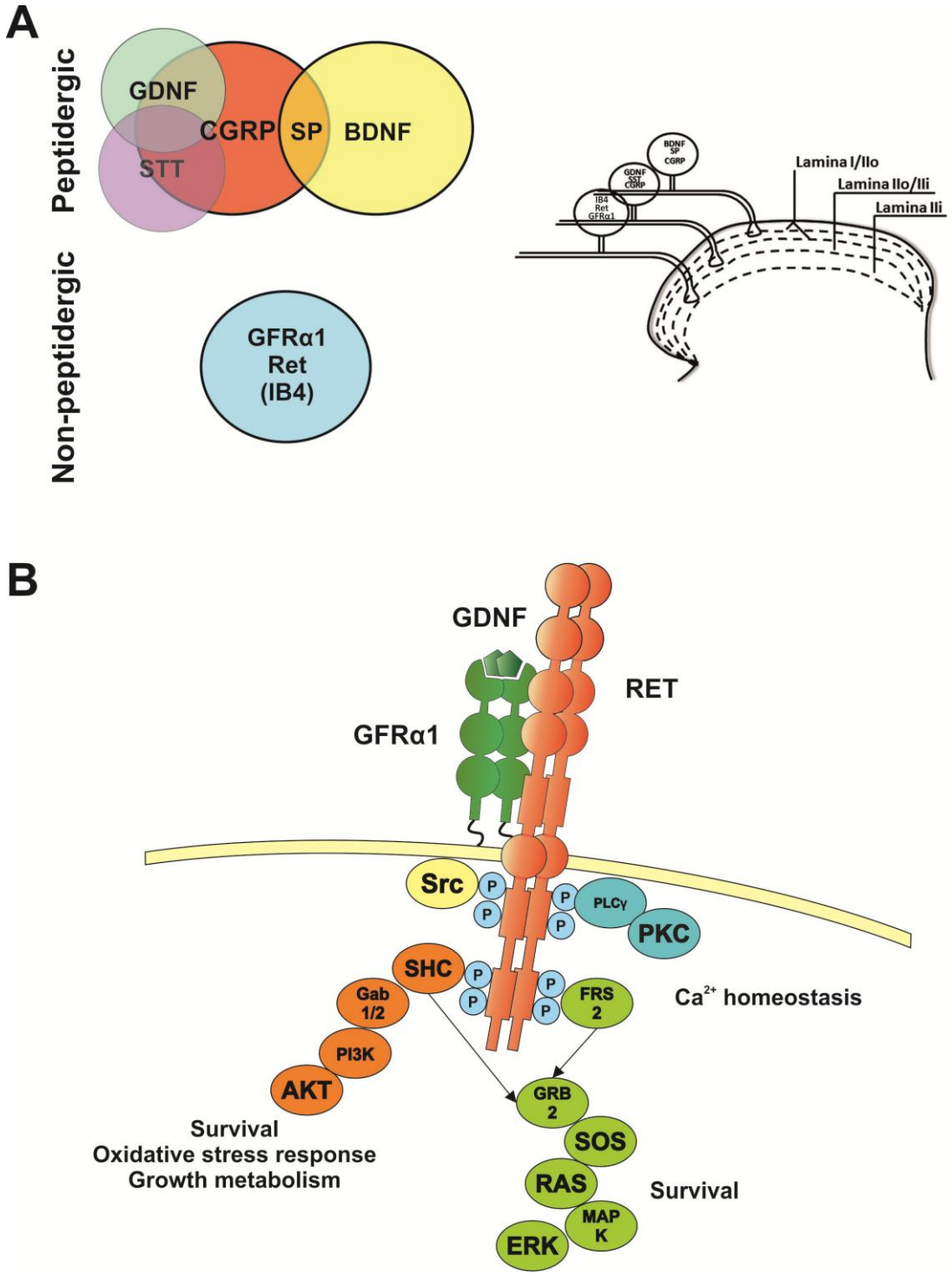

FIGURE 1.15 DIFFERENT POPULATIONS OF SENSORY NEURONS AND GDNF SIGNALING NETWORK **A** Venn diagram of different sensory neurons populations in DRG, based on neurotrophic and peptidergic content (modified from Salio and Ferrini, 2016). **B** GDNF binding to GFRα1 receptor activates different signaling pathways via Ret tyrosine kinase transduction: Ras/ERK, PI3K/Akt, Src and PLCγ/PKC. Each of them regulates diverse processes as differentiation, survival, oxidative stress response, Ca^{2+} homeostasis and growth metabolism.

Regarding the **pronociceptive** role, GDNF was able to increase the expression of pain-related receptors such as TRPV1 in rat DRGs (Ogun-Muyiwa et al., 1999), while in mouse DRGs this effect was not observed because TRPV1 is not expressed on GDNF-sensitive neurons (Zwick et al., 2002). Different mechanisms may underlie the enhancement of TRPV1, as the activation of the MAP/ERK pathway (Bron et al., 2003), with a subsequent expression of novel receptors, or the upregulation of transcripts Nav1.8/Nav1.9, which can cause a depolarizing shift in the membrane and thus facilitating the voltage-dependent component of activation (Gomtsyan and Faltynek, 2010). In addition, a study on a Nav1.8-null model showed that GDNF administration induces a strong increase in Nav1.9 conduction, the main Na^+ channel in IB4+ neurons. Consistent with this result, NGF exerted a major effect on Nav1.8, which is predominant in IB4- neurons (Cummins et al., 2000). Further mechanisms involve the upregulation of the ATP receptor P2X3 (Bradbury et al., 1998), the increased release of CGRP at the dorsal horn level in non-trkA neurons (Ramer et al., 2003) and the expression of SP (Ogun-Muyiwa et al., 1999)

Regarding the **antinociceptive** role, most of the literature reports antihyperalgesic effects of GDNF, particularly in neuropathic pain models. The underlying mechanism of these effects are not entirely understood, but may imply a control of sodium channel phenotype in sensory neurons (Boucher et al., 2000), an increase in the release of endogenous STT (Malcangio et al., 2002), the reduction of glutamate release from primary afferent in the dorsal horn (Salio et al., 2014). In general, GDNF can be considered as a neuroprotector that acts to reverse the morphological, metabolic and biochemical changes following peripheral nerve injuries (Wang et al., 2003). Indeed, intrathecal administration of GDNF in a model of neuropathy preserved the loss of IB4 binding, both on the soma and on the peripheral end, suppressed the expression of the transcription factor ATF3 and of TTX-S Nav1.3, blocked upregulation of pain-related galanin and NPY, thus preventing the development of thermal and tactile impairment (Wang et al., 2003). Furthermore, delayed administration of GDNF in a model of partial sciatic ligation reversed the mechanical and thermal hyperalgesia for the length of administration (Boucher et al. 2000). Importantly, GDNF was found to have protective role and restore a normal nociceptive behavior also in diabetes-induced peripheral neuropathy (Hedstrom et al., 2014; Peeraer et al., 2011). The antinociceptive effect was specifically replicated by a GFRα1 agonist topically delivered on diabetic mouse skin (Hedstrom et al., 2014).

Neurturin. Neurturin exerts its action via Ret kinase and GFRα2 on IB4+ primary sensory neurons (Kotzbauer et al., 1996). Electrophysiological analysis showed that neurturin/GFRα2 signaling is involved in pain signal transduction of noxious heat but not mechanical stimuli (Stucky

et al., 2002). Even if GDNF binds with low affinity GFRα2, it is not able to substitute neurturin in supporting GFRα2-expressing cells (Heuckeroth et al., 1999). In neuropathic background, neurturin level are reduced, suggesting an antinociceptive role (Merighi, 2016).

Artemin. Artemin selectively binds the high affinity receptor GFRα3 (Baloh et al., 1998). GFRα3 is mainly found in peptidergic TRPV1+ neurons and rarely in non-peptidergic IB4+ one (Orozco et al., 2001). Its main role seems to be the modulation of response properties of certain sensory neurons, rather than neuronal survival and growth (Elitt et al., 2006). Artemin induces both pro- and antinociceptive effects: systemic delivery of artemin reduces both mechanical and thermal hypersensitivity in a model of neuropathic pain (Gardell et al., 2003b), but over-expression of artemin induced sensitization of nociceptors via upregulation of TRPV1 (Elitt et al., 2006).

Persephin. Persephin acts via the GFRa4 receptor on CNS and kidney, but not on peripheral neurons (Milbrandt et al., 1998).

1.5 AIMS OF THE THESIS

Mechanisms underlying diabetic neuropathic pain and the involvement of DRG neurons have been extensively studied, from physiological and molecular alterations to morphological impairments. Despite this, limited advancements have been made in the treatment of this pathological condition and a number of functional aspects remain to be understood. Several lines of evidence suggest that GDNF receptor agonists may represent an effective therapeutic tool for counteracting altered nociception in neuropathic pain, although the role of neurotrophic factor in nociception is controversial and may vary, depending on the biological context, from anti-nociceptive to pro-nociceptive.

The experiments performed and described in this thesis were aimed to give a contribution in understanding the type of alterations caused by diabetes in DRG sensory neurons, both at a functional and morphological level. The study was performed in a whole-mount preparation of DRGs from both control mice and mice with streptozotocin-induced type 1 diabetes. Using intact DRGs allowed, in fact, to analyze functional and phenotypical properties of sensory neurons at the single cell level by preserving at the same time the structural organization of DRGs *in vivo.*

The aims of my investigation were:

- to study the morphological and cytoarchitectural alterations in DRGs in a mouse model of type I diabetes;
- to assess the functional alterations induced by diabetes in specific populations of sensory neurons;
- to analyze the effect of GDNF in the modulation of cell excitability of nociceptors under control and diabetic conditions.

2 MATERIALS AND METHODS

2.1 ANIMALS

Male CD1 mice (20-30 g) were housed in a controlled environment maintained on a 12/12 hour light/dark cycle with food and water ad libitum. To induce diabetes, animals were injected with one single intraperitoneal injection of streptozotocin (STZ, 150 mg/Kg; Sigma, St. Louis, MO, USA) at P30. STZ was freshly dissolved in 0.1M citrate buffer (pH 4.5), while control mice received buffer only. Four weeks after injection, glycemia was measured in 5 hours fasted animals following tail venipuncture using a glucose oxidase impregnated test strip (Glucocard sensor, Menarini, Firenze, Italy). Only mice with glucose concentration higher than 300 mg/dl were considered diabetic and used for the experiments.

2.2 ETHICS

All experimental procedures were approved by the Italian Ministry of Health and the Committee of Bioethics and Animal Welfare of the University of Torino. Animals were maintained according to NIH Guide for the Care and Use of Laboratory Animals.

2.3 INTACT DORSAL ROOT GANGLION (DRG) PREPARATION

All the experiments presented in this thesis were performed on entire dorsal root ganglia following a new approach published in Ciglieri et al.(2016) and summarized in Figure 2.1.
For preparation of intact DRGs, 2 month-old CD1 mice (CTR n=76, DIAB n=67) were anesthetized with a lethal dose of sodium pentobarbital (30 mg/kg, intraperitoneal). DRGs dissection was performed by constantly maintaining the tissues in ice-cold cutting solution, containing: sucrose 252 mM, KCl 2.5 mM, $NaHCO_3$ 26 mM, NaH_2PO_4 1.25 mM, D-glucose 10 mM, kynurenate 1 mM, $MgCl_2$ 3 mM, $CaCl_2$ 1.5 mM, saturated with 95% O_2-5% CO_2. DRGs were removed after cutting the spinal column along the midline; then, they were incubated for 1 h at 37°C in constantly oxygenated aCSF containing collagenase (7 mg/mL, collagenase type 3; Worthington, NJ, USA) to degrade the outer connective layer.

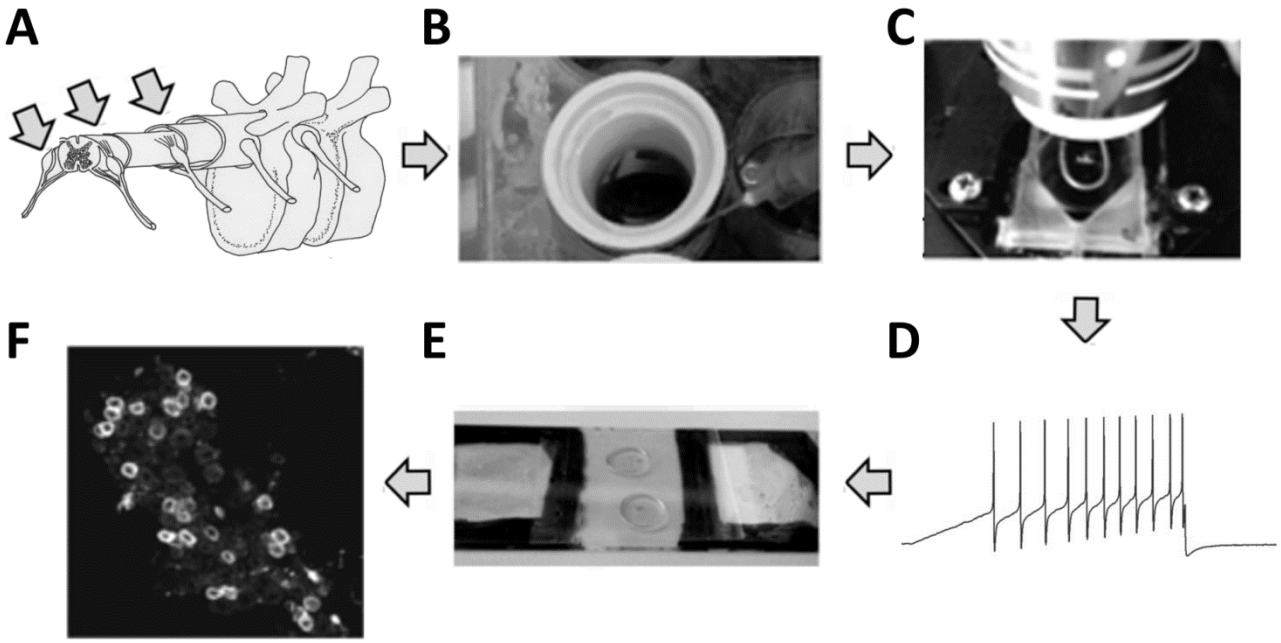

FIGURE 2.1 GRAPHIC REPRESENTATION OF THE METHOD ADOPTED.
Spinal column was cut along the midline and DRGs (**A** arrows) were harvested and incubated in constantly oxygenated aCSF in presence of collagenase (7 mg/mL), to remove the outer connective layer (**B**). After incubation, DRGs were placed in the recording chamber (**C**) and electrophysiologically recorded (**D**). Afterwards, DRGs were fixed in 4% PFA, processed for fluorescent labeling and mounted with an anti-fade mounting medium on *ad hoc* modified slide to preserve their volume (**E**). Eventually, z-stacks were collected with a confocal microscope (**F**).
From *"An improved method for in vitro morphofunctional analysis of mouse dorsal root ganglia"*, Ciglieri et al. (2016).

2.4 ELECTROPHYSIOLOGICAL RECORDING

Whole-cell current clamp and voltage-clamp recording experiments were performed at room temperature (23-25°C). After incubation, each ganglion was transferred into a recording chamber through which artificial cerebrospinal fluid (aCSF) was constantly perfused (2 mL/min) at room temperature (RT). aCSF was constantly bubbled with 95% O_2 – 5% CO_2 and contained: NaCl 126 mM, KCl 2.5 mM, D-glucose 10 mM, $NaHCO_3$ 26 mM, NaH_2PO_4 1.25 mM, $CaCl_2$ 2mM, $MgCl_2$ 1.5 mM. For isolating potassium conductances and blocking voltage gated Ca^{2+} channels, aCSF was replaced with ChCL-aCSF, containing 126 mM choline chloride, 2,5 mM KCl, 1,5 mM $MgCl_2$, 2 mM $CaCl_2$, 0.5 CdCl, 10 mM Hepes, 10 mM glucose, 11 mM sucrose, pH 7.4 with KOH, and constantly oxygenated with 100% O_2. Neurons were visualized using a fixed stage microscope (Eclipse FN-1; Nikon inc, Melville, NY, USA) equipped with infrared gradient contrast optics and a 16x water immersion objective (Nikon) and with an infrared-sensitive CCD camera (W118C; Watec Corp., Yamagata, Japan). Patch-clamp whole-cell recordings were obtained with a Multiclamp 700B amplifier (Molecular Devices, Sunnyvale, CA, USA) connected to a Digidata

interface (Digidata 1440A; Axon Instruments, Union City, CA, USA), sampled at 10 kHz and filtered at 10 kHz. Signals were recorded and stored using pCLAMP 10.2 (Molecular Devices, Sunnyvale, CA, USA). Patch pipettes were prepared using a horizontal puller (MP225; Sutter, Novato, CA, USA). Pipette resistances were around 5 MΩ. In current clamp experiments, intracellular solution contained: K gluconate 135 mM, KCl 5 mM, HEPES 10 mM, ATP-Na 4 mM, GTP-Na 0.4 mM, $MgCl_2$ 2 mM, pH 7.2 (with KOH). In voltage clamp experiments, EGTA 5 mM was added to the solution. Liquid junction potential at 25°C was 15.2 mV and 14.8 mV, respectively and was corrected offline. To allow post-recording visualization of recorded neurons, 20 µM of Alexa Fluor 568 (Thermo Fisher Scientific, Waltham, MA, USA) was added to the intracellular solution.

Recordings were included for the subsequent analysis only if: (i) membrane potential was more negative than -50 mV; (ii) access resistance changed less than 20% throughout the recording session.

In current clamp, passive and active neuronal properties were recorded. Firing was obtained by applying two different current clamp protocols: a ramp protocol, which consists in a single injection of current for 500 ms ranging from 0 nA to 1 nA; a step protocol, which consists in 12 injections of current of 20 pA in increasing steps lasting for 500 ms. Both protocols were applied from the voltage membrane $V_m$of each neurons, set at the beginning of the recording.

In voltage clamp, 3 step protocols were applied:

- a hyperpolarizing protocol in which the holding potential was fixed at -50 mV and neurons were hyperpolarized to -130 mV in -10 mV incrementing steps, with 500 ms in duration;
- a depolarizing protocol in which each neuron was kept at a holding potential of -80 mV and depolarized to -30 mV in 10 mV incrementing steps, with 500 ms in duration;
- a depolarizing protocol in which the holding potential was fixed at -80 mV and currents were elicited between -130 mV and +50 mV in 20 mV depolarizing steps, with a duration of 200 ms, after a 20 ms pre-pulse at -100 mV.

To examine K^+ current, the following step protocols were applied in presence of ChCl-aCSF:

- a hyperpolarizing protocol (as above);
- a depolarizing protocol in which, after a pre-pulse of 1 s at -100 mV, a test pulse was elicited from -60 to +50 mV in 10 mV increments to investigate the total Kv current;
- a depolarizing protocol in which, after a pre-pulse of 1 s at -40 mV, a test pulse was elicited from -60 to +50 mV in 10 mV increments to investigate sustained Kv current.

The transient Kv current was obtained by subtracting sustained Kv current from total Kv current (Tang et al., 2016).

2.5 ELECTROPHYSIOLOGICAL DATA ANALYSIS

Electrophysiologically recorded neurons were classified based on the size in small (diameter <25 µm) or medium-to-large (diameter >25 µm; Barabas et al., 2014) neurons. Moreover, some recorded neuron were also injected with 20 µM of Alexa Fluor 568 and phenotypically identified as IB4+ or CGRP+ by immunofluorescence after fixation (see below). In current clamp experiments, the identity of recorded neurons as IB4+ or IB4- cells was assessed based on functional criteria previously proposed by Choi et al. (2006). Briefly, the firing discharge following a ramp current in IB4- neurons produces a higher number of action potentials (APs) with a slower decrease of peak amplitude during the stimulation; conversely, IB4+ exhibits stronger adaptation and reduced number of APs. Passive membrane properties were analyzed with Clampfit software (Molecular Devices) and include: resting membrane potential (Vm), membrane capacitance (Cm), input resistance (Rin).

AP properties were analyzed with Stimfit Software analysis (courtesy of C. Schmidt-Hieber; http://www.stimfit.org; Guzman et al., 2014) and the following measurements were obtained: AP threshold (defined as the point of depolarization at which an AP is generated), rheobase (the minimum amount of current to trigger a AP), latency (time from the beginning of the depolarizing step to AP), AP width (defined as the duration of an AP measured at half-maximal amplitude), AP overshoot (peak measured from 0 mV), AP afterhyperpolarization amplitude, maximum rise slope (defined as the maximum value of the slope in the rising phase of an AP), time of maximum rise slope (defined as the time needed to reach the maximum rise slope), rise time 20-80% (defined as the time needed by an AP to pass from the 20% to the 80% of the rising phase), maximum decay slope (defined as the maximum value of the slope in the falling phase of an AP). When multiple APs were generated during ramp or step stimulation, AP frequency (inter-event interval) and number were also calculated.

To minimize variations due to differences in cell size, current amplitudes were expressed as current densities (pA/pF). I-V curves of hyperpolarizing protocols were obtained by measuring the current at the beginning of each voltage step (instantaneous current, I_{ist}), in the middle region, and at the end of the pulse (steady state current, I_{ss}). Hyperpolarizing I_h currents were obtained by the difference between I_{ss} and I_{ist} (Rateau, 2006). Tail currents amplitude following the voltage steps was also measured. In depolarizing protocols, current amplitude was measured at peak (i.e. at beginning of the voltage step).

2.6 DRUGS

The following drugs were bath applied:
glial cell line-derived neurotrophic factor (GDNF; Peprotech, NJ, USA), tetraethylammonium (TEA; Sigma), barium chloride (Merck, Darmstadt, Germany) and 4-aminopyridine (4-AP; Sigma). All drugs were prepared in distilled water as stock solution, kept frozen in aliquots and then added to the bath solution to obtain a concentration of 100 ng/mL (GDNF; Matheson et al., 1996), 25 mM (TEA; Tang et al. 2016), 100 µM (barium chloride; Tang et al. 2010) and 5mM (4-AP; Winkelman et al. 2005).

2.7 IMMUNOFLUORESCENCE

Acutely dissected and collagenase-treated entire DRGs were fixed for 30 min with 4% paraformaldehyde in phosphate buffer (PB, 0.1 M, pH 7.4) washed several times in phosphate buffered saline (PBS; 0.02 M, pH 7.4), and then processed for immunofluorescence. Depending on the type of marker used to label DRG neurons and/or SGCs, the following protocols were performed:
IB4-labeling: DRGs were pre-incubated in PBS containing 6% bovine serum albumin for 1 h, incubated overnight at 4°C in biotin-conjugated IB4 (1:250; L2140, Sigma), then incubated for 1 h with Extravidin-FITC (1:500; Sigma).
CGRP labeling: DRGs were pre-incubated in PBS containing 1:100 Normal Goat Serum and 0.1% Triton X-100 for 1 h, incubated overnight at 4°C in rabbit anti-CGRP (1:500; C8198, Sigma), then incubated for 1 h with anti-rabbit Alexa 594 or 633 secondary antibody (1:1000; Thermo Fisher, Waltham; MA, USA).
Glutamine synthetase labeling: DRGs were preincubated in PBS containing 1:100 Normal Goat Serum and 0.1% Triton X-100 for 1 h, incubated overnight at 4°C in mouse anti-glutamine synthetase (1:50; MAB302, Merck, Darmstadt, Germany) then incubated for 1 h with anti-mouse Alexa 546 secondary antibody (1:1000; Thermo Fisher).
Immunofluorescence was acquired using a confocal microscope (TCS SP5; Leica Microsystems, Wetzlar, Germany) with 20x lens. To obtain Z-series reconstructions, immunostained DRGs were transferred on slides modified *ad hoc* to maintain the 3D volume and to avoid movements due to the immersion lens of microscope. To avoid the interferences link to the different fluorophores, confocal optical sections were acquired at 3.5 µm intervals in a sequential mode.

2.8 PRIMARY ANTIBODIES

Anti-CGRP antibody. This polyclonal antibody was raised in rabbit against synthetic CGRP conjugated to KLH as the immunogen. Working dilution was 1:500. The specificity of the CGRP antiserum was previously characterized in several publications (Merighi et al., 1991; Salio and Ferrini, 2016).

IB4-biotin conjugate. IB4 is a protein of non-immune origin capable of binding glycoproteins expressed on the surface of non-peptidergic sensory neurons. Working dilution was 1:250. The specificity was previously characterized (Ciglieri et al., 2016a).

Anti-glutamine synthetase. This monoclonal antibody was purified from sheep brain. Working dilution was 1:50. Detection of glutamine synthetase in SGCs by this antibody has been reported on mice with immunofluorescence technique (Rajasekhar et al., 2015).

2.9 IMMUNOHISTOCHEMICAL CONTROLS

In order to verify the specificity of immunohystochemical reactions, the following control experiments were performed:

- specificity controls, by pre-adsorbing primary antibodies with their respective control peptides;
- negative controls, by omitting primary antibodies.

2.10 SOFTWARE-BASED ANALYSIS OF NOCICEPTORS DISTRIBUTION IN MICE DRGS

To better elucidate the cellular organization of DRGs and the possible alterations that can occur in diabetic conditions, a software-based analysis of 3D configuration, named *3DRG*, was developed in collaboration with the Department of Control and Computer Engineering of Polytechnic of Turin. Entire DRGs were collected for electrophysiological recordings and then fixed in PFA 4% to be processed for immunofluorescence staining of IB4+ and CGRP+ nociceptors (as described before). Z-stack images of 20-30 µm of depth and 3.51 µm of thickness were acquired with the confocal microscope and then sent to software-based analysis to make semi-automated a quantitative analysis on entire DRGs.

To distinguish the positive stained neuronal cells from noise and artifacts (e.g. spurious fluorescence, black spots, etc. which are intrinsic limitations of immunofluorescence) a 3D segmentation technique, comprising different specific steps, was applied (Figure 2.2):

- - images were optimized acting on contrast and background parameters in a way that did not alter the original immunostaining, and a filter was applied to remove fake signal and preserve significant details as neurons borders;
- - a fuzzy c-mean algorithm was applied to distinguish fluorescent objects from the dark background. Fuzzy c-mean is a clustering technique that assigns a membership value to each data to organize data with similar values in proper cluster, reducing noise and spurious blobs;
- - a refinement of the cell segmentation was performed by separating the positive objects in single cells, based on the assumption that individual cells are approximately circular;
- - the objects collected from a single image were projected to the neighborough slices of the z-stack to discriminate the type of object: if the neighborough slices contained an object that was at least the 50% of the object projected, it was interpreted as part of the positive cells, otherwise the corresponding object was considered as a sham fluorescence and discarded.

Figure 2.3 shows some examples of 2D and 3D reconstructions of DRGs obtained with this software.

Math formulas used to calculating parameters are showed in Table 2.1

TABLE 2.1 FORMULAS USED BY *3DRG* TOOL.

NUMEROSITY	VOLUMETRIC ANALYSIS
$\bar{n}_{cell} = \sum_{i=1}^{Ncls} \frac{V_{cls}^{i}}{V_{ref}}$ $\quad \%cluster\ 1 = \frac{N_{cls}}{N_V} * 100$	$V_{med\ cls} = \frac{med\ (V_{cls})}{V_{ref}}$ $\quad \%cluster\ 2 = \frac{V_{cls}}{V} * 100$

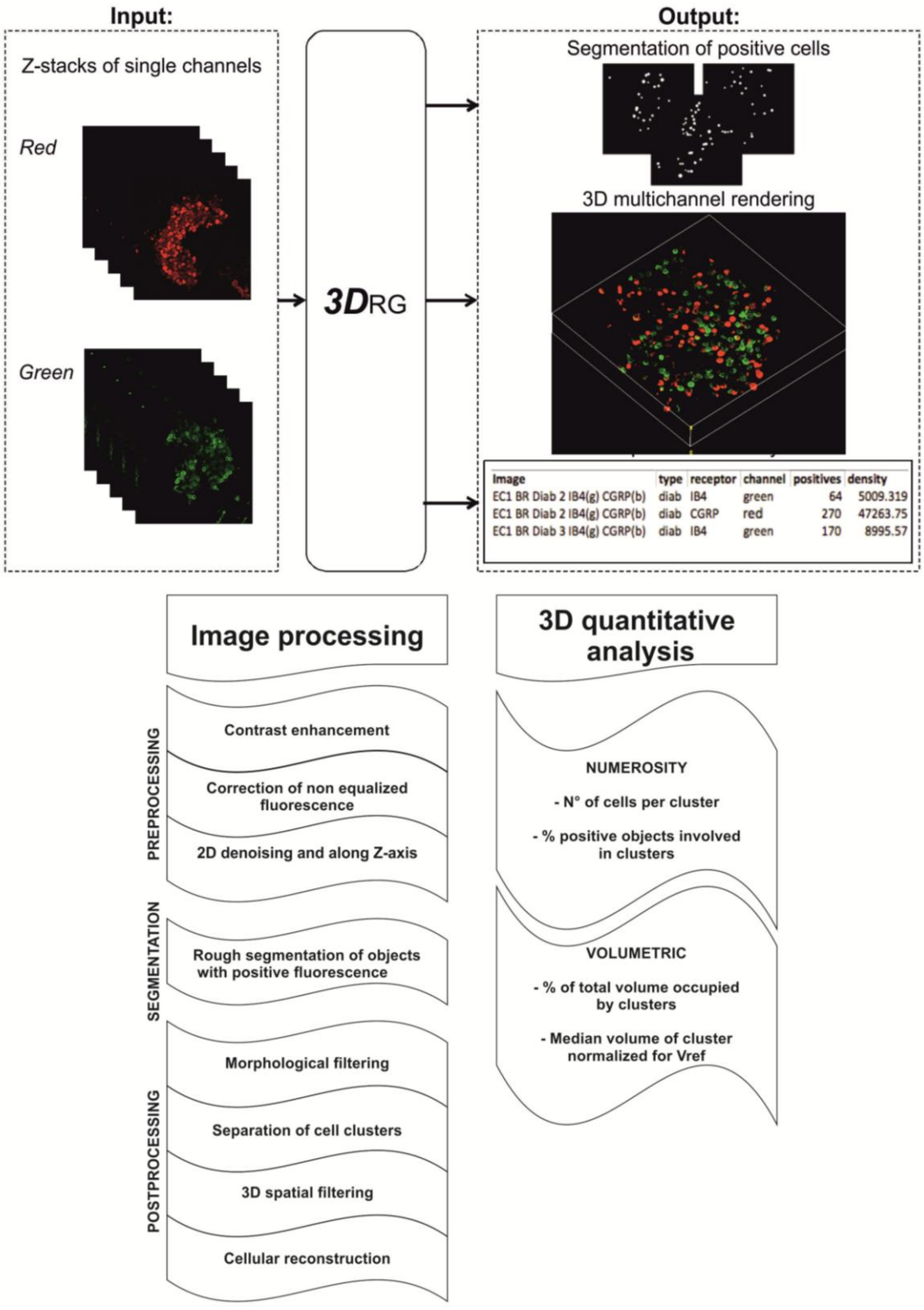

FIGURE 2.2 SIMPLIFIED STEP-BY-STEP INPUT/OUTPUT OF *3DRG*.
From *"Automated 3D immunofluorescence analysis of dorsal root ganglia for the investigation of neural circuit alterations: a preliminary study"*, (Cataldo et al., 2016)

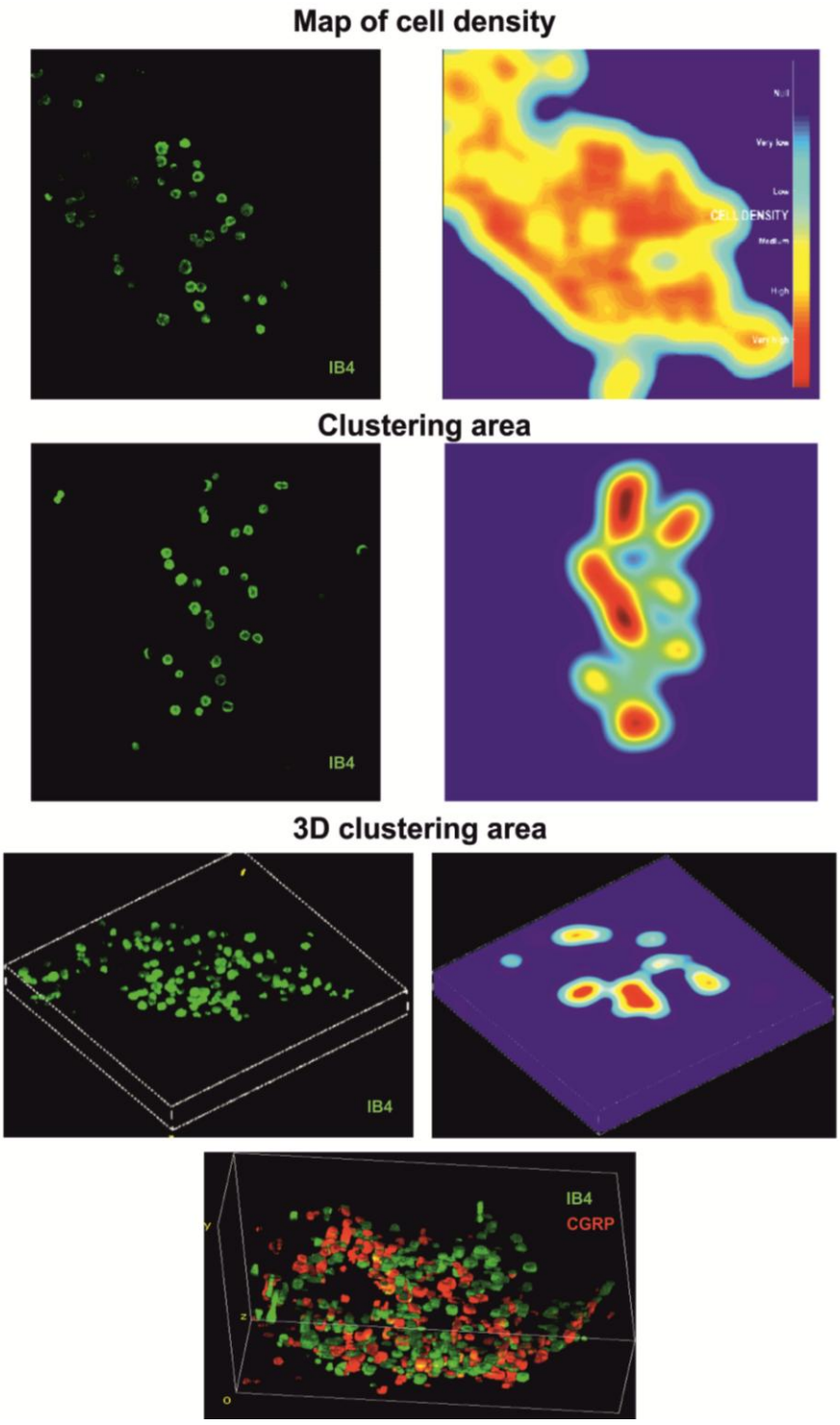

FIGURE 2.3 EXAMPLES OF SOME OUTPUTS OF *3DRG* TOOL.

2.11 ANALYSIS OF SGCS ENSHEATMENT

Cell-specific SGCs ensheatment was analyzed in 5 CTR DRGs and 5 DIAB DRGs, for a total account of 47 CTR neurons and 54 DIAB neurons. To analyze the level of SGC coverage associated with specific populations of nociceptors, entire DRGs were collected and triple immunostained for IB4, CGRP and α-glutamine synthetase (GS). DRGs images were collected using the confocal microscope (as described above) and analyzed with a technique to quantify the GS staining around neurons. GS staining was analyzed on single optical sections at the level of the neuron equator, where the neuronal cell body has the largest diameter. GS fluorescence was measured along four lines crossing the sensory neuron from side to side and passing through the cell center. Since GS staining is concentrated on the outer aspect of the sensory neuron membrane where SGCs are located, the peak of GS fluorescence surrounding the neuron was detected where the 4 lines crossed the neuronal membrane (8 points). In these points the fluorescence intensity was calculated by averaging the fluorescence of three consecutive values. As shown in Figure 2.4, the 8-point values were ordered from the higher to the lower, which correspond to the maximum and the minimum level of GS expression around the neuron. This analysis was performed in IB4+ and CGRP+ subpopulations, in the presence of diabetes or not.

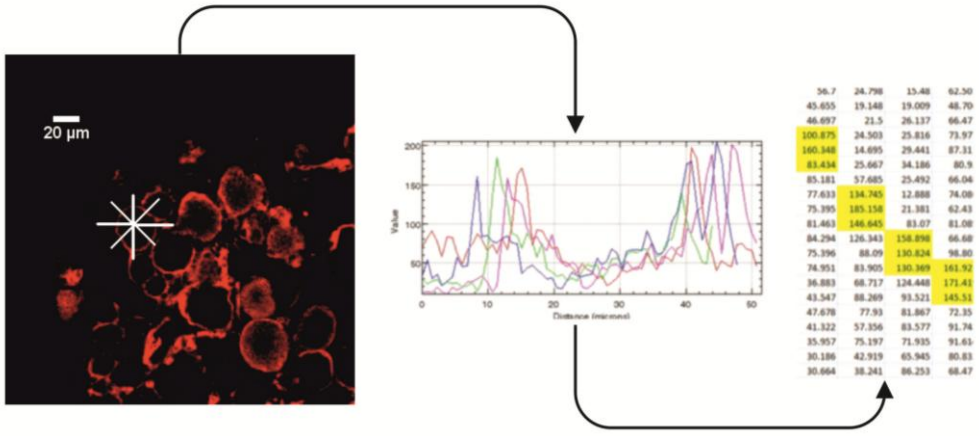

FIGURE 2.4 ANALYSIS OF SGCS ENSHEATMENT.

2.12 STATISTICS

Statistical analysis was performed with GraphPad Prism 7 (GraphPad Software, La Jolla, CA USA). Since values in our dataset did not follow a normal distribution, they were analyzed by appropriate non-parametric tests (Wilcoxon test for paired samples, Mann-Whitney for independent samples, Friedman test for multiple paired samples with Dunn's test as post-hoc).

All data were reported as mean ±SEM, with *n* indicating the number of neurons (unless otherwise stated). Values of $P<0.05$ were considered statistically significant.

3 RESULTS

3.1 PATCH-CLAMP CHARACTERIZATION OF DRG NEURONS IN CONTROL AND DIABETIC MICE

3.1.1 ACTIVE AND PASSIVE MEMBRANE PROPERTIES OF DRG NEURONS IN CONTROL AND DIABETIC MICE

Active and passive membrane properties were investigated in whole-cell current clamp mode (data are summarized in Table 3.1). Passive properties and, in particular, membrane capacitance (C_m), membrane resistance (R_m), and resting potential (V_m) were not significantly different between neurons from control (CTR) and diabetic (DIAB) mice. Also the mean cell area was not different between groups, indicating a randomized sampling of DIAB and CTR neurons unbiased by the cell size. To investigate action potential (AP) firing activity in DRG neurons, step and ramp depolarizing protocols were used in whole cell current-clamp mode. For the step protocol (Figure 3.1 A), a train of depolarizing steps current (Δ = 20 pA) with a duration of 500 ms was injected through electrode until an AP firing was evoked. The interval of each trace was 300 ms. For the ramp protocol (Figure 3.1 B), a unique step increasing from 0 nA to 1 nA or 1.5 nA with a duration of 500 ms was injected. In both cases, the injection of current was performed from the V_m of each neurons (mean values for CTR neurons of -60 mV and for DIAB neurons of -58 mV), set at the beginning of recording.

TABLE 3.1

	CTR neurons (n=19)	Diab neurons (n=17)
C_m (pF)	38.26 ± 4.03	38.29 ± 3.00
R_m (Mohm)	258 ± 50.79	310 ± 63.67
Area (um^2)	548.75 ± 58.22	575.19 ± 59.64
V_m (mV)	-74.99 ± 1.70	-70.37 ± 3.75
Rheobase (pA/pF)	8.54 ± 1.45	8.27 ± 1.57
Threshold (mV)	-39.10 ± 1.64*	-33.44 ± 1.63
Latency (ms)	31.16 ± 17.55	19.02 ± 3.54
Overshoot (mV)	46.40 ± 2.10	46.56 ± 3.32
Max rise slope (mV/ms)	131.16 ± 14.36*	90.28 ± 13.31
Time of max rise slope (ms)	14.76 ± 0.19	14.71 ± 0.14
Rise time 20-80% (ms)	0.39 ± 0.04	0.59 ± 0.08
Max decay slope (mV/ms)	63.84 ± 10.20	44.00 ± 5.54
Time of max decay slope (ms)	18.03 ± 0.60	18.91 ± 0.82

*P<0.05, Mann-Whitney test.

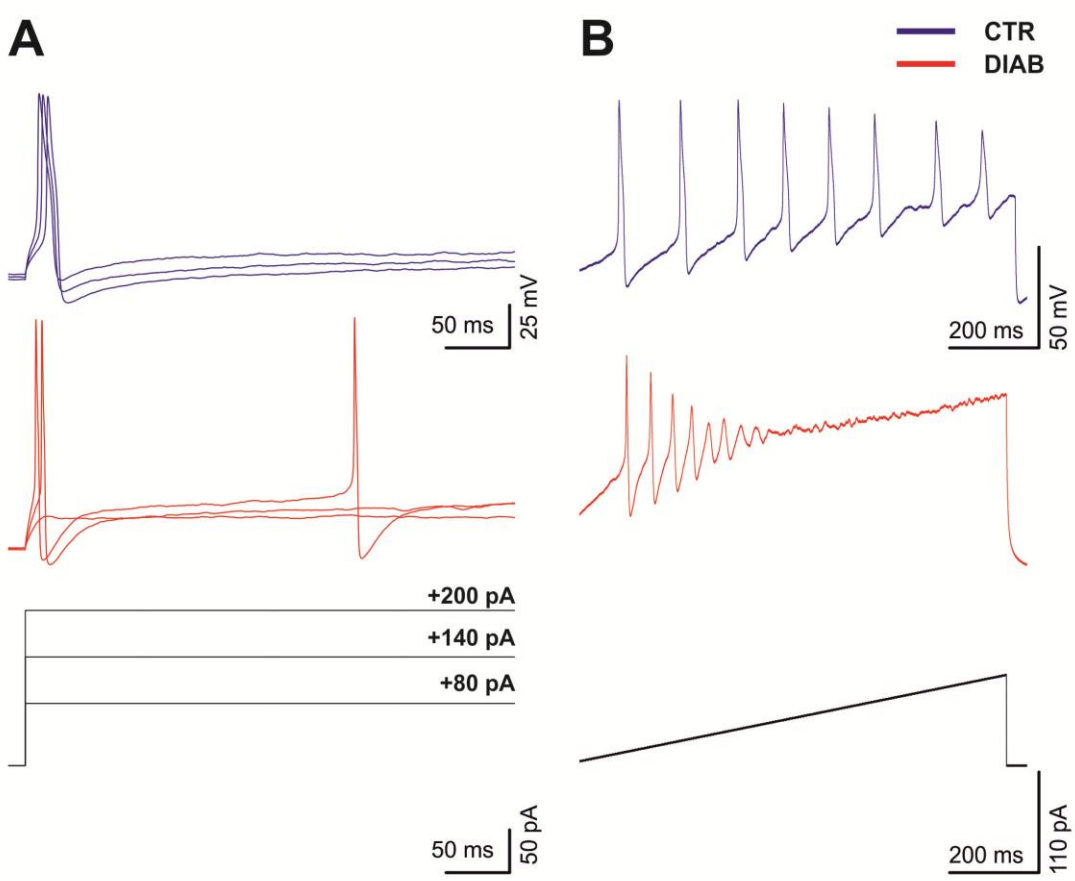

FIGURE 3.1 ACTION POTENTIALS EVOKED IN CURRENT-CLAMP CONFIGURATION.
Firing patterns obtained after injection of a depolarizing **A** step protocol and a **B** ramp protocol from V_m (mean values for CTR neurons of -60 mV and for DIAB neurons of -58 mV). Notice lower AP threshold in neurons from (**blue**) control as compared to (**red**) diabetic mice. On the bottom, representation of the protocols applied.

We measured the AP-related parameters from all recordings and compared their values between CTR and DIAB DRG neurons. As shown in Table 3.1 and Figure 3.2, the mean AP threshold in CTR neurons (n=19) was -39.10 ± 1.64 mV, while in DIAB neurons was -33.44 ± 1.63 mV (n=17, $P<0.05$, Mann-Whitney test). Moreover, the AP maximum rise slope of CTR neurons was significantly faster than the DIAB neurons ($P<0.05$, Mann-Whitney t-test). All together, these data indicate that DIAB neurons react with a slower depolarizing shift to current injections and generate APs to more positive potentials as compared to controls. Other parameters, such as rheobase and latency, were not significantly different.

To determine if there was an AP firing difference between neurons with different sizes, all the data collected were divided in two categories based on the cell area. The first category, identified/classified as "small-sized", contained neurons until 490 μm^2, while the second category "medium-sized" contained neurons between 490 μm^2 and 1100 $\mu m^{2.}$ This choice was based on our interest to analyze physiological differences in nociceptors, whose diameters sizes normally lie

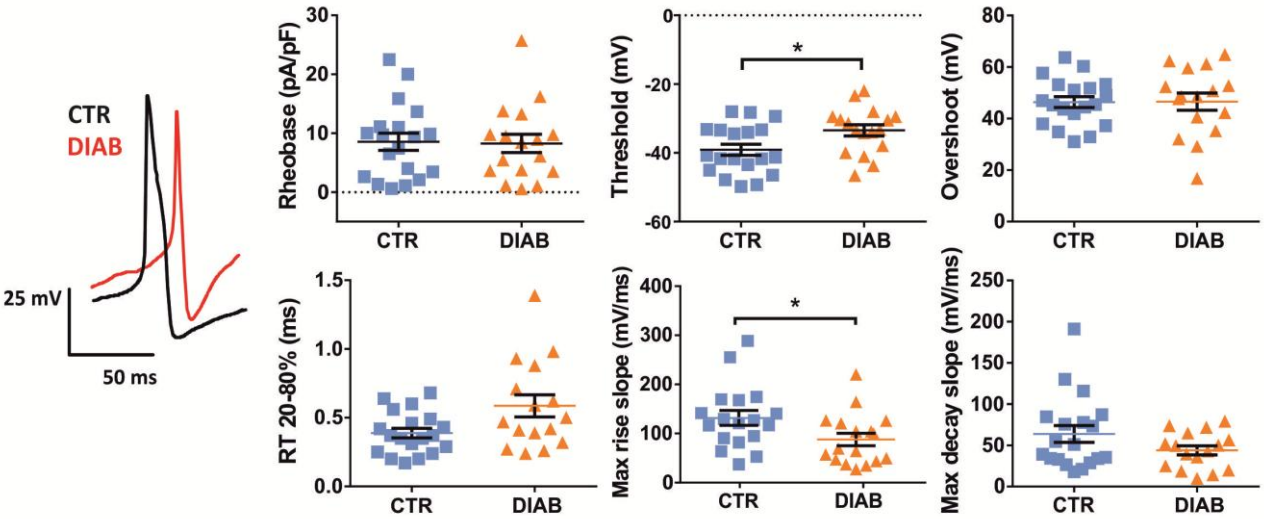

FIGURE 3.2 AP-RELATED PARAMETERS – CTR VS DIAB.
AP-related parameters were recorded from neurons of (**blue**) control and (**orange**) diabetic mice. The only parameters that differ significantly were the threshold, which was more depolarized for DIAB neurons, and the maximum rise slope, which was reduced in DIAB neurons (CTR n=19, DIAB n=17; *P<0.05, Mann-Whitney test). On the left, two AP superimposed to show the different kinetics between CTR and DIAB neurons. *Abbreviations*: CTR =control, DIAB=diabetic.

between 10 µm and 30 µm, depending on the sub-population considered (Stucky and Lewin, 1999b; Kestell et al., 2015). As shown in Table 3.2, some parameters resulted significantly different between small-sized and medium-sized cells in both control and diabetic mice, as expected. However, other parameters, such as maximum decay slope, rheobase and resting potential, were significantly different in diabetes only (*P<0.05, **P<0.01, Mann-Whitney test).

TABLE 3.2

	Small-size CTR (n=11)	Medium-size CTR (n=8)	Small-size DIAB (n=9)	Medium-size DIAB (n=8)
C_m (pF)	28.82 ± 2.83**	51.25 ± 6.46	30.22 ± 2.88***	47.38 ± 3.28
R_m (Mohm)	358.91 ± 72.66*	118.50 ± 24.58	434.78 ± 103.12*	170.25 ± 26.96
Area (um^2)	367.71 ± 23.69***	797.67 ± 65.64	386.15 ± 21.71***	787.85 ± 66.84
V_m (mV)	-59.55 ± 2.33	-75.33 ± 2.65	-54.22 ± 2.29*	-78.33 ± 2.52
Rheobase (pA/pF)	7.52 ± 1.86	9.95 ± 2.38	4.40 ± 1.08**	12.44 ± 2.28
Threshold (mV)	-37.78 ± 2.15	-40.92 ± 2.53	-33.97 ± 1.57	-32.85 ± 3.10
Latency (ms)	46.95 ± 29.93	9.46 ± 2.74	27.79 ± 4.89	9.16 ± 1.96
Overshoot (mV)	47.52 ± 3.12	44.85 ± 2.69	49.15 ± 3.17	43.23 ± 6.52
Max rise slope (mV/ms)	112.33 ± 18.59	157.05 ± 20.38	82.04 ± 19.89	100.87 ± 17.36
Time of max rise slope (ms)	14.58 ± 0.32	15.01 ± 0.13	14.62 ± 0.14	14.81 ± 0.28
Rise time 20-80% (ms)	0.45 ± 0.05*	0.30 ± 0.03	0.64 ± 0.08	0.51 ± 0.15
Max decay slope (mV/ms)	47.94 ± 9.49*	85.70 ± 18.47	32.50 ± 5.47*	58.78 ± 7.70
Time of max decay slope (ms)	18.54 ± 0.88	17.32 ± 0.76	20.14 ± 1.24	17.33 ± 0.68

*P<0.05, **P<0.01, ***P<0.001, Mann-Whitney test between small-sized and medium-sized, within CTR and DIAB categories. No differences between CTR and DIAB.

To unveil any voltage-dependency under the observed diabetes-induced effects, current-clamp protocols were applied after imposing an hyperpolarized holding potential (-85 mV; Table 3.3).

TABLE 3.3

	CTR (n=19)	CTR hyper	DIAB (n=17)	DIAB hyper
Rheobase (pA/pF)	8.54 ± 1.45*	11.80 ± 1.29	8.18 ± 1.54*	11.38 ± 1.59
Threshold (mV)	-39.10 ± 1.64***	-44.21 ± 1.87	-33.44 ± 1.63*	-36.62 ± 2.39
Latency (ms)	31.16 ± 17.55***	71.81 ± 27.83	19.02 ± 3.54	35.46 ± 22.95
Overshoot (mV)	46.40 ± 2.10**	42.29 ± 2.61	46.56 ± 3.32	47.65 ± 2.87
Rise time 20-80% (ms)	0.39 ± 0.04	0.39 ± 0.04	0.59 ± 0.08	0.52 ± 0.06
Max rise slope (mV/ms)	131.16 ± 14.36	128.96 ± 14.20	90.28 ± 13.31	106.60 ± 14.66
Time of max rise slope (ms)	14.76 ± 0.19	14.59 ± 0.16	14.71 ± 0.14	15.94 ± 1.31
Max decay slope (mV/ms)	63.84 ± 10.20	61.32 ± 9.21	43.99 ± 5.54	49.27 ± 7.61
Time of max decay slope (ms)	18.03 ± 0.60*	17.43 ± 0.60	18.73 ± 0.80	19.57 ± 1.26

*P<0.05, **P<0.01, ***P<0.001, Wilcoxon test between resting and hyperpolarized condition, within CTR and DIAB categories. P<0.05 Mann-Whitney test between CTR and DIAB.

After hyperpolarization, AP threshold was the only parameter remaining significantly different between control and diabetic mice. No differences were observed in parameters associated with AP kinetics (maximum rise slope and rise time). Interestingly, hyperpolarized state significantly affected several AP properties of CTR neurons as compared to their respective resting values, and namely threshold, latency, overshoot, timing of maximum decay (CTR n=19, DIAB n=17; *P<0.05, **P<0.01, ***P<0.001, Wilcoxon test; Figure 3.3). Conversely, small or no detectable differences were observed in DIAB cells.

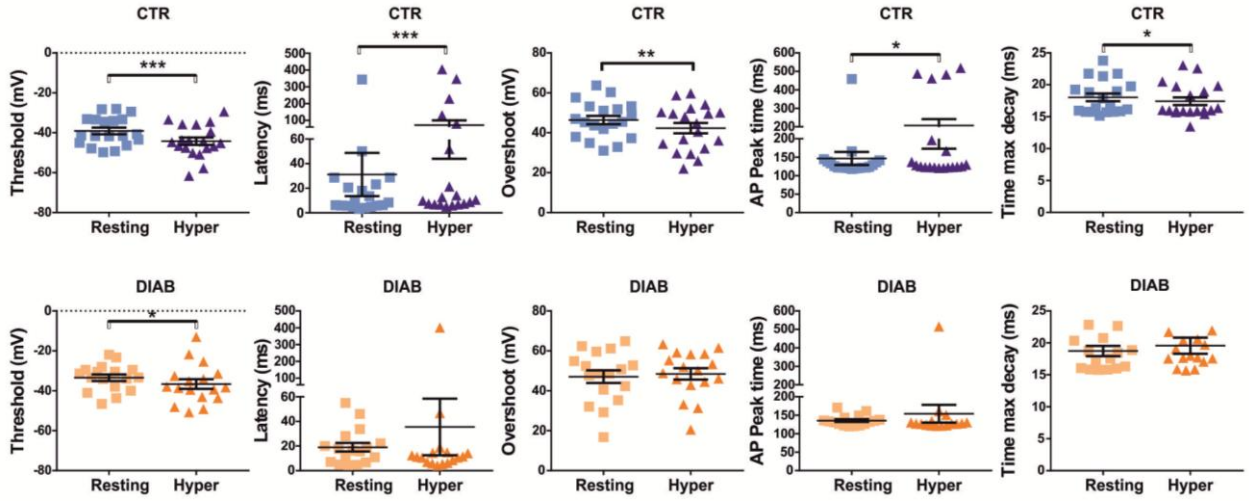

FIGURE 3.3 AP RELATED PARAMETERS – RESTING VS HYPER.
AP related parameters were recorded from neurons of (**top**) control and (**bottom**) diabetic mice. For each neurons, the same protocols were repeated in resting and hyperpolarized (i.e. -85 mV) conditions, to analyze voltage-dependent differences. Interestingly, only CTR neurons showed significant differences in hyperpolarized condition in parameters as threshold, latency, overshoot, AP peak time and time of max decay (CTR n=19, DIAB n=17, *P<0.05, **P<0.01, ***P<0.001, Wilcoxon test). *Abbreviations:* CTR=control, DIAB= diabetic.

The effects of hyperpolarization were analyzed by considering the categories “small-sized” and “medium-sized” (Table 3.4). In small CTR neurons, a significant decrease in AP overshoot was measured, which passed from 47.52 ± 3.12 mV to 43.20 ± 3.71 mV, while an increase resulted in threshold, which passed from -37.78 ± 2.15 mV to -43.99 ± 3.07 mV, and in latency, which varied from 46.95 ± 29.93 ms to 62.49 ± 30.77 ms (*P<0.05, **P<0.01 respectively, Wilcoxon test). Medium-sized CTR neurons also reacted to hyperpolarization with a significant change in threshold, which passed from -40.92 ± 2.53 mV to -44.51 ± 1.70 mV and latency, from 9.46 ± 2.74 ms to 7.40 ± 0.52 ms (P<0.05, Wilcoxon test). Parameters in DIAB neurons, as above stated, were little affected by hyperpolarization. The only AP feature that changed was rheobase in small-sized cells, which increased from 4.40 ± 1.08 pA to 10.89 ± 2.31 pA (P<0.01, Wilcoxon test).

TABLE 3.4

	Small-size CTR (n=11)	Small-size hyper CTR	Medium-size CTR (n=8)	Medium-size hyper CTR
Rheobase (pA/pF)	7.52 ± 1.86	11.23 ± 1.98	9.95 ± 2.38	12.57 ± 1.55
Threshold (mV)	-37.78 ± 2.15**	-43.99 ± 3.07	-40.92 ± 2.53*	-44.51 ± 1.70
Latency (ms)	46.95 ± 29.93*	62.49 ± 30.77	9.46 ± 2.74*	7.40 ± 0.52
Overshoot (mV)	47.52 ± 3.12*	43.20 ± 3.71	44.85 ± 2.69	41.02 ± 3.75
Max rise slope (mV/ms)	112.33 ± 18.59	111.33 ± 16.17	157.05 ± 20.38	153.20 ± 23.93
Time of max rise slope (ms)	14.58 ± 0.32	14.63 ± 0.14	15.01 ± 0.13	15.00 ± 0.14
Rise time 20-80% (ms)	0.45 ± 0.05	0.44 ± 0.05	0.30 ± 0.03	0.33 ± 0.05
Max decay slope (mV/ms)	47.94 ± 9.49	46.45 ± 7.71	85.70 ± 18.47	81.76 ± 17.28
Time of max decay slope (ms)	18.54 ± 0.88	18.54 ± 0.86	17.32 ± 0.76	16.98 ± 0.70
	Small-size DIAB (n=11)	Small-size hyper DIAB	Medium-size DIAB (n=8)	Medium-size hyper DIAB
Rheobase (pA/pF)	4.40 ± 1.08**	10.89 ± 2.31	12.44 ± 2.28	14.63 ± 2.17
Threshold (mV)	-33.97 ± 1.57	-36.73 ± 2.23	-32.85 ± 3.10	-36.50 ± 4.63
Latency (ms)	27.79 ± 4.89	60.32 ± 42.72	9.16 ± 1.96	7.50 ± 0.97
Overshoot (mV)	49.15 ± 3.17	49.11 ± 2.66	43.23 ± 6.52	45.77 ± 5.83
Max rise slope (mV/ms)	82.04 ± 19.89	88.60 ± 16.58	100.87 ± 17.36	129.75 ± 24.47
Time of max rise slope (ms)	14.62 ± 0.14	16.63 ± 2.35	14.81 ± 0.28	14.89 ± 0.18
Rise time 20-80% (ms)	0.64 ± 0.08	0.60 ± 0.07	0.51 ± 0.15	0.41 ± 0.09
Max decay slope (mV/ms)	32.50 ± 5.47	34.32 ± 4.30	58.78 ± 7.70	68.49 ± 13.78
Time of max decay slope (ms)	20.14 ± 1.24	19.67 ± 0.99	17.33 ± 0.68	17.19 ± 0.63

*P<0.05, **P<0.01, ***P<0.001, Wilcoxon test between resting and hyperpolarized condition, within CTR small/medium-sized and DIAB small/medium-sized categories. No difference between CTR and DIAB.

Eventually, the above analysis was repeated further dividing the small-sized category into putative IB4+ and IB4- subsets. This subdivision was based on data published by Choi et al. (2006) and Fang et al. (2006), who demonstrated that IB4+ neurons adapt quickly to ramp stimuli, showing a rapid decrement of AP amplitude and a longer AP duration. Conversely, IB4- neurons did not show the decline in AP amplitude during ramp current injection and present a shorter AP (Figure 3.4 C).

This correlation was confirmed in a subset of neurons dye-injected during the electrophysiological recordings and subsequently processed for identification of IB4+ and CGRP+ neurons by immunostaining (Figure 3.4 A). Our data showed that threshold was more positive in IB4- neurons (n=4) than in IB4+ ones (n=4) (-25.74 ± 2.57 mV and -43.10 ± 4.00 mV, respectively; $P<0.05$, Mann-Whitney test). Conversely, this difference was lost in diabetic mice. Interestingly, the main effect induced by diabetes on AP threshold was detected in IB4+ neurons (Figure 3.4 B). By using a two-ways ANOVA, the increase in threshold induced by diabetes was shown to be clearly associated with cellular phenotype (CTR n=4, DIAB n=4; **$P<0.01$,two-way ANOVA).

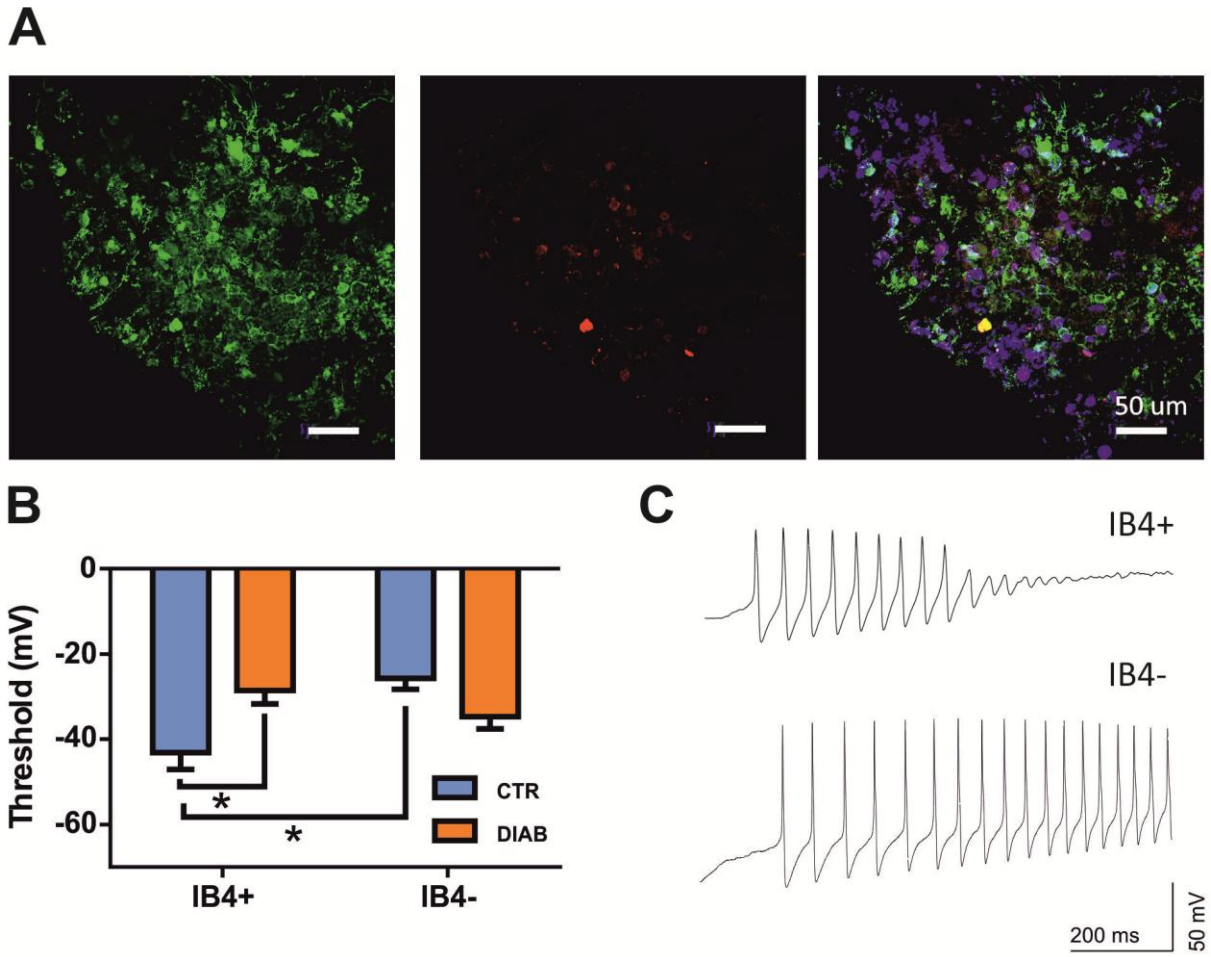

FIGURE 3.4 IB4+ AND IB4- SENSORY NEURONS.
A Dye injected neuron during electrophysiological recording and subsequently processed for identification with immunostaining. The fluorescent label indicates a IB4+ non-peptidergic neuron. **B** Two-way ANOVA to compare the different effect exerted by diabetes on IB4+ and IB4- neurons. IB4+ neurons showed significant depolarization of the threshold in diabetic condition, while IB4- not. In addition, IB4+ CTR neurons were more hyperpolarized than IB4- CTR one (CTR n=4, DIAB n=4;*$P<0.05$, two-way ANOVA). **C** IB4+ neurons can be recognized from IB4- based on a different kinetics of adaptation (Choi et al., 2006).

All together, these data indicate that DIAB neurons exhibit a reduced excitability as compared to CTR neurons. This effect is particularly obvious in small IB4+ neurons. Since the observed effect is differentially influenced by hyperpolarization in diabetic and control mice, it might involve voltage-dependent channels, such as K^+ channels.

3.1.2 VOLTAGE-CLAMP CHARACTERIZATION OF DRG NEURONS IN CONTROL AND DIABETIC MICE

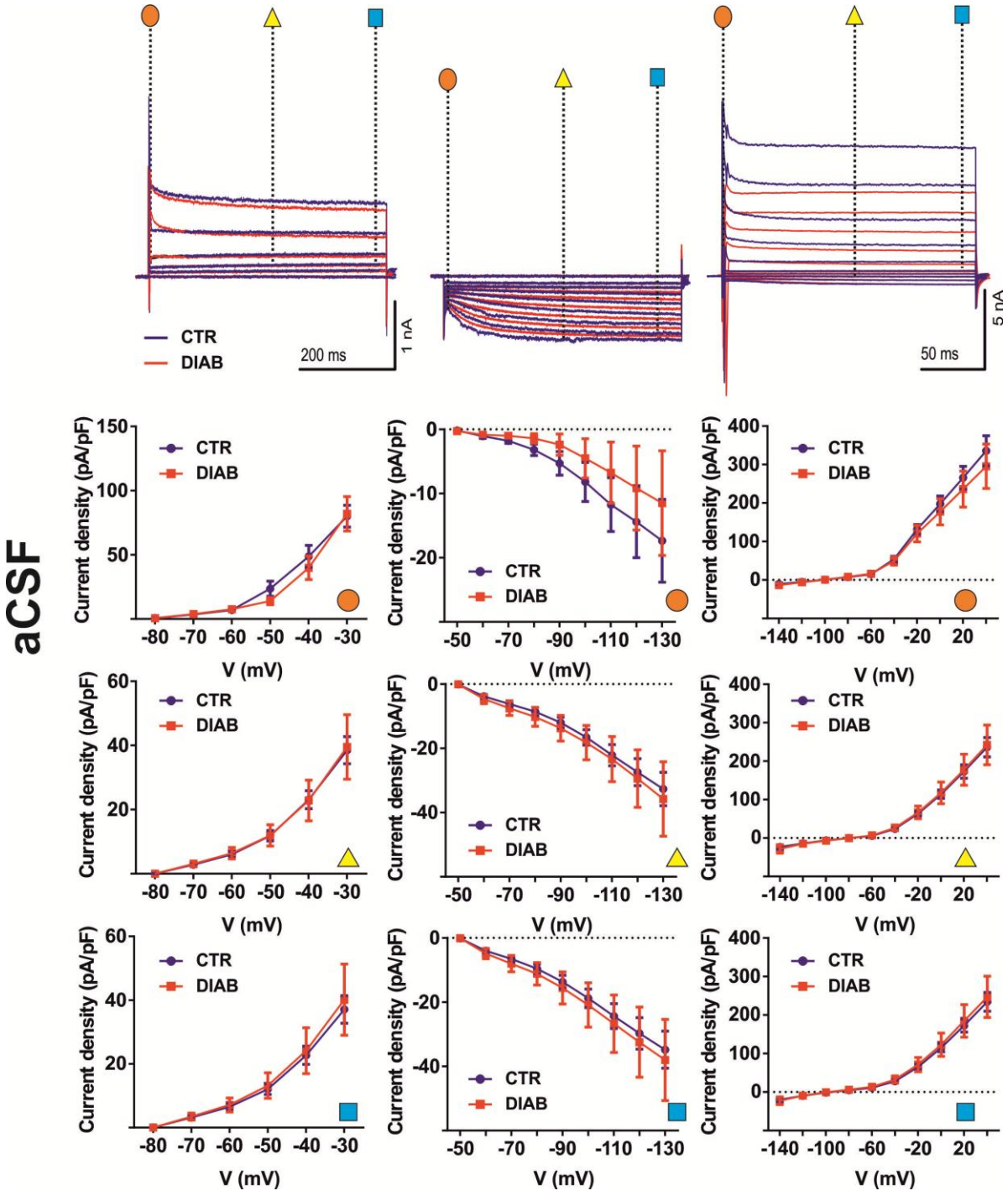

FIGURE 3.5 TOTAL CURRENTS ELICITED IN CTR AND DIAB NEURONS IN ACSF.
Top Representative traces of the current elicited by two depolarizing and one hyperpolarizing protocols in voltage-clamp configuration. Currents were measured at the start (**orange circle**), the middle (**yellow triangle**) and at the end (**blue square**) of the traces. **Bottom** Analyzing the mean density of current no difference were observed (CTR n=16, DIAB n=17). *Abbreviations:* CTR=control, DIAB= diabetic.

To better isolate voltage-dependent components underlying diabetes-induced effects in DRG neurons, current-voltage (I-V) relationship were further investigated in voltage clamp. Both depolarizing and hyperpolarizing step protocols were applied (Figure 3.5, upper panel). Depolarizing protocols ranged from -80 mV to -30 mV (500 ms, Δ=10 mV) or from -140 mV to +40 mV (200 ms, Δ=20 mV). Hyperpolarizing protocol considered voltage steps from -50 mV to -130 mV (500 ms, Δ=20 mV). Currents were measured at three different time-points (start, middle, end of the step pulse; see Figure 3.5). Comparing the mean currents evoked in neurons from control (n=14) and diabetic mice (n=14), no significant differences were observed.

Subsequently, to isolate K^+ conductances, Na^+ conductances were minimized by substituting NaCl with choline chloride in aCSF and by adding Cd^{2+} (500 µM) to block Ca^{2+} conductances. First, hyperpolarizing protocol was applied as described above (Figure 3.6).
The mean current measured in neurons from diabetic mice (n=15) was significantly greater compared to neurons from control mice (n=15; $P<0.05$, Mann-Whitney test). This difference was mostly due to small-sized neurons contribute.

Hyperpolarizing voltage steps often induce a hyperpolarization-activated inward current (I_h) whose amplitude can be calculated as the difference between the steady state current measured at the end of the step (I_{ss}, blue squares) and the instantaneous current I_{ist} (orange circles) at the beginning of voltage step. In this case, no significant difference were measured in I_h currents between CTR and DIAB neurons (Figure 3.7).

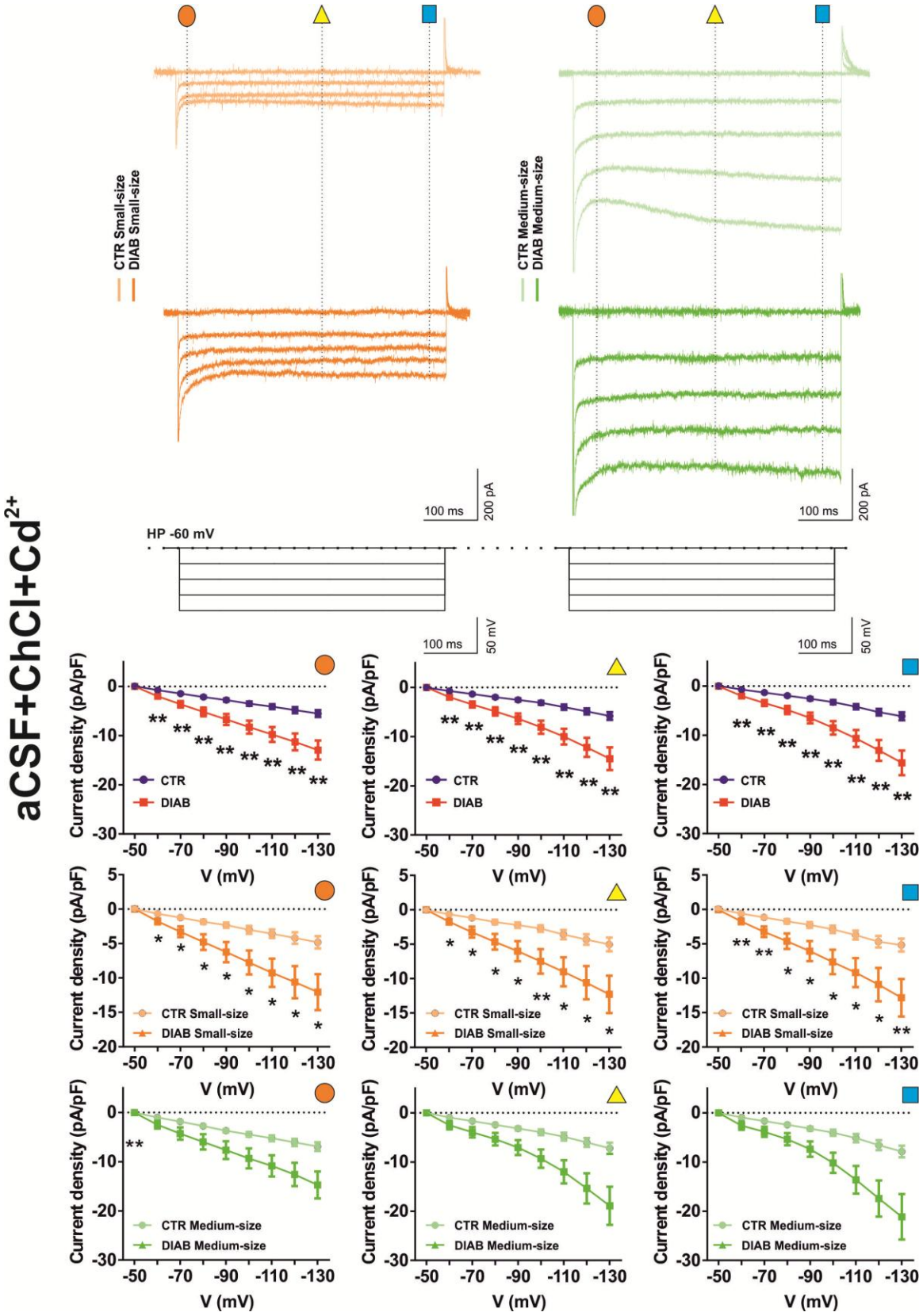

FIGURE 3.6 CURRENTS ELICITED BY HYPERPOLARIZING PROTOCOL IN NA+-FREE ACSF.
Top Representative traces of the current elicited by the hyperpolarizing protocols from -50 mV to -130 mV (500 ms, Δ=20 mV). Currents were measured at the start (**orange circle**), the middle (**yellow triangle**) and at the end (**blue square**) of the traces. **Bottom** The mean density of current in DIAB neurons was significantly greater than in CTR neurons, mostly due to the effect in small-sized cells (CTR n=15, DIAB n=15; *P<0,05, **P<0.01, Mann-Whitney test). *Abbreviations:* CTR=control, DIAB= diabetic.

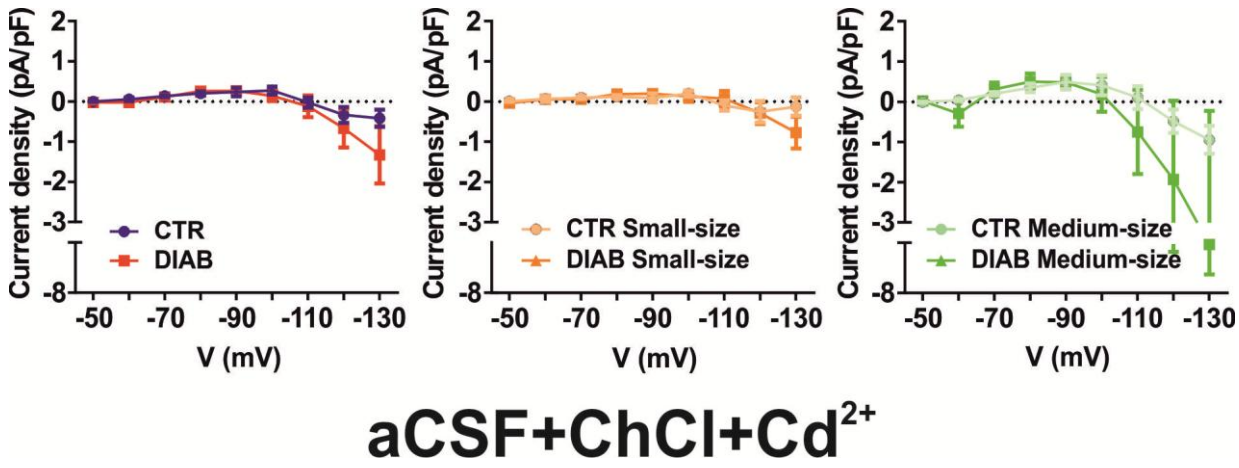

FIGURE 3.7 IH CURRENTS IN NA+-FREE ACSF.
Hyperpolarization-activated inward current (I_h) calculated as the difference between the steady state I_{ss} and the istantaneous I_{ist} currents. No significant difference were measured in I_h currents between CTR and DIAB neurons (CTR n=15, DIAB n=15). *Abbreviations:* CTR=control, DIAB=diabetic.

Then, depolarizing protocols were optimized to distinguish sustained (I_K) and a transient (I_A) component within the total K^+ current (Kv), as described in Fan et al. (2011). Total Kv current was evoked by voltage steps ranging from -60 mV to + 50 mV with 500 ms of duration, preceded by a 1000 ms prepulse of -100 mV. A prepulse of -40 mV was instead applied for inactivating transient Kv current and filtering out I_K. The subtraction of the respective current traces induced by these two protocols yielded the transient I_A (Figure 3.8). The mean of steady-state total Kv currents in neurons from diabetic mice (n=14) was significantly greater than in neurons from control animals (n=12) at more negative voltages, (*P<0.05, **P<0.01, ***P<0.001, Mann-Whitney test). This difference was lost for I_K currents while it was amplified for I_A currents. Differences were observed again at more negative voltages (from -60 to -20 mV), where at the peak currents were nearly 2 times larger in cells from diabetic than control mice. When neurons were pooled according to the size, differences were still significant in small-sized neurons only (Figure 3.9).

All together these data indicate that the activity of voltage dependent Kv channels is increased in DRG neurons of diabetic mice. The effect is mainly due to a potentiation of I_A conductance, particularly in small sized cells.

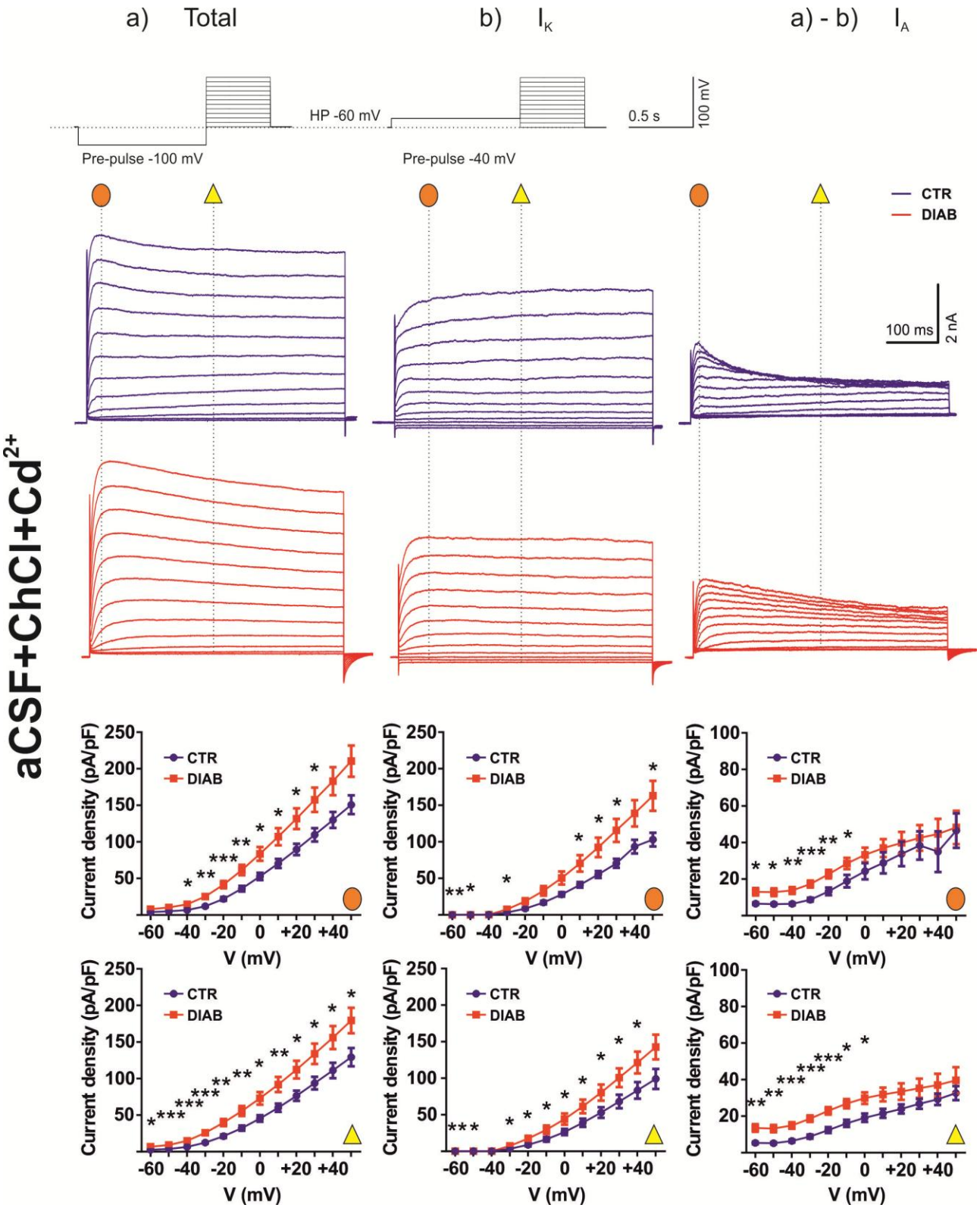

FIGURE 3.8 KV CURRENTS FROM CTR AND DIAB NEURONS IN NA+-FREE ACSF.

Top Representative traces of the total Kv current (left), sustained (centre) and transient Kv currents (right). **Bottom** The mean density of total, sustained and transient Kv currents of DIAB neurons was significantly higher than that of CTR neurons, both measured at the start (orange circle) and at the middle (yellow triangle) points (CTR n=12, DIAB n=14; *P<0.05, **P<0.01, ***P<0.01, Mann-Whitney test). *Abbreviations:* CTR=control, DIAB=diabetic.

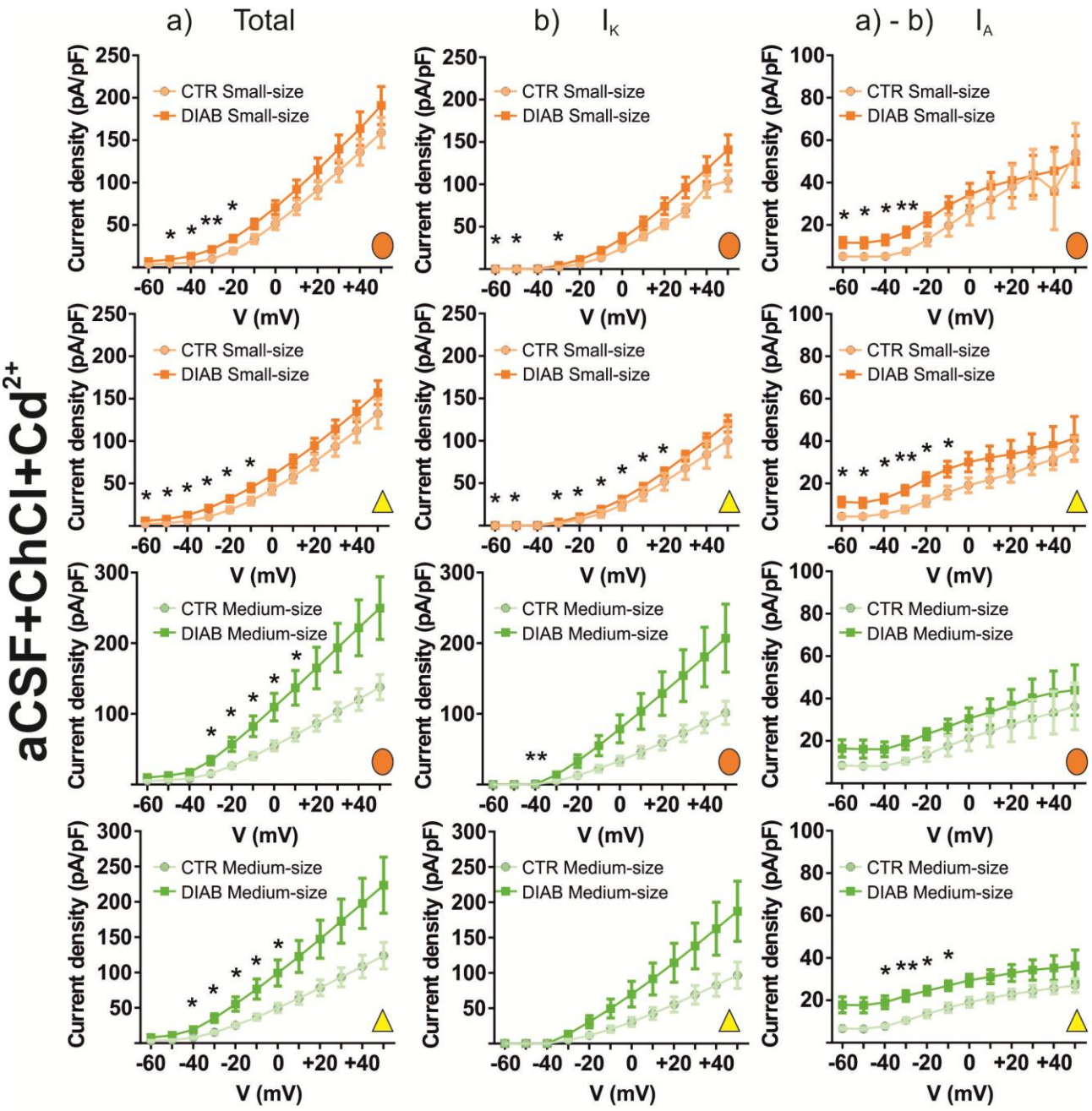

FIGURE 3.9 KV CURRENTS IN NA+-FREE ACSF ACCORDING TO THE NEURONS SIZE.
The mean density of total, sustained and transient Kv currents was significantly higher in DIAB small-sized neurons than in CTR small-sized one, while there was no difference between CTR and DIAB neurons in the medium-sized class. This difference was particularly high measuring the current at the middle point (yellow triangle) (CTR small-sized n=9, medium-sized n=5;DIAB small-sized n=10, medium-sized n=5; *P<0.05, **P<0.01, Mann-Whitney test). *Abbreviations:* CTR=control, DIAB=diabetic.

3.1.3 EFFECT OF GLUCOSE-ENRICHED PERFUSION ON DRG NEURONS ON CONTROL AND DIABETIC MICE

In order to verify if a standard aCSF perfusion was suitable for studying neurons from diabetic mice, which adapted to a glucose-rich extracellular environment, the effect of high glucose concentration on Kv currents was investigated. Depolarizing and a hyperpolarizing protocols were applied as previously described (Figure 3.10). At the end of each experiment, DRGs were perfused for 5 minutes with aCSF containing 20 mM glucose (twice the regular concentration). A significant increase in currents at negative voltage steps was observed in control neurons only (-50 mV and -60 mV with depolarization and -70 mV to -80 mV with hyperpolarization; CTR n=10, DIAB n=9; $P<0.05$, Wilcoxon test). This difference was not noticed in neurons from diabetic mice. This indicates that Kv currents in control neurons can be potentially affected by an increase of extracellular glucose; on the other hand, recording neurons from diabetic mice in normal aCSF does not significantly affect these conductances.

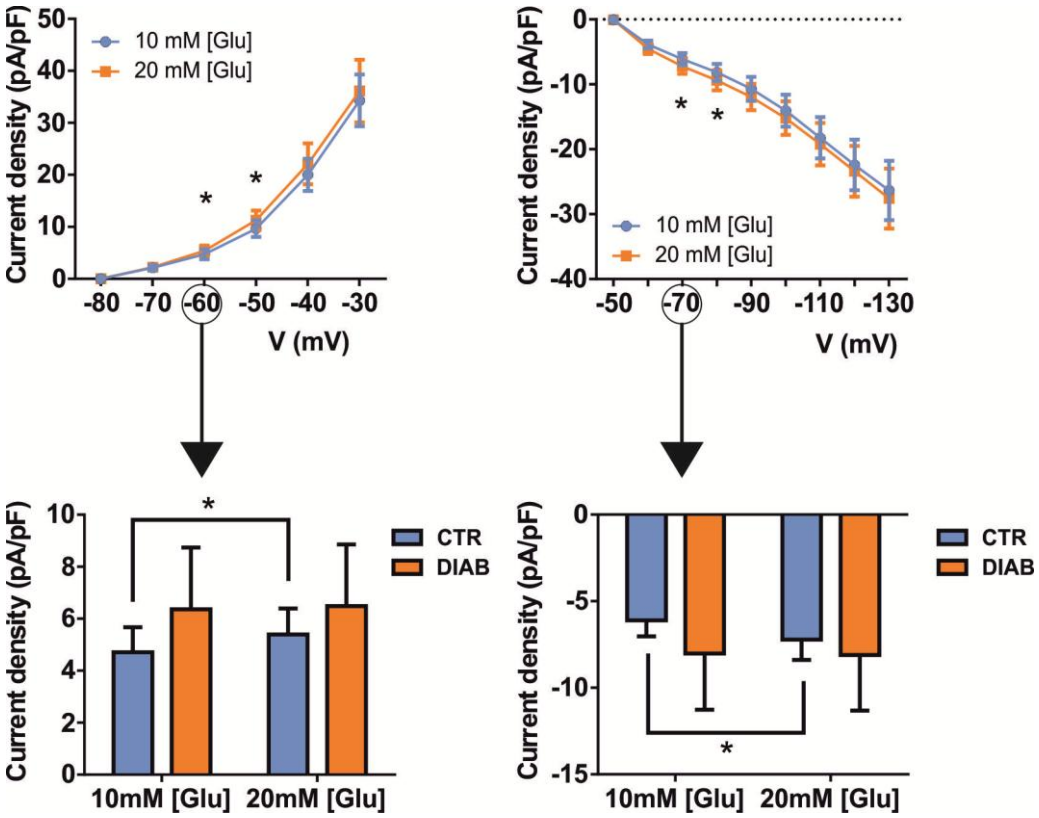

FIGURE 3. 10 CURRENTS IN GLUCOSE-ENRICHED ACSF.
Mean currents measured after perfusion with normal aCSF (10mM[Glu]) and glucose-enriched aCSF (20mM[Glu]) to mimic hyperglycemia. DRG CTR neurons showed an higher mean current after perfusion with glucose-enriched aCSF, while DIAB neurons did not show any change (CTR n=10, DIAB n=9; *P<0.05, Wilcoxon test). *Abbreviations:* CTR= control, DIAB=diabetic, Glu=glucose).

3.2 PHYSIOLOGICAL EFFECT OF GDNF ADMINISTRATION ON DRG NEURONS IN CONTROL AND DIABETIC MICE

3.2.1 PATCH-CLAMP CHARACTERIZATION OF DRG NEURONS AFTER GDNF ADMINISTRATION.

The aim of the present study was to test whether acute application of GDNF modulates neuronal excitability of DRG neurons and whether such modulation is altered in diabetic condition. The concentration of GDNF used (100 ng/mL) was based on dose-response curves from a previous report (Matheson et al., 1996) to provide the maximal effect for sensory neurons. All the protocols described in the previous section were repeated in presence of GDNF (bath-applied for 5-10 min).

GDNF effects on active membrane properties in current clamp mode are reported in Table 3.5 and two representative recorded traces in Figure 3.11. In CTR neurons (n = 19), GDNF induced a significant increase in the AP latency (from 31.16 ± 17.55 ms to 66.43 ± 26.33 ms; $P<0.05$, Wilcoxon test). This effect was not observed in diabetes, in which GDNF only induced a slight hyperpolarization of action potential threshold (from -33.44 ± 1.63 mV to -37.90 ± 3.13 mV; $P<0.05$, Wilcoxon test).

TABLE 3.5

	CTR (n=19)	CTR + GDNF	DIAB (n=17)	DIAB + GDNF
Rheobase (pA/pF)	8.54 ± 1.45	9.43 ± 1.47	8.18 ± 1.54	8.84 ± 1.44
Threshold (mV)	-39.10 ± 1.64	-36.91 ± 2.32	-33.44 ± 1.63*	-37.90 ± 3.13
Latency (ms)	31.16 ± 17.55*	66.43 ± 26.33	19.02 ± 3.54	18.57 ± 3.59
Overshoot (mV)	46.40 ± 2.10	45.04 ± 3.03	46.56 ± 3.32	46.66 ± 3.01
Rise time 20-80% (ms)	0.39 ± 0.04	0.40 ± 0.03	0.59 ± 0.08	0.56 ± 0.06
Max rise slope (mV/ms)	131.16 ± 14.36	122.09 ± 15.54	90.28 ± 13.31	89.19 ± 11.59
Time of max rise slope (ms)	14.76 ± 0.19	14.38 ± 0.42	14.71 ± 0.14	14.84 ± 0.24
Max decay slope (mV/ms)	63.84 ± 10.20	58.80 ± 9.98	43.99 ± 5.54	46.10 ± 7.06
Time of max decay slope (ms)	18.03 ± 0.60	18.40 ± 1.18	18.73 ± 0.80	18.52 ± 0.73

*P<0.05, Wilcoxon test between pre and post GDNF administration, within CTR and DIAB categories. P<0.05 Mann-Whitney test between CTR and DIAB.

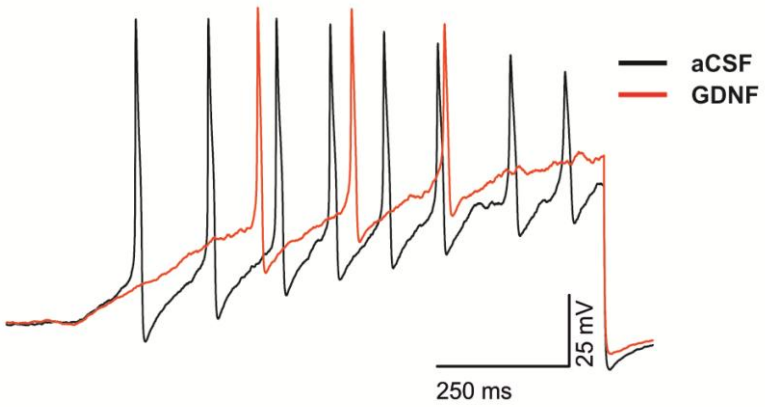

FIGURE 3.11 SUPERIMPOSED APS BEFORE AND AFTER GDNF.

Interestingly, previously described differences between CTR (n=19) and DIAB (n=17) neurons in threshold and kinetics were abolished in presence of GDNF.

As previously described, the involvement of putative voltage-sensitive mechanisms was evaluated by replicating current clamp protocols under hyperpolarized conditions (V_m -85 mV). In CTR neurons, the effect of GDNF on action potential latency observed under resting conditions was inverted (from 71.81 ± 27.83 ms to 39.44 ± 19.11 ms; P<0.01, Wilcoxon test). Other parameters were instead significantly increased (i.e. rheobase, threshold), indicating an overall higher resistance to fire following GDNF application (Table 3.6). No major effects were instead observed in DIAB neurons, except for small changes in action potential kinetics (Table 3.6).

TABLE 3.6

	CTR (n=19) hyper	CTR hyper + GDNF	DIAB (n=17) hyper	DIAB hyper + GDNF
Rheobase (pA/pF)	11.80 ± 1.29*	14.32 ± 2.11	11.38 ± 1.59	11.86 ± 1.58
Threshold (mV)	-44.21 ± 1.87*	-39.85 ± 2.60	-36.62 ± 2.39	-36.11 ± 2.21
Latency (ms)	71.81 ± 27.83**	39.44 ± 19.11	35.46 ± 22.95	73.73 ± 34.66
Overshoot (mV)	42.29 ± 2.61	41.18 ± 2.91	47.65 ± 2.87	47.13 ± 3.16
Rise time 20-80% (ms)	0.39 ± 0.04	0.41 ± 0.03	0.52 ± 0.06*	0.57 ± 0.05
Max rise slope (mV/ms)	128.96 ± 14.20	120.74 ± 16.29	106.60 ± 14.66*	96.69 ± 12.71
Time of max rise slope (ms)	14.59 ± 0.16	14.71 ± 0.13	15.87 ± 1.31	16.08 ± 1.20
Max decay slope (mV/ms)	61.32 ± 9.21	62.03 ± 8.95	49.27 ± 7.61	47.07 ± 7.57
Time of max decay slope (ms)	17.43 ± 0.60*	17.27 ± 0.49	19.69 ± 1.20	19.66 ± 1.20

*P<0.05, **P<0.01, Wilcoxon test between pre and post GDNF administration in hyperpolarized condition, within CTR and DIAB categories. P<0.05 Mann-Whitney test between CTR and DIAB.

The same parameters were analyzed after pooling the data according to "small-sized" and "medium-sized" categories (Figure 3.12). Under resting condition, GDNF increased the rheobase in small-sized CTR neurons only (from 7.52 ± 1.86 pA/pF to 9.35 ± 1.91 pA/pF; CTR n=11, DIAB n=9; P<0.05, Wilcoxon test) and, after hyperpolarization, also increased the threshold (-44.00 ± 3.07 mV to -38.10 ± 3.97 mV; *P<0.05, **P<0.01, Wilcoxon test).

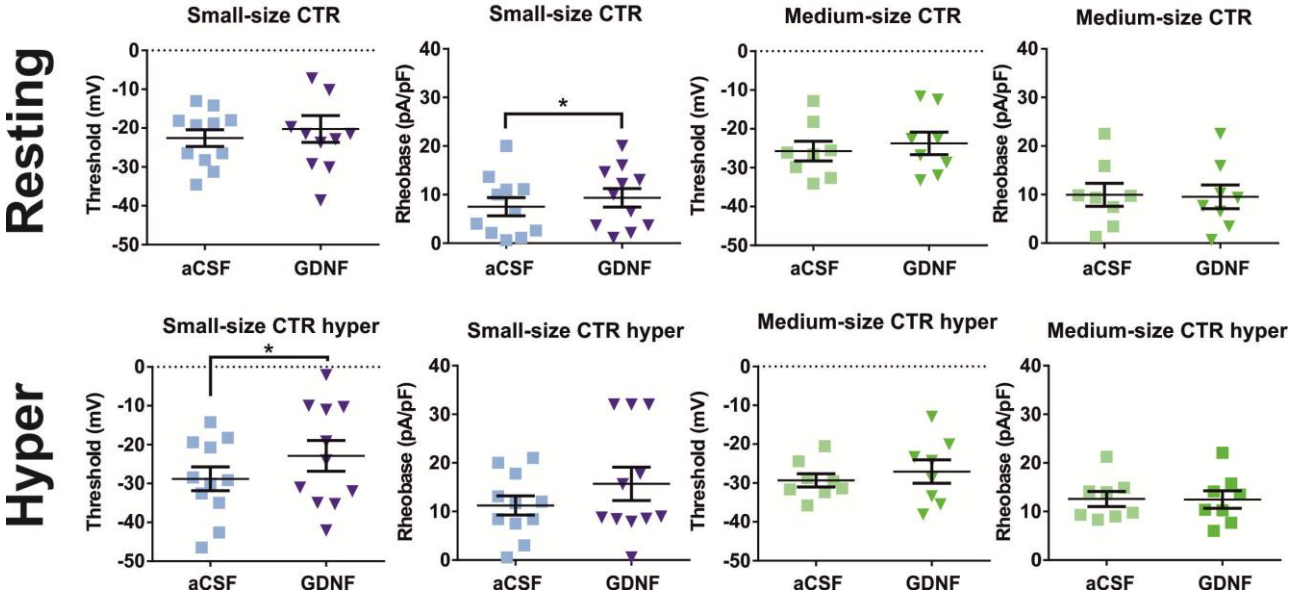

FIGURE 3.12 AP-RELATED PARAMETERS IN CTR – RESTING VS HYPERPOLARIZATION.
AP-related parameters were recorded from CTR (**blue**) small-sized and (**green**) medium-sized neurons before and after GDNF administration and a comparison was made with hyperpolarized condition. The only parameters that differ significantly were in small-sized neurons and were the rheobase, which was lower before GDNF administration, but only in resting condition; and threshold, which was depolarized after GDNF administration, but only in hyperpolarized condition (small-sized n=11, medium-sized n=8; *P<0.05, Wilcoxon test). *Abbreviations*: CTR =control.

In medium-sized neurons, GDNF affected only some action potential kinetics as the maximum decay slope, which was significantly slowed down from 81.76 ± 17.27 mV/ms to 77.55 ± 16.97 mV/ms. No GDNF effects were observed within "small-sized" or "medium-sized" DIAB neurons (Figure 3.13).

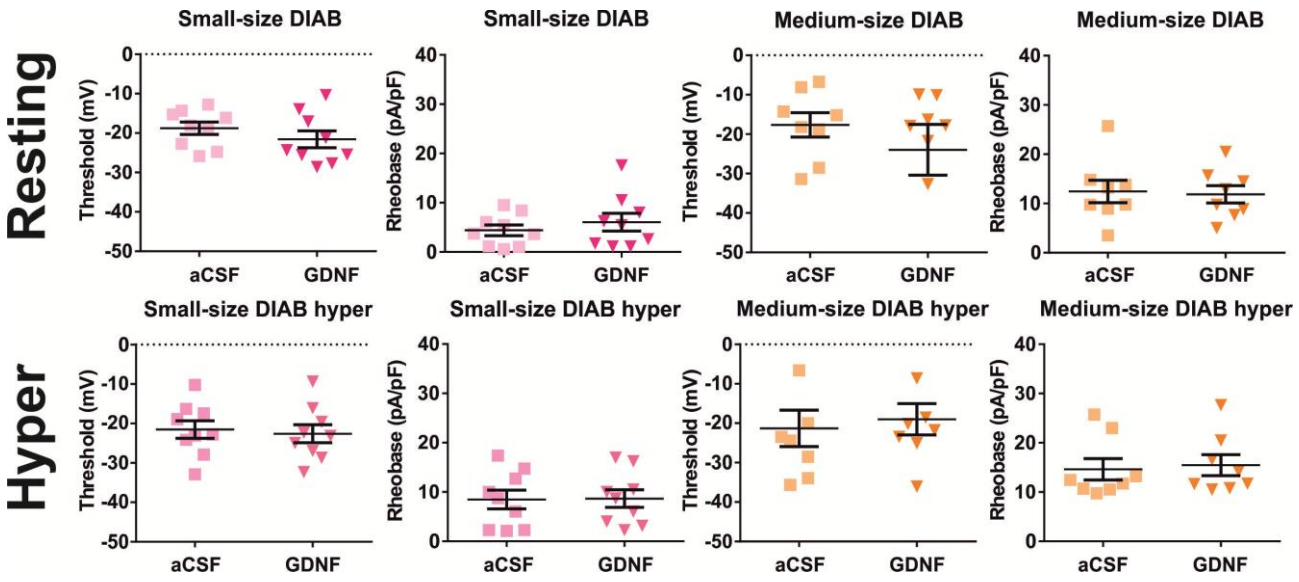

FIGURE 3.13 AP-RELATED PARAMETERS IN DIAB – RESTING VS HYPERPOLARIZATION.
AP-related parameters were recorded from DIAB (**pink**) small-sized and (**orange**) medium-sized neurons before and after GDNF administration and a comparison was made with hyperpolarized condition. No parameters differ significantly in both the condition and size-class (small-sized n=9, medium-sized n=8). *Abbreviations*: DIAB =diabetic.

All together, these data suggest that GDNF may reduce the excitability of DRG neurons from control mice, especially affecting firing properties in small-sized neurons. However, the neurotrophic factor seems to have little effects in neurons from diabetic animals, which already exhibit reduced excitability as compared to control neurons.

3.2.2 VOLTAGE-CLAMP ANALYSIS OF GDNF ADMINISTRATION

The effect of GDNF in voltage clamp was then analyzed applying the same protocols used to investigate the differences between CTR and DIAB neurons in the previous section (Figure 3.5).
First, we performed experiments in regular aCSF by bath-applying GDNF (100 ng/mL) for 5-10 minutes. I-V curves obtained from hyperpolarizing and depolarizing protocols are reported in Figure 3.14.

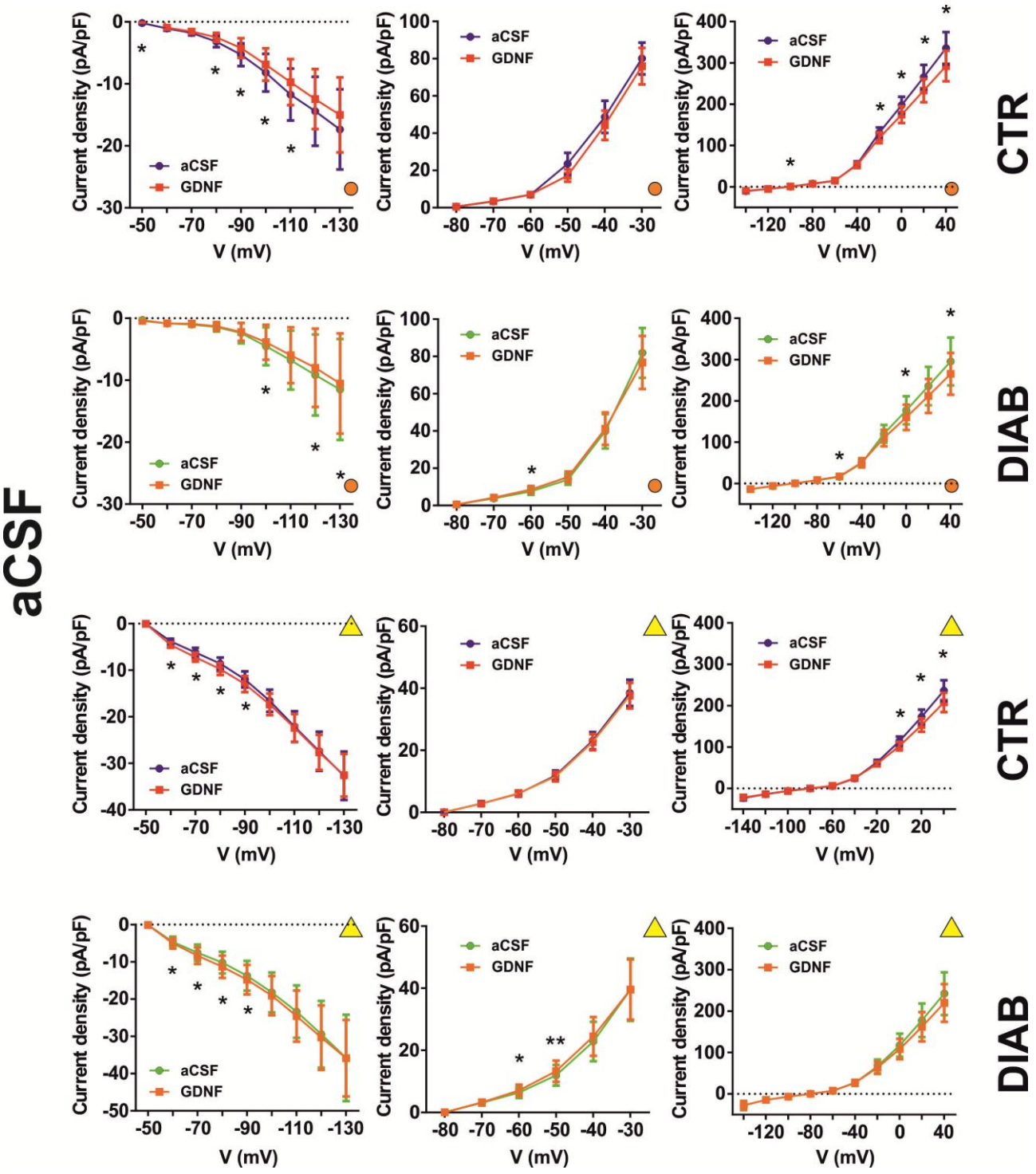

FIGURE 3.14 TOTAL CURRENTS ELICITED IN CTR AND DIAB NEURONS IN ACSF.
Currents were measured at the start (orange circle) and at the middle (yellow triangle) of the traces. Conflicting results were observed analyzing the mean density current, and this contrast depended on the measured point: at the start point, both CTR and DIAB neurons showed a decreased current after GDNF administration, while an increase if measured at the middle point (CTR n=16, DIAB n=17). *Abbreviations:* CTR=control, DIAB= diabetic.

Under these experimental conditions, only slight and conflicting effects can be detected. Indeed, when current measurements (orange circles) were performed at the beginning of the voltage step, GDNF induced a small reduction of the total current in both CTR (n=16) and DIAB (n=17) neurons, even though the effect appeared most prominent in the former. Conversely, a slight current increase of total Kv current was observed when measurements were made on the middle region of the step pulse (yellow triangle). Considering this latter region of measurement (Figure 3.15), the GDNF effect was mostly seen in small-sized CTR neurons as response to the hyperpolarizing protocol (n=9; P<0.05, Wilcoxon test). These data support a putative effect of GDNF in small-sized CTR neurons, as observed in current clamp experiments.

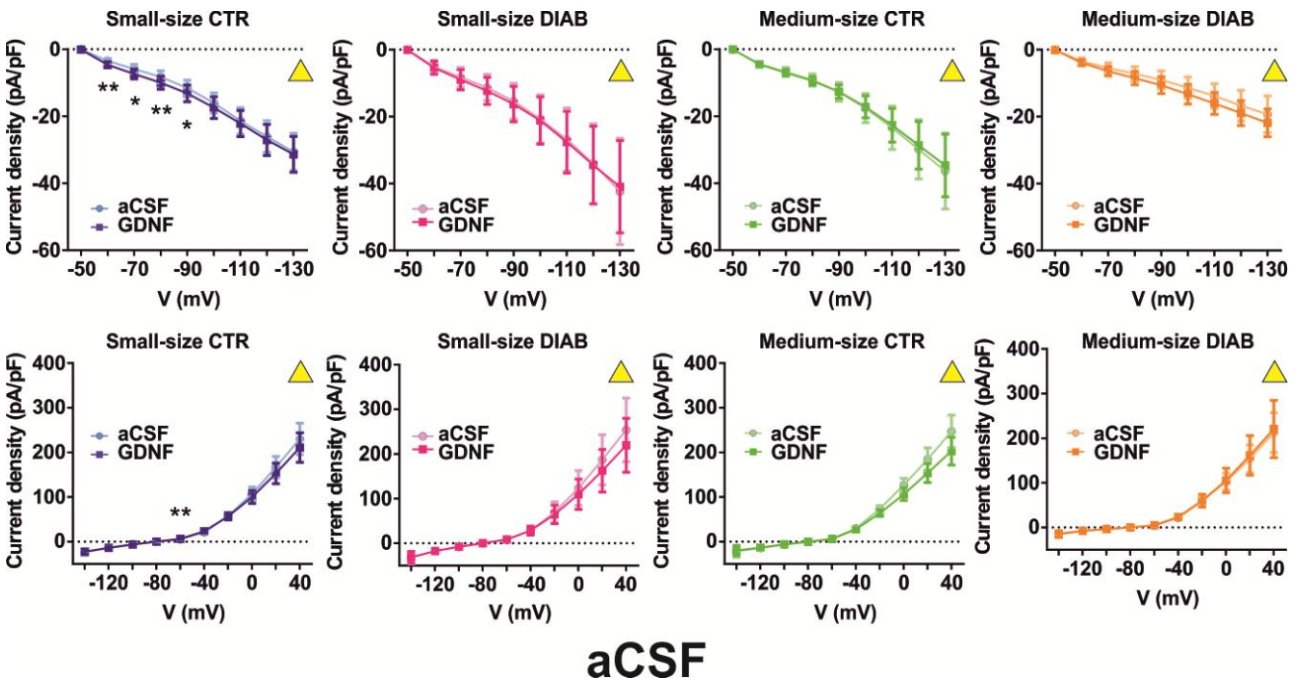

FIGURE 3.15 TOTAL CURRENTS ELICITED IN CTR AND DIAB NEURONS IN ACSF.
Were considered only currents measure at the middle point of the traces (yellow triangle). Analyzing the mean density currents, we observed an increase only in small-sized CTR neurons after GDNF administration (CTR small-sized n=9, medium-sized n=5; DIAB small-sized n=10, medium-sized n=5; *P<0.05, **P<0.01, Wilcoxon test). *Abbreviations:* CTR=control, DIAB= diabetic.

As results obtained in aCSF were rather contradictory, GDNF effect was also analyzed in a ChCl-based aCSF solution (see above) to better explore the putative contribution of voltage-gated K channels in reducing firing activity. First, we analyzed K^+ conductances by applying hyperpolarizing protocol (CTR n=15, DIAB n=15; Figure 3.16). Although an increase of the instantaneous current at the beginning of voltage step (I_{inst}) was observed, it was not statistically significant.

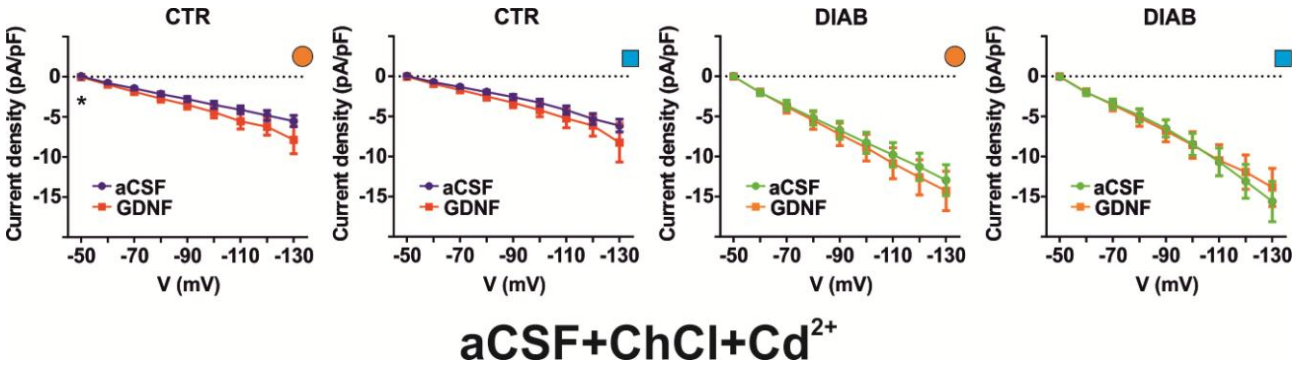

FIGURE 3.16 CURRENTS ELICITED BY HYPERPOLARIZATION IN NA+FREE-ACSF.
No significant difference were noticed before and after the administration of GDNF recurring to an hyperpolarizing protocol (CTR n=15, DIAB n=15).

However, when considering only small-sized neurons, the effect was partially significant at negative voltage steps (CTR n=9, DIAB n=10; P<0.05, Wilcoxon test; Figure 3.17).

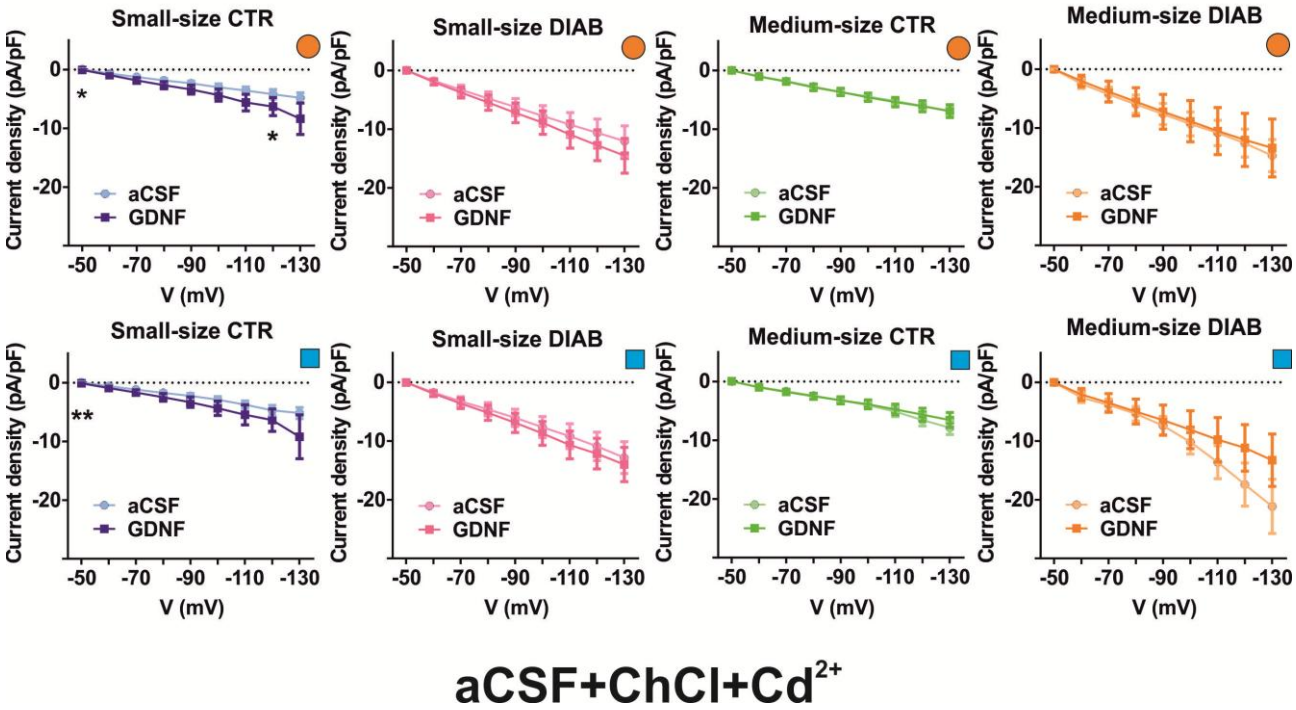

FIGURE 3.17 CURRENTS ELICITED BY HYPERPOLARIZATION IN NA+FREE-ACSF.
The mean density current was significantly increased after GDNF administration, but only in small-sized CTR neurons and at high negative voltages (CTR small-sized n=9, medium-sized n=5;DIAB small-sized n=10, medium-sized n=5; *p<0.05, **p<0.01, Wilcoxon test).

Hyperpolarizing voltage steps often induce a hyperpolarization-activated inward current (I_h) whose amplitude can be calculated as the difference between I_{ss} and I_{ist} (see above). GDNF significantly reduced the amplitude of I_h currents (Figure 3.18). The effect was observed in both CTR (n=15; **P<0.01 and ***P<0.001, Wilcoxon test) and DIAB neurons (n=15; **P<0.01, Wilcoxon test).

This difference was recorded only in small-sized neurons (CTR n=10, DIAB n=10; *P<0.05 and **P<0.01, Wilcoxon test).

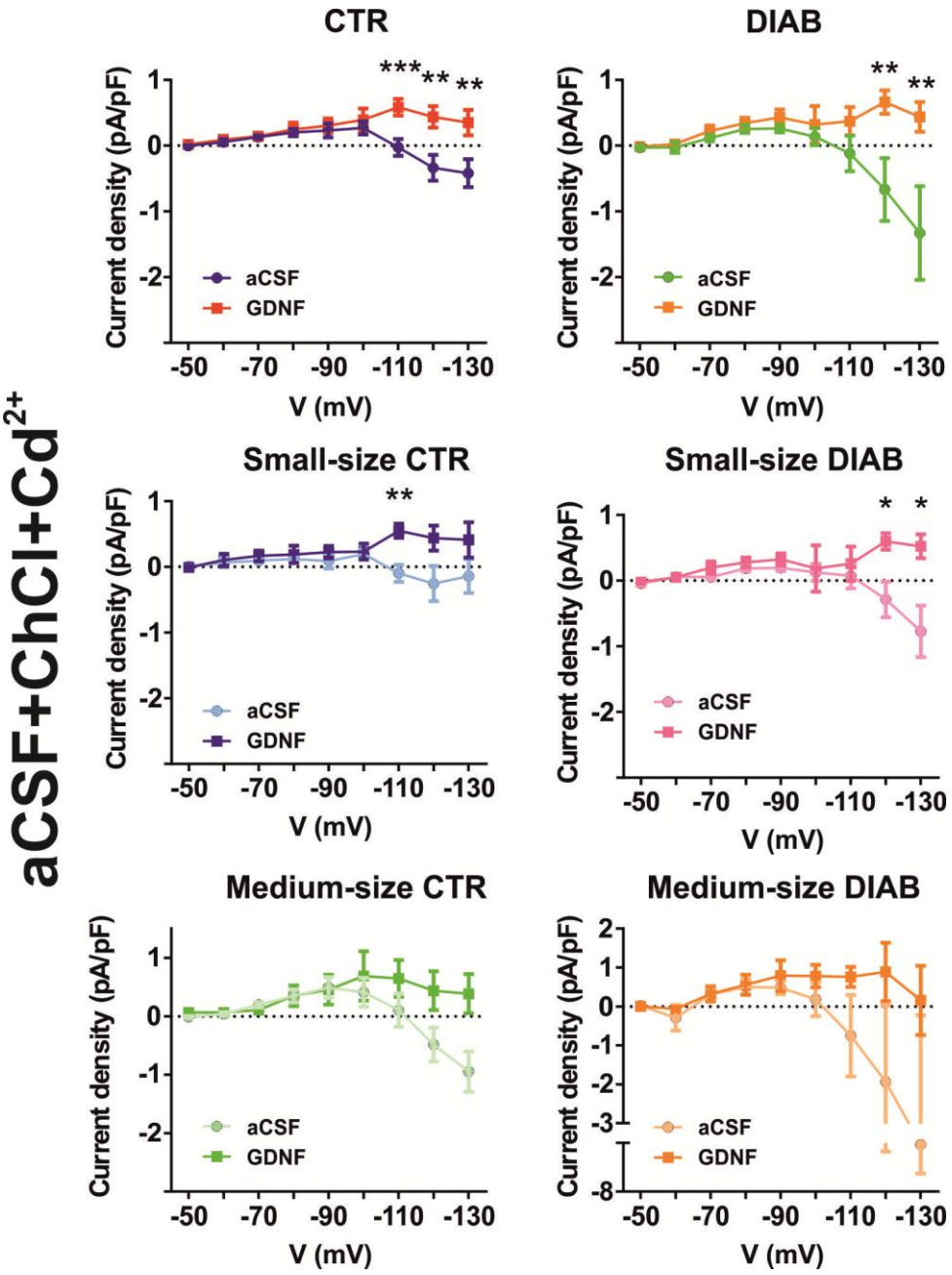

FIGURE 3.18 IH CURRENTS IN NA+-FREE ACSF.
Hyperpolarization-activated inward current (I_h) calculated as the difference between the steady state I_{ss} and I_{ist}. A significant difference was noticed at high negative voltages only in small-sized neurons, both in CTR and DIAB animals. GDNF seemed to block the I_h currents (CTR small-sized n=9, medium-sized n=5;DIAB small-sized n=10, medium-sized n=5; *p<0.05, **p<0.01, Wilcoxon test).

In depolarizing protocols, GDNF administration in CTR neurons did not induce significant changes in total Kv current. However, while delayed rectifying I_K currents were inhibited, transient I_A currents were significantly increased (n=13; *P<0.05,**P<0.01, Wilcoxon test, Figure 3.19). A

similar effect was also detected in DIAB neurons, especially in I_A currents (n=15; *P<0.05, **P<0.01, ***P<0.001, Wilcoxon test).

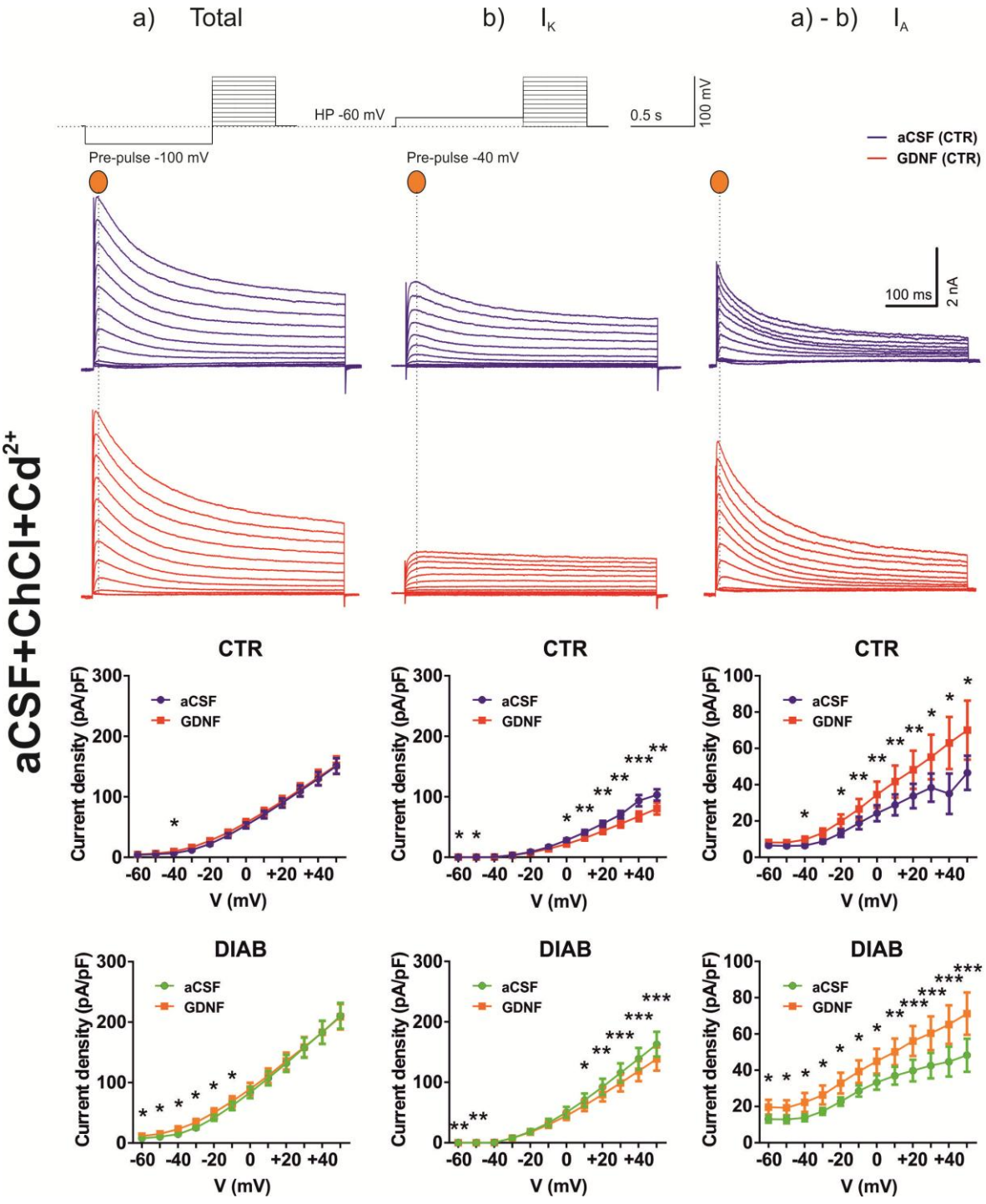

FIGURE 3.19 KV CURRENTS FROM CTR AND DIAB NEURONS IN NA+-FREE ACSF.
Top Representative traces of the total Kv current (left), sustained (centre) and transient Kv currents (right). **Bottom** The mean density of sustained and transient Kv currents of both CTR and DIAB neurons was significantly different after GDNF administration, with a decrease of the sustained component and an increase of the transient component. Contrariwise, the total Kv current did not vary significantly (CTR n=14, DIAB n=15; *P<0.05, **P<0.01, ***P<0.001, Wilcoxon test).

After pooling data according to the cell sizes (Figure 3.20), both small-sized CTR and DIAB neurons showed significant variations after GDNF administration (small-sized CTR n=9, DIAB=10; *P<0.05, **P<0.01, ***P<0.001, Wilcoxon test).

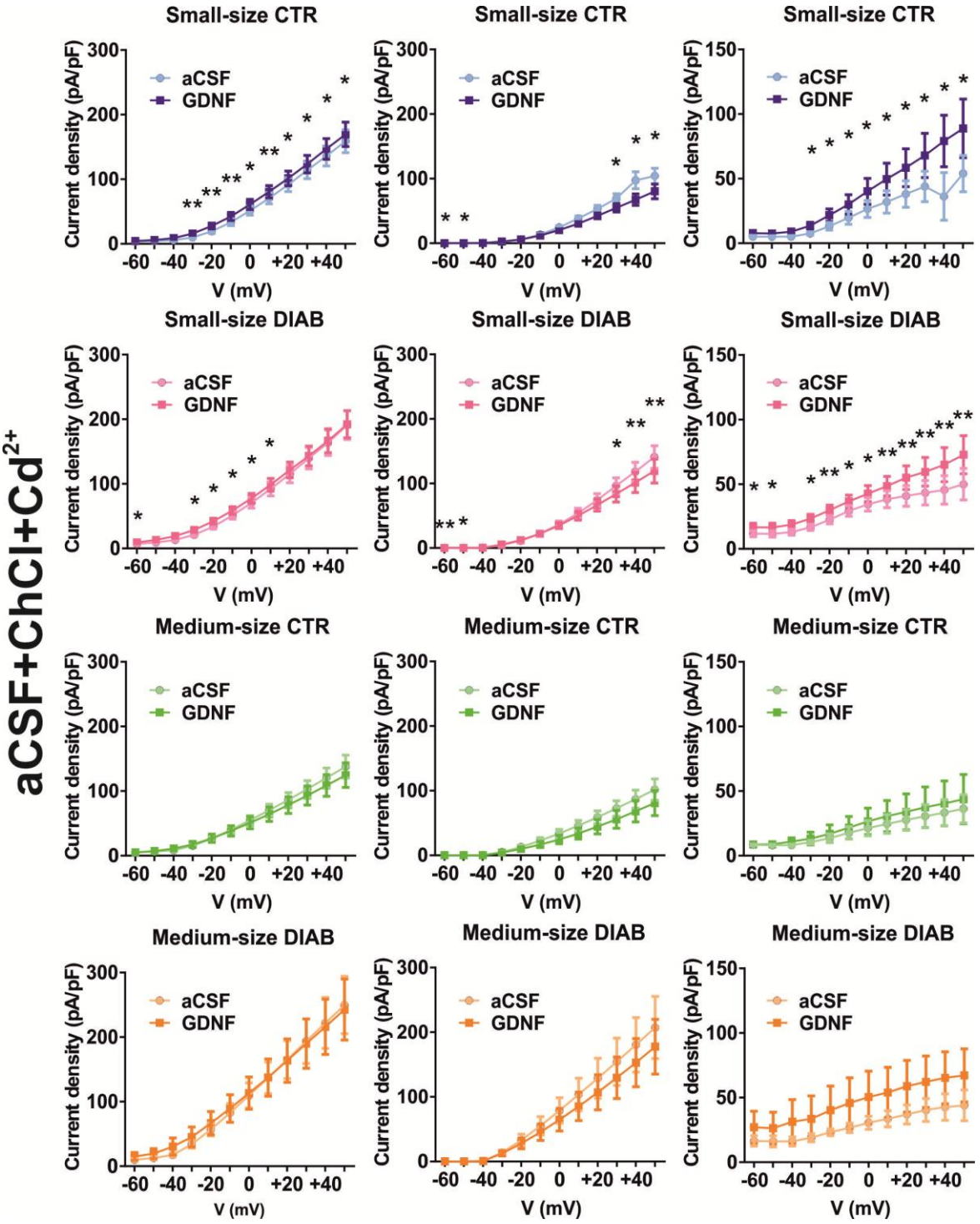

FIGURE 3.20 KV CURRENTS FROM CTR AND DIAB NEURONS IN NA+-FREE ACSF.
The mean density of sustained and transient Kv currents of CTR small-sized neurons was significantly different after GDNF administration, with a decrease of the sustained component and an increase of the transient component. Contrariwise, the total Kv current did not vary significantly. This effect was not measured in small-sized DIAB neurons or in medium-sized both CTR and DIAB (CTR small-sized n=9, medium-sized n=5;DIAB small-sized n=10, medium-sized n=5; *p<0.05, Wilcoxon test

The effect of GDNF persisted, or even increased, for 5-10 minutes after switching to a GDNF-free aCSF solution (Figure 3.21). The persistance of the effect after removing GDNF was particularly evident in small-sized CTR neurons (small-sized CTR n=5; *P<0.05, **P<0.01, ***P<0.001, Friedman test), while in small-sized DIAB neurons only I_A current increased (small-sized DIAB n=5; P<0.05, **P<0.01, ***P<0.001, Friedman test).

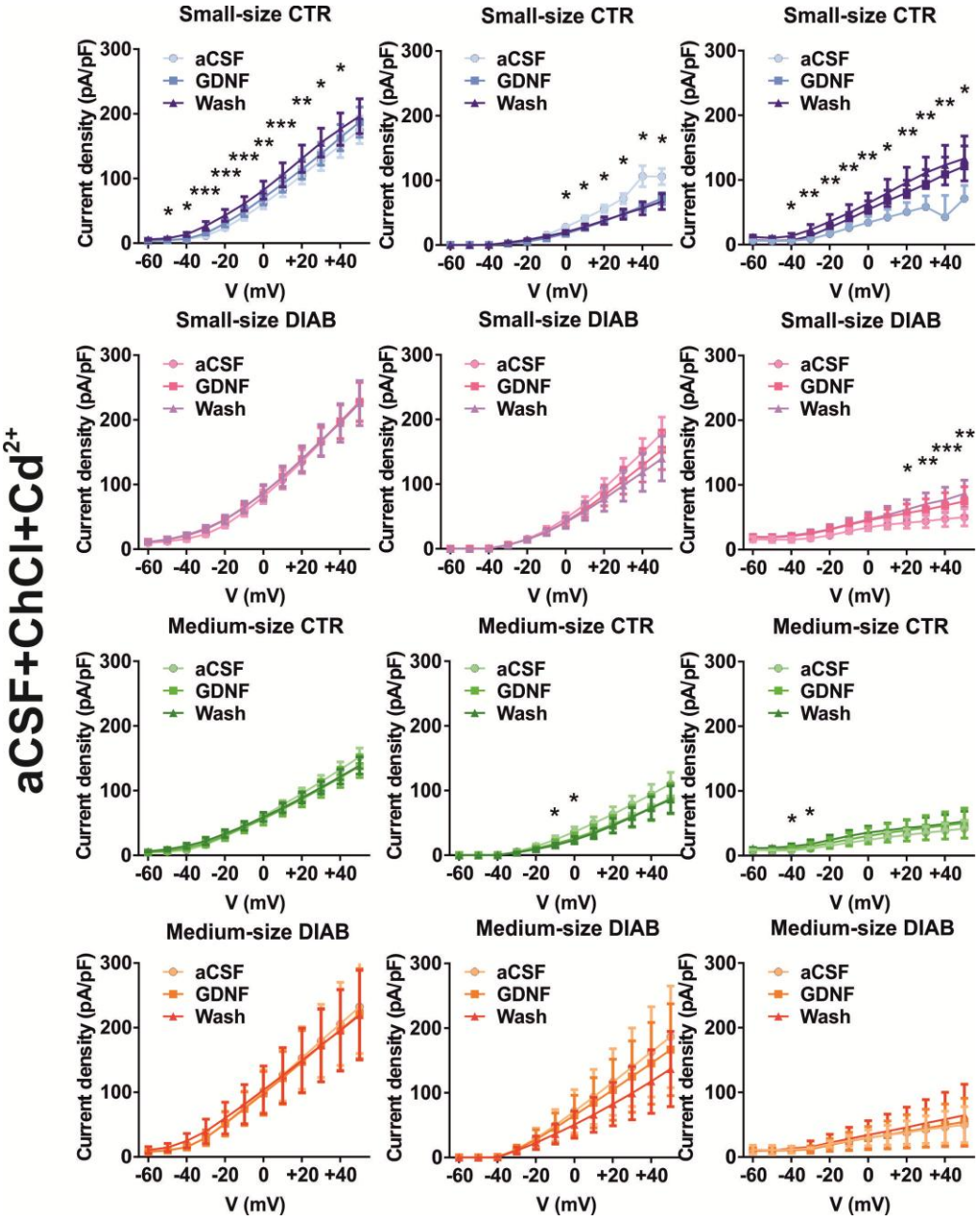

FIGURE 3.21 EFFECTS ELICITED BY GDNF INCREASED IN THE WASH STEP.
Currents were measured at the middle of the traces in CTR and DIAB neurons. The increase of the currents induced by the administration of GDNF was not wash out by 5-min perfusion with ChCl-based aCSF. The major effect was induced in small-sized CTR neurons (small-size CTR n=5, DIAB n=5, medium-sized CTR n=4, DIAB n=3; *P<0.05, **P<0.01, ***P<0.001, Friedman test).

Altought it was not possible to properly washout the GDNF effect in our experimental settings, no significant changes were detected when the same protocols, with similar timing, were applied without GDNF (n=5; not shown).

3.2.3 GDNF EFFECT IN PRESENCE OF VOLTAGE-DEPENDENT K+ CHANNEL BLOCKER

Effects on hyperpolarizing currents were analyzed in presence of Ba^{2+} (100 µM, Tang et al., 2010) to block inwardly rectifying potassium channels (Kir).

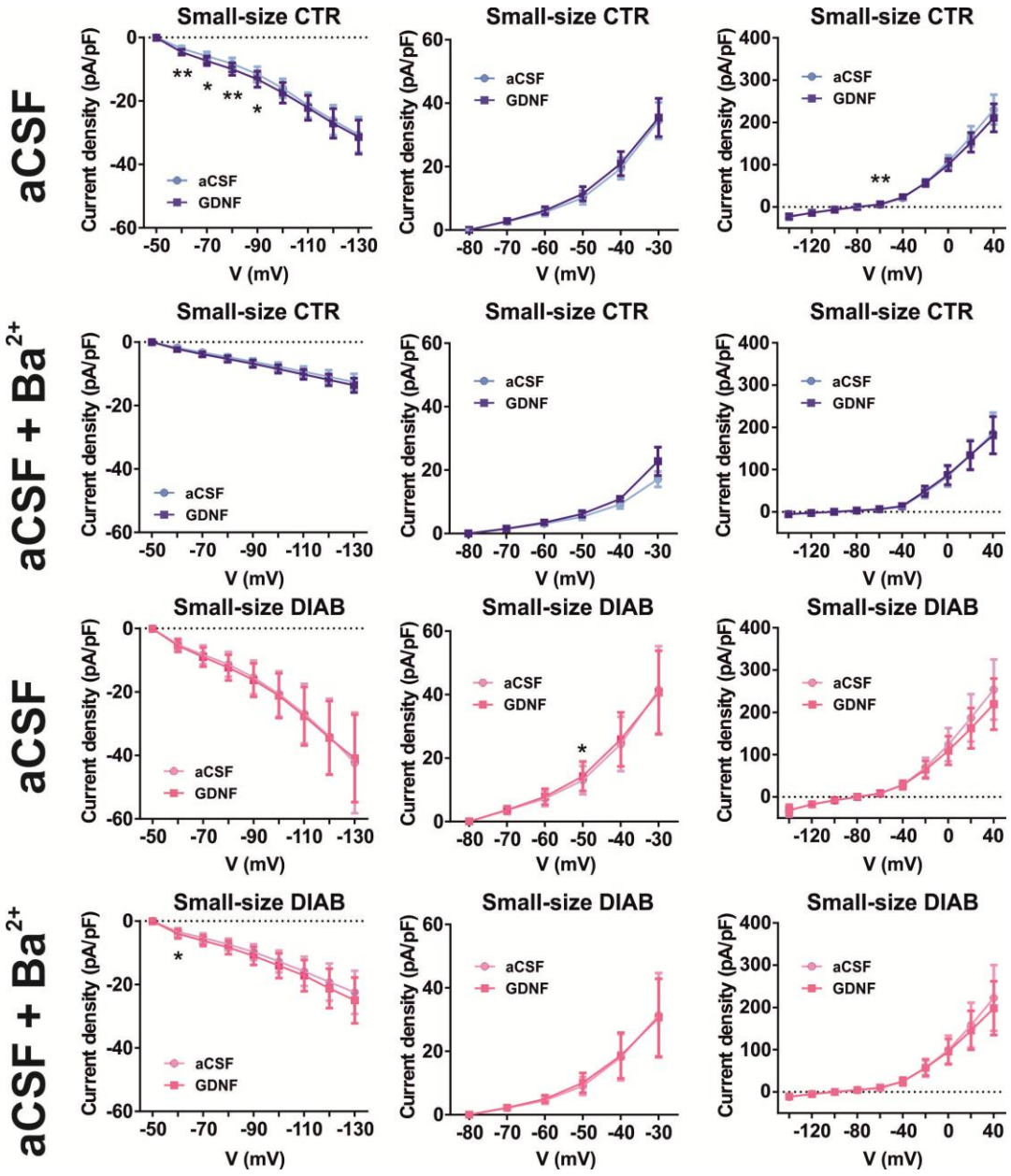

FIGURE 3.22 CURRENTS ELICITED IN CTR AND DIAB NEURONS IN ACSF AND ACSF+BARIUM. Currents were measured at the middle of the traces only in small-sized neurons. The increase of the current induced by the administration of GDNF was detected in CTR neurons. The same experiment was repeated in Barium containing aCSF (100µM) and the effect was lost. However, isolate the specific effect of GDNF in this experimental condition was difficult, so no strong conclusion can be drawn (small-sized CTR n=4, small-sized DIAB n=6).

Experiments were performed in Ba^{2+}-containing normal aCSF with special focus on small-sized CTR (n = 4) and DIAB (n = 6) neurons which are more sensitive to GDNF than medium-sized (Figure 3.22). However, as GDNF effects were difficult to isolate under these experimental conditions (see above), no strong conclusions can be drawn.

In depolarizing protocols, the non-selective K-channels blocker tetraethylammonium (TEA, 25 mM; Tang et al., 2016) was added to the ChCl-based aCSF. Traces shown in Figure 3.23 were recorded from a single small-sized CTR neuron. Despite the presence of TEA, the reduction of I_K currents and the increment of I_A currents following the administration of GDNF was still detectable.

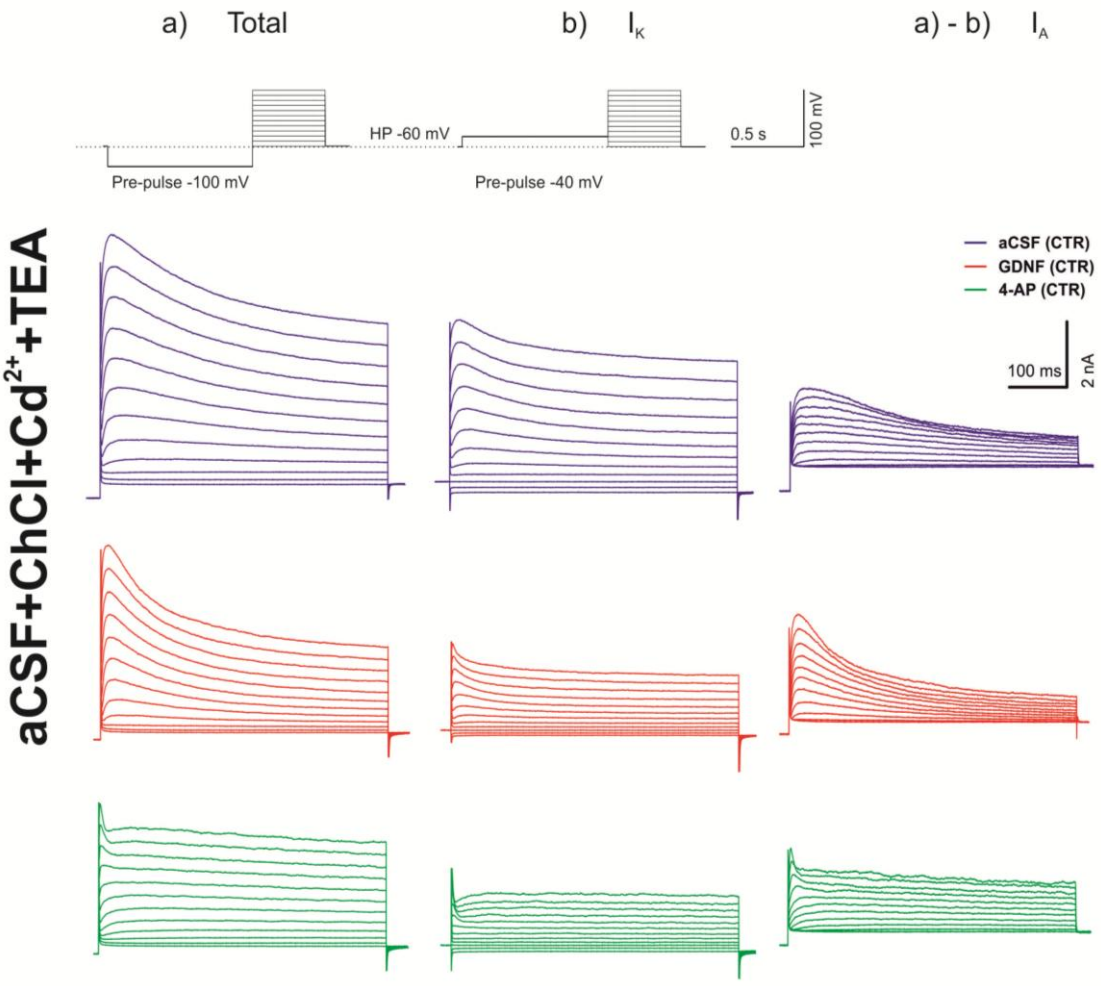

FIGURE 3.23 KV CURRENTS FROM CTR AND DIAB NEURONS IN NA+-FREE ACSF, TEA AND 4-AP. Representative traces of the total Kv current (left), sustained (centre) and transient Kv currents (right) of a small-sized CTR neuron are shown. Despite the presence of the K-channel blocker TEA, the reduction of the sustained component and the increment of the transient component of Kv current were still detectable. The administration of the K-channel blocker 4-AP at the end of the experiment confirm an involvement of the transient component of Kv current in GDNF-mediated effect.

This suggests that at least part of the effect of GDNF is TEA-insensitive. However, bath-applying 4-AP (5 mM; Winkelman et al., 2005) at the end of the experiment, selectively blocked the transient component, confirming a major involvement of I_A currents in GDNF-dependent effects.

The data collected suggest multiple effect of GDNF on K^+ currents, including an increase of the transient component I_A, which seems to be TEA-insensitive 4-AP-sensitive, and an inhibition of the sustained component.

3.3 MORPHOLOGICAL CHARACTERIZATION OF NOCICEPTORS IN DRG IN CONTROL AND DIABETIC MICE

3.3.1 CLUSTERIZATION OF IB4+ NOCICEPTOR SUB-POPULATION IN MICE DRGS

Primary sensory neurons subpopulations can be distinguished using immunofluorescence labeling: peptidergic sensory neurons are labeled by the antibody recognizing CGRP, while non-peptidergic are bound by the marker isolectin B4 dye-conjugated (for in-depth description see Paragraph 1.2.2). During z-stacks confocal acquisition of entire DRGs, a particular distribution of IB4+ nociceptors was observed, as shown in Figure 3.24. IB4+ neurons tended to aggregate in structures that can be called “clusters”, in which some cell’s surfaces seem in direct contact to each other. Conversely, CGRP+ neurons did not show this type of cell distribution, being completely separated each other. The *3DRG* tool, used for 3D reconstruction of entire DRGs, was optimized and employed to have a validating analysis of the cluster distribution and to verify if these structures could be altered in the presence of diabetes.

Being a semi-automated software, *3DRG* required some manual inputs that were inserted by an operator: *i)* the size of the cells of interest (*Vref*); *ii)* the size threshold between single cell and cluster (V_{cls}). *Vref* was set considering a diameter size of 20 µm for IB4+ neurons and a diameter size of 25 µm for CGRP+ neurons. These diameter sizes are consistent with manual measurements performed on our images (Figure 3.24), as well as with previously published literature data (Stucky and Lewin, 1999b; Kestell et al., 2015). Then, all the positive objects found during the preprocessing were normalized for *Vref* and only the objects with a value higher than the 85^{th} percentile were accounted as clusters. This decision was justified by the need to face the internal variance of cellular sizes, mostly for CGRP+ neurons, which sizes ranged in a broad spectrum (Figure 3.24).

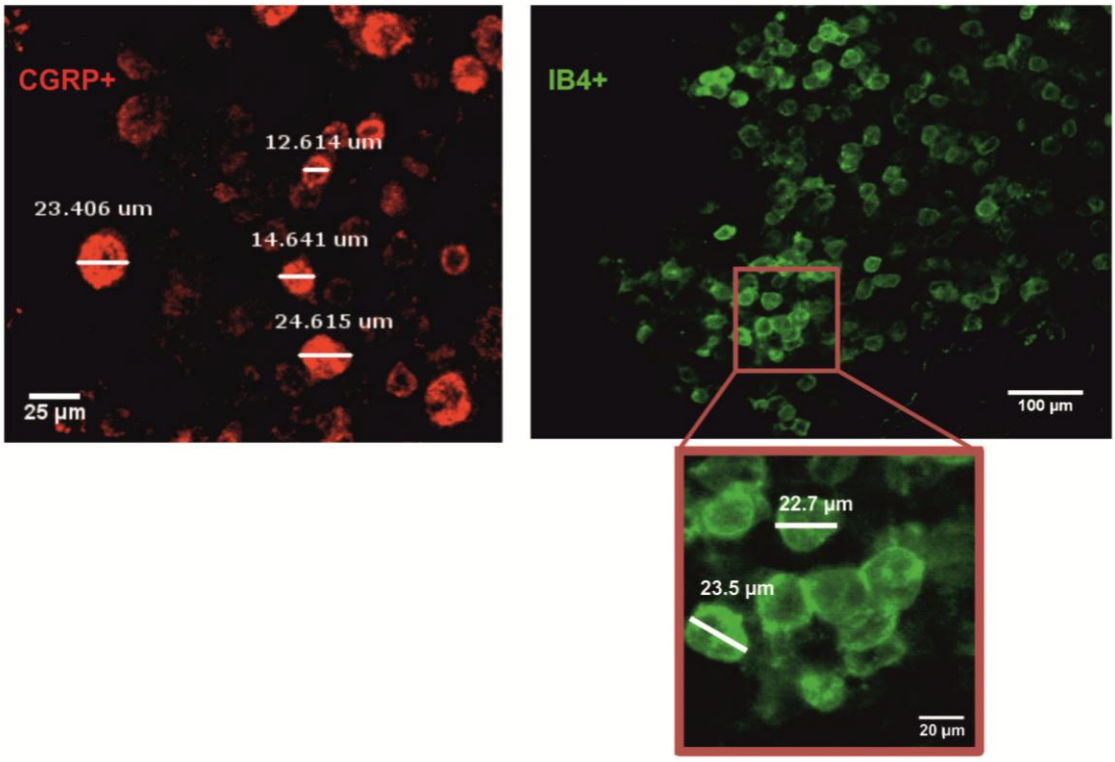

FIGURE 3.24 DIFFERENT SIZES OF PEPTIDERGIC AND NON-PEPTIDERGIC POPULATIONS

Parameters obtained were: the median volume of cluster normalized for *Vref* ($V_{med\ cls}$), the mean number of cells per cluster ($N°_{cell}$), the percentage of cells involved in cluster on the total amount of cells (%cluster 1) and the percentage of volume belonging to cluster on the total amount of volume (% cluster 2) (Table 2.1). Analysis was carried out on 147 different DRGs, which includes 48 CTR samples and 57 DIAB samples for IB4+ neurons, and 58 CTR samples and 56 DIAB samples for CGRP+ neurons. Data obtained from semi-automated analysis not only confirmed the tendency of IB4+ cells to form clusters but also provided other features of this configuration: around 15% of the total positive objects found were clusters and this 15% occupied around 80% of the total positive volume (Table 3.7; Figure 3.25). IB4+ clusters were usually composed of 4/5 cells each and the $V_{med\ cls}$ was about 2.5 times V_{ref}. The discrepancies between this two latter data can be explained by the fact that the mean number of cells present in each cluster is the mean obtained dividing the volume of clusters higher than 75th percentile for V_{ref}, while the $V_{med\ cls}$ is the median of all clusters' volume divided for V_{ref}.

TABLE 3.7 Output of *3DRG* software analysis

Marker	Treatment	N° cell per cluster	% cluster 1	% cluster 2	$V_{med\ cls}$	Positive volume (mm^3)	ROD
IB4+	CTR	4.70±0.26	15.24±0.65	80.36±1.09	2.40±0.09	0.0194±0.001	140.14±18.64
	DIAB	4.28±0.24	15.08±0.55	78.21±1.39	2.34±0.09	0.0196±0.001	201.17±25.84
CGRP+	CTR	1.89±0.11	8.45±0.37	56.87±2.02	1.75±0.04	0.0176±0.001	192.54±8.48
	DIAB	1.65±0.08	7.84±0.35	52.79±2.18	1.81±0.06	0.015±0.001	189.53±12.02

As shown in Figure 3.25, the comparison of all these parameters between IB4+ and CGRP+ neurons resulted significantly different (P<0.001, Mann-Whitney test). CGRP+ neurons do not form clusters, thus both the number of cells per cluster and the $V_{med\ cls}$ are expected to be 1.

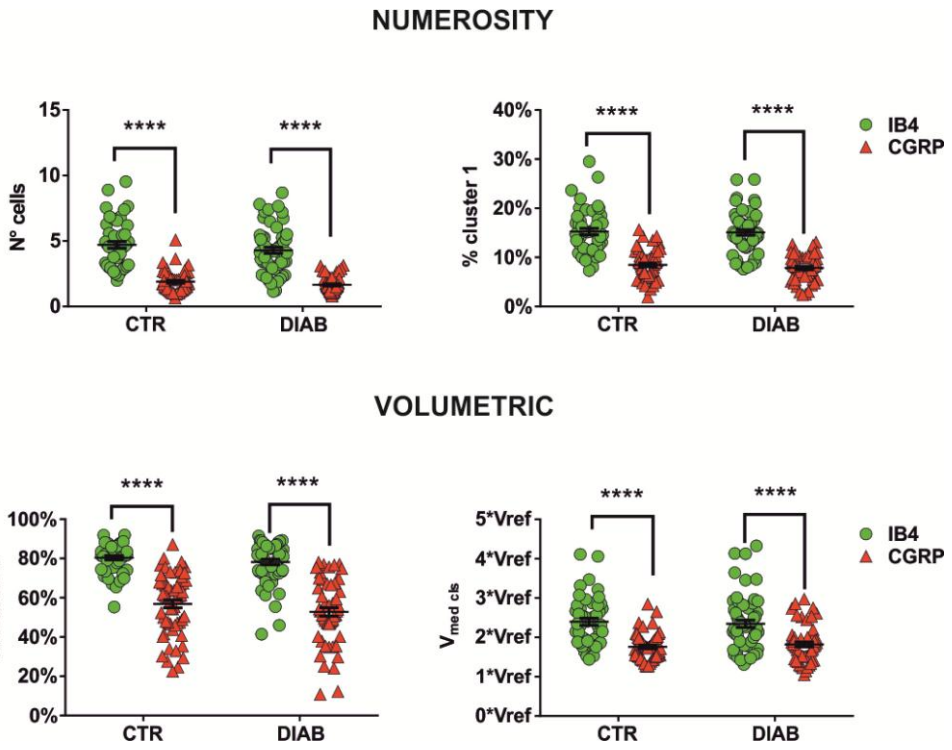

FIGURE 3.25 STATISTICAL ANALYSIS OF *3DRG* OUTPUT DATASET.
Parameters analyzed were the number of cells per cluster, the percentage of the total volume detected as positive fluorescence that is involved in cluster (%cluster1), the percentage of volume occupied by cluster on the total volume of the DRGs (%cluster2) and the size relationship with Vref.

In our samples, the number of cells/cluster was 1.89 and the $V_{med\ cls}$ 1.76, both in CTR and DIAB. This deviation from the expected values was due to the heterogeneous sizes that characterize CGRP+ neurons in respect to IB4+ cells. Regarding the comparison between CTR and DIAB samples, no significant differences were outlined in both the cellular subpopulations.

The cluster organization of IB4+ neurons was not described previously. We hypothesized that the cluster distribution may have a role in the cross-talk between IB4+ neuronal somata.

3.3.2 Alterations in satellite glial cell morphological organization in DRG from diabetic mice

Direct neuron-to-neuron communication in DRGs is limited by the presence of a thin layer of satellite glial cells (SGCs) which individually ensheats and insulates sensory neurons. At the same time, SGCs may indirectly mediate cross-talk between neuronal somata by forming "sandwich synapses" (Rozanski et al., 2013).

Since different neuronal populations exhibit different patterns of spatial organization, the level of cell coverage by SGCs may differ within specific cell populations and may be differentially compromised in pathological conditions.

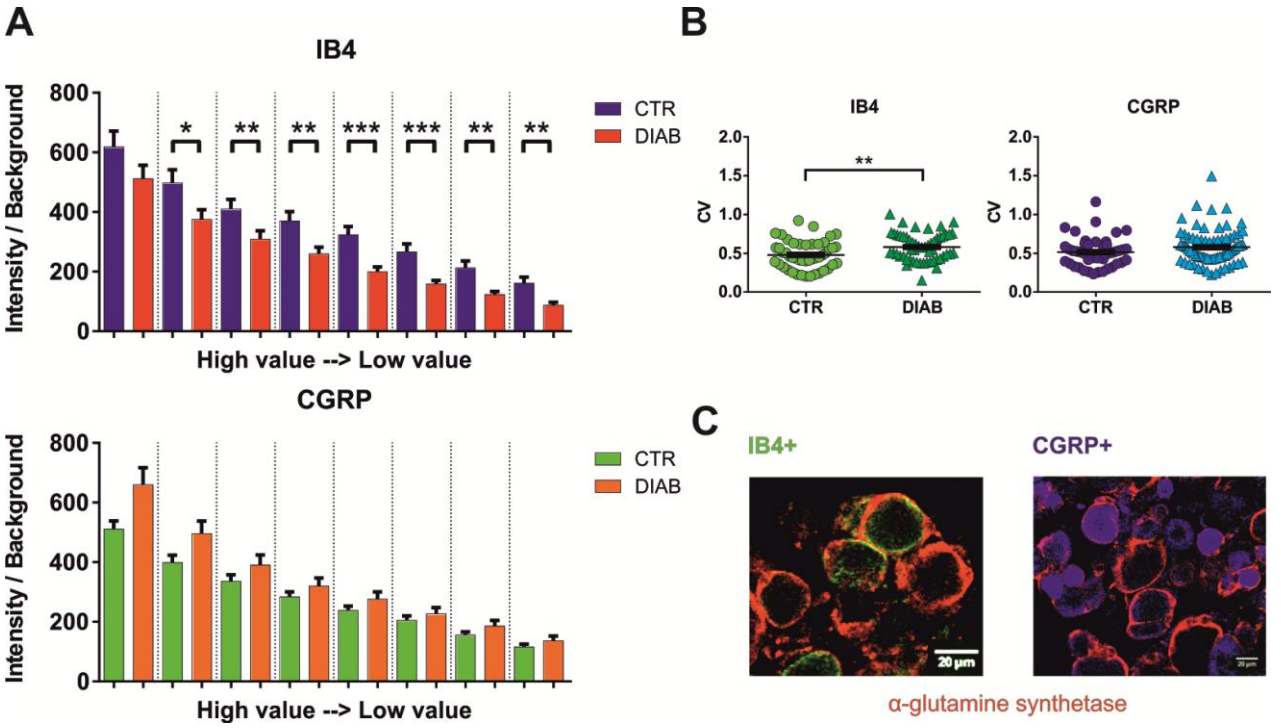

FIGURE 3.26 ANALYSIS OF SGCS ENSHEATMENT.
A Graphs of the mean intensity values of SGCs ensheathment measured around CGRP+ and IB4+ neurons; **B** Graphs of the coefficient of variation; **C** images showing the three different population (**red** SGCs, **green** IB4, **blue** CGRP). Statistic for the analysis performed: *P<0.05, **P<0.01, ***P<0.001, Mann-Whitney test).

To test this hypothesis the cell-specific SGCs ensheathment was analyzed in 7 CTR DRGs and 8 DIAB DRGs, for a total account of 47 CTR neurons and 54 DIAB neurons. Entire DRGs were harvested and triple stained for IB4+, CGRP+ and α-glutamine synthetase (GS), a marker of SGCs. The staining for these two markers allowed their characterization, while the stain for the latter the analysis of the ensheatment degree (for in-depth description of the method, see Paragraph 2.11).

This analysis was performed in IB4+ and CGRP+ subpopulations (Figure 3.26 C), in the presence of diabetes or not. Interestingly, a significant difference existed in IB4+ subset between CTR and DIAB neurons (Figure 3.26 A), with a decrease of the fluorescence in the latter, suggesting a reduction of the coverage due to SGCs in diabetic conditions (*P<0.05; **P<0.01, ***P<0,001, Mann-Whitney test).

On the contrary, SGCs staining upon CGRP+ neurons was increased around DIAB neurons, but it was not significant. Moreover, the coefficient of variation of fluorescence around the cell circumferences appeared to be significantly higher in DIAB IB4+ neurons as compared to CTR (P<0.01, Mann-Whitney test; Figure 3.26 B), indicating a higher degree of variance of fluorescence around the cell membrane, which might reflect defective SGCs covertures. This difference was not present in CGRP+ neurons.

These data suggest a putative alteration of SGCs in diabetic condition, with a reduction of the ensheatment around IB4+ neurons and an increase around CGRP+ neurons. The reduction of SGC coverage in cells with high tendency to cluster may promote direct cross-talk between neurons and account for aberrant encoding in pathological settings.

4 DISCUSSION

4.1 FUNCTIONAL ALTERATIONS IN SENSORY NEURONS ASSOCIATED WITH DIABETES AND ROLE OF GDNF

4.1.1 FUNCTIONAL ALTERATIONS OF SENSORY NEURONS IN DRG OF DIABETIC MICE

Diabetic peripheral neuropathy (DPN) is characterized by a length-dependent alteration of the sensory system. Neuropathy typically starts at small nerve fibers, giving rise to hyperalgesia and allodynia, which consists in an increased sensitivity to painful and non-painful stimuli, respectively (Callaghan et al., 2012). Then a further advancement causes dysfunction and degeneration of larger myelinated fibers, with the consequent sensory ataxia and decreased proprioception (Tesfaye and Selvarajah, 2012). Eventually, hypoalgesia and completely sensory loss characterizes the advanced stage of peripheral neuropathy (Callaghan et al., 2012), although a highly variable constellation of sensory loss- and gain-of-function can be expressed (Themistocleous et al., 2016).
In the present study, functional properties of primary sensory neurons were analyzed in a STZ-induced model of type 1 diabetes in mice. The model was chosen as it induces a strong diabetic phenotype in few days after a single high dose of STZ and thus allows to generate highly reproducible diabetic phenotypes (see King, 2012 for review). To further maintain reproducibility, mice were all sacrificed one month after diabetes induction. At this stage, it was reported that CD1 male mice exhibit thermal and mechanical hypersensitivity (Courteix et al., 1996; Pabbidi et al., 2008). Finally, to preserve the anatomical configuration and cell-to-cell interactions, functional experiments were performed ex vivo on intact DRGs rather than in dissociated DRG cultures, allowing to analyze physiological cell properties in experimental conditions mimicking *in vivo* settings (Ciglieri et al., 2016b; Gong et al., 2016).

One of the main findings emerging by this study was that neurons from diabetic mice exhibit reduced excitability and higher resistance to fire. Action potentials showed indeed a higher threshold and slower kinetics as compared to neurons from control mice. By sorting neurons according to the size (Stucky and Lewin, 1999b; Kestell et al., 2015), differences in firing properties between small and medium populations were more prominent in diabetes, with a substantial increase of action potential latency and kinetics in small neurons. Moreover, not only

small neurons appeared more sensitive to diabetes-induced changes but among them, non-peptidergic IB4+ neurons turned out to be the more affected population. These observations are consistent with firing profiling published by Choi et al. (2006), in which IB4+ neurons presented a physiological more negative AP threshold than IB4- ones. Interestingly, this difference was lost in diabetes. All together, these data indicate a reduced excitability of DRG neurons from diabetic mice, particularly in the non-peptidergic population.

Several voltage-gated channels (Nav channels, Kv channels, Cav channels) may have an altered expression and/or function in DPN (Hong et al., 2004; Cao et al., 2010; Waxman and Zamponi, 2014). Interestingly, while firing properties in control DRG were very sensitive to hyperpolarization (increase in rheobase, threshold, latency), the effect was largely lost in diabetes. This observation led to speculate that voltage-dependent potassium conductance might play a role in the observed differences.

Results from voltage clamp experiments confirmed this hypothesis suggesting an upregulation of Kv channels activity in diabetes, with a major involvement of fast inactivating component A-type (I_A) isolated in depolarizing protocols and of the leak current in hyperpolarizing protocols, which are likely mediated by inward rectifier potassium channels (Rateau, 2006). Importantly, this enhancement was only found in small-sized neurons, while in the medium-sized ones K^+ conductances resulted unvaried.

The observation of an overall impairment of cell excitability in small DRG neurons well support clinical observations indicating a decreased conduction velocity in peripheral nerves with particular reference to small fibers neuropathy (Cummins and Dorfman, 1981; Erdoğan et al., 2013), as well as preclinical studies in STZ diabetic mice which confirm the hypofunction of peripheral nerves in diabetes (Murakami et al., 2013). Interestingly, the observation that reduced excitability might be particularly prominent in IB4+ neurons is in strongly agreement with histological investigations indicating that non-peptidergic fibers in STZ diabetic mice were more vulnerable to diabetes (Akkina et al. 2001). Of course, reduced conduction velocity may be due to the degeneration process at distal peripheral afferent or to segmental demyelination rather than alterations in the cell soma (Toth et al., 2004); however, impaired nerve function is observed at early stage of diabetes, when degenerative process and reduction of fiber number is not detected yet (Shaikh and Somani, 2010), suggesting more complex molecular alterations likely involving ion channels.

On the other hand, most of the in vitro studies reported increased excitability of sensory neurons from diabetic animals (Cao et al., 2010; Hirade et al., 1999). Specifically, in a rat model of diabetes

a marked reduction of the densities of total Kv, A-type (I_A) and sustained delayed (I_K) currents was observed, particularly in medium- and large-sized neurons in diabetic condition, while small-sized neurons resulted unaffected (Cao et al., 2010). These results are partly in contrast with the findings in the present study. However, it should be pointed out that, besides methodological differences in time point and type of animals, all the above studies were performed on dissociated DRG cell cultures rather than intact DRGs, leaving open the question of whether in vitro modifications in molecular profiles and neuroanatomical relationships might have affected the results. It is also important to note that hyperalgesia and allodynia associated with diabetes do not necessarily correlate with increased excitability into sensory neurons. Aberrant encoding in specific cell populations and the synthesis and release of specific factors from pathological sensory neurons, may induce a neurimflammatory state in the dorsal horn of the spinal cord, which eventually may undergo to central sensitization mechanisms (Latremoliere and Woolf, 2009).

4.1.2 FUNCTIONAL EFFECT OF GDNF ADMINISTRATION ON DRG NEURONS

Several studies highlighted the crucial role of neurotrophic factors in regulating DRG sensory neurons survival and function also in adulthood (Ernfors et al., 1994; Lewin et al., 1994; Trupp, 1999; Bardoni et al., 2007; Bardoni and Merighi, 2009). In addition, their effect is specifically associated with certain neuronal subpopulations, as peptidergic and non-peptidergic neurons for NGF and GDNF, respectively (Bennett et al., 1998; Molliver et al., 1997b). The majority of small-sized DRG sensory neurons are involved in nociceptive signaling and our data, in concert with previous studies, suggested a crucial role of their afferents in the development of DPN (Akkina et al., 2001). In particular in this study, non-peptidergic nociceptors appeared as the population of sensory neurons most sensitive to diabetes-induced alterations in excitability. Since this population also expresses the GDNF receptor complex GFRα1/Ret (Salio et al., 2014), the role of the neurotrophic factor GDNF in modulating sensory neurons function was investigated in control and diabetic mice.

The acute administration of GDNF on entire DRGs from control mice induced a substantial increase in the AP latency and threshold, especially from hyperpolarized membrane potentials. As expected, the effect was more prominent in small-sized neurons. Interestingly, GDNF had little effect on firing properties of sensory neurons from diabetic mice. Actually, the previously reported differences between neurons from control and diabetic mice were abolished after GDNF administration, suggesting that GDNF recapitulates in normal neurons some of the mechanisms leading to reduced excitability in pathology. Indeed, GDNF potentiated A-type K+ currents and

hyperpolarizing leak currents in small-sized neurons from control mice, the same potassium conductances that were increased in small-sized neurons from diabetic mice. The potentiation of these conductances may account for the altered AP properties observed in current clamp. However, it should be noted that GDNF also inhibits some specific potassium conductances, and namely, the sustained potassium currents (I_K) and the hyperpolarization-activated currents (I_h). This dual action implies the activation of multiple intracellular pathways with positive and negative effects on different voltage-dependent potassium channels. This duality may be explained by the activation, via binding of GFRα1/Ret complex (Jin et al., 2002), of several intracellular signaling cascades. Binding to GFRα1, GDNF initiates functional coupling with Ret and activates extracellular signal-regulated kinase (ERK), p38 mitogen activated protein kinase (MAPK), phosphatidylinositol 3-kinase (PI3K)/AKT and other pathways (c-Jun N-terminal kinase, Src family kinases; Tansey et al. 2000; Airaksinen and Saarma, 2002). While the activation of MAPK/ERK pathway was shown to inhibit A-type transient (Kv4.2) and K-type sustained current via phosphorylation of specific residues (Takeda et al., 2010; Yang et al., 2001), the activation of PI3K pathways via Akt kinase, by overriding the activation of MAP/ERK, may lead to a potentiation of the same conductances (Jin et al., 2002; Liu et al., 2009). MAPK/ERK pathway itself does not always produce an inhibitory effect on Kv4.2 channels. In fact, point mutations on three different Kv4.2 residues targeted by ERK kinase lead to both potentiating and inhibitory effects on the gating properties of these channels (Schrader et al., 2006). The activation of one specific pathway, and thus its biological effect, may depend upon a variety of factors, including: i) the neuronal cell type which may express different types of GFRα receptors; ii) the receptor organization/phosphorylation (Runeberg-Roos and Saarma, 2007); iii) the subcellular localization (Paratcha et al., 2001; Richardson et al., 2006); the dose of GDNF applied (Mills et al., 2007) and more in general, iv) the experimental settings. Contrasting evidence on the physiological role of GDNF in neuronal excitability follows this complexity. A recent study on dissociated sensory neurons in trigeminal ganglia has shown that GDNF increases the excitability by inhibiting transient I_A currents and sustained I_K currents (Takeda et al., 2010), while in our study we observed an inhibition of the latter and a potentiation of the former, with a net inhibitory effect. Again, as discussed above, such discrepancy may account for differences in the experimental model adopted, which in turn might influence intracellular signaling pathways. Importantly, by using the entire DRGs, the intimate relationship between SGCs and sensory neurons is preserved. On one side, SGCs physiologically act as a buffer for extracellular potassium, thus lowering the cell excitability (Pannese, 1981); moreover, SGCs may express and release trophic factors, including GDNF, in pathological conditions (Otoshi et al., 2010), thus possibly modifying subsequent responses to exogenous stimuli.

On the other hand, the observed inhibitory effects of GDNF are consistent with a broad number of published works supporting an antinociceptive role of the trophic factor, with special reference to neuropathic pain syndromes (see for review Merighi, 2016). Antinociceptive effects have been also described following topical application of GFRα1 agonist in a mouse model of diabetic neuropathy (Hedstrom et al., 2014) or the induction of GDNF overexpression in peripheral tissues (Liu et al., 2009), which support its clinical use to treat diabetes-induced neuropathic pain. In our study, however, we found that the inhibitory effect of exogenous GDNF in sensory neurons are reduced in diabetes. The more logical explanation is that the increased potassium conductances in diabetes counteract a further potentiation induced by exogenous GDNF. It can be speculated that the same signaling pathways activated by exogenous GDNF may be already activated in diabetic condition by the endogenous molecule released with protective purposes.

4.1.3 Structural alterations in sensory neurons associated with diabetes

Dorsal root ganglia present very unique features that characterize them as the site of sensory afferent somata. Their anatomical structure is characterized by nerve cell bodies in mutual contact during the development. Then, they are progressively enveloped by a satellite cell sheath, which in turn becomes enveloped by connective tissue (Pannese, 1981), thus completely isolating cell bodies from each other just before birth. Nevertheless, sparse pairs or triplets of nerve cell bodies, identified as cell clusters, surrounded by a common connective tissue, have been described in the spinal ganglia of various species (Pannese et al., 1991, 1993). This particular arrangement raises the question whether a cell-to cell communication exists in DRGs and how it develops being these cells not synaptically interconnected (Amir and Devor, 1996). In this context, even if the functional profile of these neurons has now been widely investigated (Pannese, 1981; Hanani, 2005; Nascimento et al., 2008; Rozanski et al., 2013; Hanani, 2015), little is still known on their mutual spatial relationship and distribution and whether this has an impact on their function in health and disease.

In the present study the anatomical distribution and structure of DRG nociceptors was morphologically analyzed in control and diabetic mice, by using two classically recognized markers, such as IB4 to label non-peptidergic nociceptors and CGRP for the peptidergic ones. In collaboration with the Politecnico of Turin, a 3D software-based analysis, named 3*DRG* (Cataldo et al., 2016) was set up and an innovative method developed in our laboratory, consisting in a DRG

whole-mount preparation (Ciglieri et al., 2016), was applied. In particular, based on a previously described approach used to record neurons from entire DRGs (Hayar et al., 2008; Zhang et al., 1998) a collagenase treatment was performed to remove the external fibrous connective capsule from acutely excised DRGs. Collagenase pre-treatment significantly improves antibodies and marker penetration into intact DRGs without requiring classical slicing procedures.
The interesting result emerging from this analysis, never described in literature until now, is that the non-peptidergic IB4+ population of nociceptors tend to cluster in groups of three-four, with neurons apparently in strict contact each other. In particular, considering the total positive objects identified by the software during the analysis of IB4+ fluorescence, clusters represent 15% of total IB4+-labeled volume in the DRGs. On the contrary, the CGRP+ peptidergic population of nociceptors never clusterize, being the immunolabeled cells scattered all over the DRG.

The cluster structure indicates a non random cell distribution, which may condition the spread of excitation among neighboring cells. The existence of some form of anatomical arrangement in DRGs, albeit confined to a single cell population, is in contrast with the common belief of a lack of organization in these formations (Taylor et al., 1982). We have also to take in mind that both spinal cord and cortex have a precise somatotopic organization in somatosensory pathways (Welker, 1971; Swett and Woolf, 1985), while only few observations were made about a similar organization in DRGs (Pfaller and Arvidsson, 1988; Wessels and Marani, 1993; Wessels et al., 1990). In this context, the IB4-clusters could be part of a more complex somatotopic organization, related to particular pattern of skin innervations or transduction of multi-quality stimuli. The intimate contact observed in our study between specific IB4+ nociceptor populations may have an important impact in cell-to-cell communication in DRGs, thus overcoming the classical idea of sensory neurons as independent communicating elements. Even if synapses are virtually absent in DRGs and thus cell-to-cell interactions within DRGs cannot involve synaptic junctions, the close membrane apposition in the non-peptidergic -IB4+ cluster could permit electrotonic interactions among neighboring DRG neurons. Furthermore, around 5% of DRG somata are described to be able to originate electrical impulses (Wall and Devor, 1983) and titanic stimulation of one axon can exert subthreshold activity in the neighboring neurons, even if not directly stimulated (Devor and Wall, 1990).
We then speculated whether the cluster structure observed in the IB4+ non-peptidergic population of nociceptors could have an impact also in diabetes-induced alteration, but we did not observe significant changes between normal and diabetic mice, remaining both the total number of clusters and the mean value of cells involved in the clusters unchanged.

Although the cluster structure was unaltered in DRGs from diabetic mice, a different arrangement of SGC was detected. Alterations in SGC ensheatment between the different cell populations of nociceptors may strongly affect the spread of excitability across DRG neurons. SGCs were proved to communicate between each other via gap junctions (Huang et al., 2005) and to mediate inter-soma communication via "sandwich synapses" (Rozanski et al., 2013). During systemic inflammation, SGCs resulted activated and the communication between each other potentiated (Blum et al., 2014). Moreover, SCGs are reported to undergo important changes in different pain models, contributing to chronic pain (Jasmin et al., 2010; Hanani, 2012). In a streptozotocin-induced type 1 diabetic model, SGCs were activated with a 4-fold and 5-fold increase in GFAP immunostaining in mice and rats, respectively. Being GFAP a marker of glia activation, this indicates that important functional modifications occur in diabetic condition (Hanani et al., 2014). Here, the level of SGCs ensheathing in diabetes was found to be specifically reduced around IB4+ non-peptidergic neurons only, while little changes were observed around CGRP+ peptidergic neurons. A decreased SGC ensheathment around IB4+ nociceptors in diabetes may lead to an augmentated possibility of contacts between neighboring neurons in IB4+ cell clusters. This anatomical configuration may favor direct functional crosstalk between clustered neurons in pathological conditions, that may disrupt the correct encoding of sensory input.

4.1.4 IMPACT AND FUTURE DIRECTIONS

The present study has explored *ex vivo* various features of the physiological and morphological alterations induced by diabetes in DRG sensory neurons, encompassing perturbations of neuronal membrane properties to the impairment of neuron-glia relationship. In particular, a detailed analysis of GDNF effects has elucidated the role of the neuroptrophic factor in mitigating neuronal excitability, which may represent an innovative approach to tackle altered somatosensory function in diabetes (Akkina et al., 2001; Anitha et al., 2006; Peeraer et al., 2011).

To further investigate these mechanisms and to explore their impact *in vivo* different approaches could be adopted.

Glia-neuron interactions can be better investigated by using genetically modified or virally-injected animals to induce the expression of light-inducible molecules to stimulate or inhibit selected sensory neuron populations. As shown by Iyer et al. (2014), the injection of viruses encoding excitatory and inhibitory opsin light sensitive allowed the optogenetic control of sensory neurons excitability. An alternative approach (Kim et al., 2016) consist in recurring to genetically-modified mice expressing calcium indicators in sensory neurons. These *in* vivo techniques represent a

powerful tool to explore direct interactions among sensory neurons in DRGs following physiological stimulations of peripheral tissues. Coupling activation of neighbouring neurons has been indeed demonstrated (Kim et al., 2016) and the impact of SGCs on neuronal crosstalk can be directly analyzed. Secondly, direct evidence of the effect of GDNF in restoring normal cell excitability in pathological conditions could be effectively monitored *in vivo* by delivering systemic treatments with GDNF or GDNF mimetics.

Targeting cell-to-cell communication in DRGs represents a new frontiers in the treatment of neurological diseases associate with pathological pain (Costa and Neto, 2015; Hanani, 2012; Wu et al., 2012). In this context, gap junctions and pannexin are key mediators of the communication and resulted hyperactivated following injury (Hanani et al., 2002; Hanstein et al., 2013, 2016; Wu et al., 2012). Gap junction-forming connexin is a protein that resulted hypoexpressed in pathological condition and the increase of SGCs coupling was explained with an augment of these specific channels functioning (Xu et al., 2014). On the contrary, membrane channels pannexins resulted increased in pain models, releasing signaling molecules as ATP, which is algogenic and lead to cytokine production (Silverman et al., 2009) and, eventually, to peripheral sensitization (Zhang et al., 2015). In future studies, the role of SGCs in contributing to altered pain in diabetes can thus take advantage of gap junctions and pannexin blockers, such as carbenoxolone, which are proved to dramatically reduce pain profile (Bravo et al., 2014; Hanstein et al., 2010).

Regarding the kinetics of action of GDNF in pathological situation, a different type of approach to study alterations in DRG sensory neurons could be recurring to GDNF or GFRα1-null mice. Few studies performed in the past showed that *GDNF-/-* mice embryos presented 23% losses of L5 DRG sensory neurons, while *GRFα1-/-* embryos showed a normal neuronal population (Moore et al., 1996). These findings and the lack of a massive neuronal cell loss suggested that GDNF, even if involved in cells survival, was not the key survival factor of peripheral nervous system and that GFRα1 is just one of the mediators of GDNF action (Cacalano et al., 1998; Moore et al., 1996; Pichel et al., 1996; Sánchez et al., 1996). On the contrary *Ret-/-* embryos presented a severe loss of neurons, probably due to the fact that is a signaling transducer shared by all GDNF family ligands (Cacalano et al., 1998; Schuchardt et al., 1994).

Currently, a definite role for GDNF as modulator of the nociceptive information is still controversial, considering its actions as both anti- and pro-nociceptive, depending on the system and the type of pain considered: indeed, GDNF may exert hyperalgesic effect in peripheral nervous system, and an analgesic effect in the central, as deeply rewied in Merighi (2016). Taking this in consideration, an interesting resolution is the development of neurotrophic mimetics, which are

small molecules that act as agonists of neurotrophic factors but without the poor drug-like features, as low bioavailability, poor tissue diffusion (Piltonen et al., 2009) and high-cost production. Regarding GDNF, few alternatives are currently available: gliafin, that is a peptide able to induce Ret phosphorylation, but still under study for testing pain reduction (Garcia-Bennett et al., 2013); BT13, a Ret agonist, which decreased mechanical hypersensitivity and normalized the expression of several DRG neurons markers in a model of neuropathic pain (Sidorova et al., 2017); XIB4035, a small molecule that enhances the signaling of GFRα1 (Tokugawa et al., 2003) and, administered topically, alleviates small fiber neuropathy in a rat model of diabetes (Hedstrom et al., 2014; Merighi, 2016).

A combination of the previous *in vivo* approaches together with behavioral studies in animal models of diabetic neuropathy would help to make a significant step forward in the comprehension of the molecular and cellular mechanisms underlying altered nociceptive transmission in diabetes. Moreover new insights on physiological mechanisms of GDNF kinetics are necessary for new drug design.

5 CONCLUSION

The experiments described in this thesis were carried out by combining electrophysiological and morphological approaches in order to analyze the pathological alterations of dorsal root ganglia as a consequence of the metabolic impairments typical of diabetic polyneuropathy. Sustained hyperglycemia affects the entire nervous system, with major impairments over the peripheral nervous system which is more exposed to the direct effects of systemic diseases. In particular, DRGs host the cell bodies of sensory neurons and therefore represent the center where gene expression is controlled and cell excitability modulated as a response of environment changes.

The main findings presented in this thesis can be summarize as follows:

- diabetes causes relevant alterations in sensory neurons, mainly in small-sized non-peptidergic nociceptors. These neurons exhibit reduced excitability and decreased firing activity, which is associated with a potentiation of voltage-dependent potassium channels;
- the neurotrophic factor GDNF mitigates cell excitability in small nociceptors under physiological conditions. The mechanisms implies again an increase in potassium conductances, namely driven by fast inactivating I_a and hyperpolarized-activated I_h currents;
- in neurons from diabetic animals, GDNF response is diminished or lacking;
- morphologically, diabetes does not affect the general organization of DRG neurons, while causes a disruption of the functional unit formed by neuronal somata and satellite glial cells, again mainly of small-sized non-peptidergic neurons.

Thanks to the new methodological approach developed in our laboratory, the analysis of the DRGs as entire structure was feasible and allowed to investigate the effects of diabetic polyneuropathy with a more integrated view.

Non-peptidergic neurons in DRGs appeared particularly affected by diabetes and therefore represent a strategic target for future drug development to contain altered nociceptive behavior in diabetic neuropathy. Indeed, these neurons were shown to form cluster which may favor the spread of excitation and amplify the incoming sensory input. Moreover, the insulation provided by satellite glial cells is mainly lost upon this population in diabetes, which may further favor atypical cell-to-cell communication. Finally, these neurons express the GDNF receptor complex GFRα1/Ret (Salio e al. 2014) and are the most sensitive to the inhibitory effects of this neurotrophic factor.

These results thus support the hypothesis that the administration of GDNF or GDNF analogs may exert protective and antinociceptive effects in pathological conditions in which non-peptidergic nociceptors are involved and potentially damaged. This view is supported by a broad literature that confirm a regulatory role for GDNF (Akkina et al., 2001; Mills et al., 2007; Liu et al., 2009; Hedstrom et al., 2014; Merighi, 2016). Overall, it is clear that a deeper analysis of the role of neurotrophic factors, mainly GDNF, could bring not only a broader knowledge of the mechanisms underlying nociception, but also uncover new ways to approach diseases such as diabetic polyneuropathy. Considering that the somata of the neurons sensitive to GDNF are hosted by DRGs and that these structures are easily accessible to systemic treatments, this could be translated in a more efficient administration and, possibly, in a higher therapeutic effect.

"The dorsal root ganglion (DRG) is an odder beast than most of us realize"
-Unexplained peculiarities of the dorsal root ganglion- Marshall Devor, 1999.

Publications and abstract related to the present study

Papers

- **Ciglieri E**.; Ferrini F.; Salio C. *An improved method for in vitro morphofunctional analysis of mouse dorsal root ganglia*, Annals of Anatomy - Anatomischer Anzeiger. (Vol 207, pages 62-67), September 2016; 10.1016/j.aanat.2016.04.032

- Di Cataldo, S.; Tonti, S.; **Ciglieri, E.**; Macii, E.; Ferrini, F.; Salio, C.; Ficarra, E. *Automated 3D immunofluorescence analysis of Dorsal Root Ganglia for the investigation of neural circuit alterations: a preliminary study* - Position of the 2016 Federated Conference on Computer Science and Information Systems, (Vol. 9, pages 65–70), 2016; http://dx.doi.org/10.15439/2016F569

Abstracts

- **Ciglieri E.**, Vacca M., Ferrini F., Di Cataldo S., Ficarra E., Salio C. - "Spatial distribution of peptidergic and non-peptidergic nociceptors in mouse dorsal root ganglia: a cluster story"
  XI National Congress AMV, Rome, 25th-26th May 2017 (Oral communication)

- Ciglieri E.;Ferrini F.; Salio C. -"Effects of GDNF on DRG neurons in normal and diabetic mice"
  10th FENS Forum of Neuroscience, Copenhagen, 2nd-6th of July 2016 (Poster presentation)

- Ciglieri E.; Ferrini F.; Tonti S.; Di Cataldo S.; Ficarra E.; Salio C. - " An integrated approach for morphofunctional analysis of DRGs in normal and diabetic mice"
  XVI Congress for the Italian Society for Neuroscience (SINS), Fiera Internazionale della Sardegna, Cagliari, 8th-11th October 2015 (Poster presentation)

- Ciglieri E.; Ferrini F.; Salio C. -"Role of GDNF in diabetes-induced alterations in primary sensory neurons"
  Monothematic conference of SIF: "Advances in pain research: pathophysiology and new therapeutic strategies", Naples, 18th-19th June 2015 (Poster presentation)

- Ciglieri E.; Ferrini F.; Boggio E.; Salio C. - "An improved method for in vitro morphofunctional analysis of dorsal root ganglia in the normal and diabetic mouse"
  X National Congress AMV, Rome, 21st-22nd May 2015 (Oral communication)

- Ciglieri E.; Ferrini F.; Boggio E.; Salio C. - "An improved method for in vitro morphofunctional analysis of dorsal root ganglia in the normal and diabetic mouse"
  National Meeting of PhD Students in Neuroscience, Department of Neuroscience of the University "Federico II", Naples, 26th February 2015 (Poster presentation)

6 BIBLIOGRAPHY

Airaksinen, M.S., and Saarma, M. (2002). The GDNF family: signalling, biological functions and therapeutic value. Nat. Rev. Neurosci. *3*, 383–394.

Airaksinen, M.S., Koltzenburg, M., Lewin, G.R., Masu, Y., Helbig, C., Wolf, E., Brem, G., Toyka, K.V., Thoenen, H., and Meyer, M. (1996). Specific Subtypes of Cutaneous Mechanoreceptors Require Neurotrophin-3 Following Peripheral Target Innervation. Neuron *16*, 287–295.

Akkina, S.K., Patterson, C.L., and Wright, D.E. (2001). GDNF rescues nonpeptidergic unmyelinated primary afferents in streptozotocin-treated diabetic mice. Exp. Neurol. *167*, 173–182.

Ali, Z., Ringkamp, M., Hartke, T.V., Chien, H.F., Flavahan, N.A., Campbell, J.N., and Meyer, R.A. (1999). Uninjured C-fiber nociceptors develop spontaneous activity and alpha-adrenergic sensitivity following L6 spinal nerve ligation in monkey. J. Neurophysiol. *81*, 455–466.

Amaya, F., Shimosato, G., Nagano, M., Ueda, M., Hashimoto, S., Tanaka, Y., Suzuki, H., and Tanaka, M. (2004). NGF and GDNF differentially regulate TRPV1 expression that contributes to development of inflammatory thermal hyperalgesia. Eur. J. Neurosci. *20*, 2303–2310.

Amir, R., and Devor, M. (1996). Chemically mediated cross-excitation in rat dorsal root ganglia. J. Neurosci. Off. J. Soc. Neurosci. *16*, 4733–4741.

Anitha, M., Gondha, C., Sutliff, R., Parsadanian, A., Mwangi, S., Sitaraman, S.V., and Srinivasan, S. (2006). GDNF rescues hyperglycemia-induced diabetic enteric neuropathy through activation of the PI3K/Akt pathway. J. Clin. Invest. *116*, 344–356.

Aoki, E., and Semba, R. (1992). Localization of nitric oxide-related substances in the peripheral nervous tissues. Neurosci. Res. Suppl. *17*, 109.

Averill, S., McMahon, S.B., Clary, D.O., Reichardt, L.F., and Priestley, J.V. (1995). Immunocytochemical localization of trkA receptors in chemically identified subgroups of adult rat sensory neurons. Eur. J. Neurosci. *7*, 1484–1494.

Baloh, R.H., Tansey, M.G., Lampe, P.A., Fahrner, T.J., Enomoto, H., Simburger, K.S., Leitner, M.L., Araki, T., Johnson, E.M., and Milbrandt, J. (1998). Artemin, a novel member of the GDNF ligand family, supports peripheral and central neurons and signals through the GFRalpha3-RET receptor complex. Neuron *21*, 1291–1302.

Barabas, M.E., Mattson, E.C., Aboualizadeh, E., Hirschmugl, C.J., and Stucky, C.L. (2014). Chemical Structure and Morphology of Dorsal Root Ganglion Neurons from Naive and Inflamed Mice. J. Biol. Chem. *289*, 34241–34249.

Barbacid, M. (1994). The Trk family of neurotrophin receptors. J. Neurobiol. *25*, 1386–1403.

Barde, Y.A., Edgar, D., and Thoenen, H. (1982). Purification of a new neurotrophic factor from mammalian brain. EMBO J. *1*, 549–553.

Bardoni, R., and Merighi, A. (2009). BDNF and TrkB mediated mechanisms in the spinal cord. In Synaptic Plasticity in Pain, pp. 89–108.

Bardoni, R., Ghirri, A., Salio, C., Prandini, M., and Merighi, A. (2007). BDNF-mediated modulation of GABA and glycine release in dorsal horn lamina II from postnatal rats. Dev. Neurobiol. *67*, 960–975.

Barnes, P.J., Belvisi, M.G., and Rogers, D.F. (1990). Modulation of neurogenic inflammation: novel approaches to inflammatory disease. Trends Pharmacol. Sci. *11*, 185–189.

Basbaum, A. (2011). Specificity Versus Patterning Theory: Continuing the Debate.

Basbaum, A.I., Bautista, D.M., Scherrer, G., and Julius, D. (2009). Cellular and Molecular Mechanisms of Pain. Cell *139*, 267–284.

Bell, C., and Shaw, A. (1868). Reprint of the "Idea of a New Anatomy of the Brain," with Letters, & c. J Anat Physiol *3*, 147–182.

Bencivinni, I., Ferrini, F., Salio, C., Beltramo, M., and Merighi, A. (2011). The somatostatin analogue octreotide inhibits capsaicin-mediated activation of nociceptive primary afferent fibres in spinal cord lamina II (substantia gelatinosa). Eur. J. Pain Lond. Engl. *15*, 591–599.

Bennett, D.L., Michael, G.J., Ramachandran, N., Munson, J.B., Averill, S., Yan, Q., McMahon, S.B., and Priestley, J.V. (1998). A distinct subgroup of small DRG cells express GDNF receptor components and GDNF is protective for these neurons after nerve injury. J. Neurosci. Off. J. Soc. Neurosci. *18*, 3059–3072.

Berkemeier, L.R., Winslow, J.W., Kaplan, D.R., Nikolics, K., Goeddel, D.V., and Rosenthal, A. (1991). Neurotrophin-5: A novel neurotrophic factor that activates trk and trkB. Neuron *7*, 857–866.

Besson, J.-M., and Chaouch, A. (1987). Peripheral and spinal mechanisms of nociception. Physiol. Rev. *67*, 67–186.

Bhave, G., Hu, H.-J., Glauner, K.S., Zhu, W., Wang, H., Brasier, D.J., Oxford, G.S., and Gereau, R.W. (2003). Protein kinase C phosphorylation sensitizes but does not activate the capsaicin receptor transient receptor potential vanilloid 1 (TRPV1). Proc. Natl. Acad. Sci. *100*, 12480–12485.

Black, J.A., Dib-Hajj, S., McNabola, K., Jeste, S., Rizzo, M.A., Kocsis, J.D., and Waxman, S.G. (1996). Spinal sensory neurons express multiple sodium channel alpha-subunit mRNAs. Brain Res. Mol. Brain Res. *43*, 117–131.

Black, J.A., Liu, S., Tanaka, M., Cummins, T.R., and Waxman, S.G. (2004). Changes in the expression of tetrodotoxin-sensitive sodium channels within dorsal root ganglia neurons in inflammatory pain. Pain *108*, 237–247.

Blair, N.T., and Bean, B.P. (2002). Roles of tetrodotoxin (TTX)-sensitive Na+ current, TTX-resistant Na+ current, and Ca2+ current in the action potentials of nociceptive sensory neurons. J. Neurosci. Off. J. Soc. Neurosci. *22*, 10277–10290.

Bleakman, D., Colmers, W.F., Fournier, A., and Miller, R.J. (1991). Neuropeptide Y inhibits Ca2+ influx into cultured dorsal root ganglion neurones of the rat via a Y2 receptor. Br. J. Pharmacol. *103*, 1781–1789.

Blum, E., Procacci, P., Conte, V., and Hanani, M. (2014). Systemic inflammation alters satellite glial cell function and structure. A possible contribution to pain. Neuroscience *274*, 209–217.

Boscia, F., Esposito, C.L., Casamassa, A., de Franciscis, V., Annunziato, L., and Cerchia, L. (2013). The isolectin IB4 binds RET receptor tyrosine kinase in microglia. J. Neurochem. *126*, 428–436.

Boucher, T.J., and McMahon, S.B. (2001). Neurotrophic factors and neuropathic pain. Curr. Opin. Pharmacol. *1*, 66–72.

Boucher, T.J., Okuse, K., Bennett, D.L., Munson, J.B., Wood, J.N., and McMahon, S.B. (2000). Potent analgesic effects of GDNF in neuropathic pain states. Science *290*, 124–127.

Bourane, S., Garces, A., Venteo, S., Pattyn, A., Hubert, T., Fichard, A., Puech, S., Boukhaddaoui, H., Baudet, C., Takahashi, S., et al. (2009). Low-Threshold Mechanoreceptor Subtypes Selectively Express MafA and Are Specified by Ret Signaling. Neuron *64*, 857–870.

Bradbury, E.J., Burnstock, G., and McMahon, S.B. (1998). The Expression of P2X3Purinoreceptors in Sensory Neurons: Effects of Axotomy and Glial-Derived Neurotrophic Factor. Mol. Cell. Neurosci. *12*, 256–268.

Bravo, D., Ibarra, P., Retamal, J., Pelissier, T., Laurido, C., Hernandez, A., and Constandil, L. (2014). Pannexin 1: a novel participant in neuropathic pain signaling in the rat spinal cord. Pain *155*, 2108–2115.

Brehm, M.A., Powers, A.C., Shultz, L.D., and Greiner, D.L. (2012). Advancing animal models of human type 1 diabetes by engraftment of functional human tissues in immunodeficient mice. Cold Spring Harb. Perspect. Med. *2*, a007757.

Brodal, A. (1969). Neurological anatomy in relation to clinical medicine (Oxford University Press).

Bron, R., Klesse, L.J., Shah, K., Parada, L.F., and Winter, J. (2003). Activation of Ras is necessary and sufficient for upregulation of vanilloid receptor type 1 in sensory neurons by neurotrophic factors. Mol. Cell. Neurosci. *22*, 118–132.

Brumovsky, P., Watanabe, M., and Hökfelt, T. (2007). Expression of the vesicular glutamate transporters-1 and -2 in adult mouse dorsal root ganglia and spinal cord and their regulation by nerve injury. Neuroscience *147*, 469–490.

Cacalano, G., Fariñas, I., Wang, L.-C., Hagler, K., Forgie, A., Moore, M., Armanini, M., Phillips, H., Ryan, A.M., Reichardt, L.F., et al. (1998). GFRα1 Is an Essential Receptor Component for GDNF in the Developing Nervous System and Kidney. Neuron *21*, 53–62.

Calcutt, N.A., Freshwater, J.D., and Mizisin, A.P. (2004). Prevention of sensory disorders in diabetic Sprague-Dawley rats by aldose reductase inhibition or treatment with ciliary neurotrophic factor. Diabetologia *47*, 718–724.

Callaghan, B.C., Cheng, H., Stables, C.L., Smith, A.L., and Feldman, E.L. (2012). Diabetic neuropathy: Clinical manifestations and current treatments. Lancet Neurol. *11*, 521–534.

Campbell, J.N., and Meyer, R.A. (1983). Sensitization of unmyelinated nociceptive afferents in monkey varies with skin type. J. Neurophysiol. *49*, 98–110.

Cao, X.-H., Byun, H.-S., Chen, S.-R., Cai, Y.-Q., and Pan, H.-L. (2010). Reduction in Voltage-Gated K+ Channel Activity in Primary Sensory Neurons in Painful Diabetic Neuropathy: Role of Brain-Derived Neurotrophic Factor. J. Neurochem. *114*, 1460–1475.

Carnicella, S., and Ron, D. (2009). GDNF — A potential target to treat addiction. Pharmacol. Ther. *122*, 9–18.

Carroll, P., Lewin, G.R., Koltzenburg, M., Toyka, K.V., and Thoenen, H. (1998). A role for BDNF in mechanosensation. Nat. Neurosci. *1*, 42–46.

Cataldo, S.D., Tonti, S., Ciglieri, E., Ferrini, F., Macii, E., Ficarra, E., and Salio, C. (2016). Automated 3D immunofluorescence analysis of Dorsal Root Ganglia for the investigation of neural circuit alterations: a preliminary study. Ann. Comput. Sci. Inf. Syst. *9*, 65–70.

Caterina, M.J., and Julius, D. (1999). Sense and specificity: a molecular identity for nociceptors. Curr. Opin. Neurobiol. *9*, 525–530.

Caterina, M.J., Leffler, A., Malmberg, A.B., Martin, W.J., Trafton, J., Petersen-Zeitz, K.R., Koltzenburg, M., Basbaum, A.I., and Julius, D. (2000). Impaired nociception and pain sensation in mice lacking the capsaicin receptor. Science *288*, 306–313.

Cauna, N., and Mannan, G. (1958). The structure of human digital pacinian corpuscles (corpus cula lamellosa) and its functional significance. J. Anat. *92*, 1–20.

Cauna, N., and Ross, L.L. (1960). The fine structure of Meissner's touch corpuscles of human fingers. J. Biophys. Biochem. Cytol. *8*, 467–482.

Cavanaugh, D.J., Chesler, A.T., Bráz, J.M., Shah, N.M., Julius, D., and Basbaum, A.I. (2011). Restriction of transient receptor potential vanilloid-1 to the peptidergic subset of primary afferent neurons follows its developmental downregulation in nonpeptidergic neurons. J. Neurosci. Off. J. Soc. Neurosci. *31*, 10119–10127.

Cesare, P., Dekker, L.V., Sardini, A., Parker, P.J., and McNaughton, P.A. (1999). Specific Involvement of PKC-ε in Sensitization of the Neuronal Response to Painful Heat. Neuron *23*, 617–624.

Chen, X., and Levine, J.D. (2001). Hyper-responsivity in a subset of C-fiber nociceptors in a model of painful diabetic neuropathy in the rat. Neuroscience *102*, 185–192.

Chéry-Croze, S. (1983). Painful sensation induced by a thermal cutaneous stimulus. Pain *17*, 109–137.

Choi, J.-S., Dib-Hajj, S.D., and Waxman, S.G. (2006). Differential Slow Inactivation and Use-Dependent Inhibition of Nav1.8 Channels Contribute to Distinct Firing Properties in IB4+ and IB4- DRG Neurons. J. Neurophysiol. *97*, 1258–1265.

Chu, Q., Moreland, R., Yew, N.S., Foley, J., Ziegler, R., and Scheule, R.K. (2008). Systemic Insulin-like Growth Factor-1 Reverses Hypoalgesia and Improves Mobility in a Mouse Model of Diabetic Peripheral Neuropathy. Mol. Ther. *16*, 1400–1408.

Ciglieri, E., Ferrini, F., Boggio, E., and Salio, C. (2016a). An improved method for in vitro morphofunctional analysis of mouse dorsal root ganglia. Ann. Anat. - Anat. Anz. *207*.

Ciglieri, E., Ferrini, F., Boggio, E., and Salio, C. (2016b). An improved method for in vitro morphofunctional analysis of mouse dorsal root ganglia. Ann. Anat. - Anat. Anz.

Connor, B., and Dragunow, M. (1998). The role of neuronal growth factors in neurodegenerative disorders of the human brain. Brain Res. Rev. *27*, 1–39.

Costa, F.A.L., and Neto, F.L.M. (2015). Satellite glial cells in sensory ganglia: its role in pain. Braz. J. Anesthesiol. Engl. Ed. *65*, 73–81.

Coull, J.A.M., Beggs, S., Boudreau, D., Boivin, D., Tsuda, M., Inoue, K., Gravel, C., Salter, M.W., and De Koninck, Y. (2005). BDNF from microglia causes the shift in neuronal anion gradient underlying neuropathic pain. Nature *438*, 1017–1021.

Courteix, C., Bardin, M., Massol, J., Fialip, J., Lavarenne, J., and Eschalier, A. (1996). Daily insulin treatment relieves long-term hyperalgesia in streptozocin diabetic rats. Neuroreport *7*, 1922–1924.

Cozzi, B., Granato, A., and Merighi, A. (2009). Neuroanatomia dell'uomo (Roma: A. Delfino medicina scienze).

Creedon, D.J., Tansey, M.G., Baloh, R.H., Osborne, P.A., Lampe, P.A., Fahrner, T.J., Heuckeroth, R.O., Milbrandt, J., and Johnson, E.M. (1997). Neurturin shares receptors and signal transduction pathways with glial cell line-derived neurotrophic factor in sympathetic neurons. Proc. Natl. Acad. Sci. U. S. A. *94*, 7018–7023.

Crowley, C., Spencer, S.D., Nishimura, M.C., Chen, K.S., Pitts-Meek, S., Armanini, M.P., Ling, L.H., McMahon, S.B., Shelton, D.L., and Levinson, A.D. (1994). Mice lacking nerve growth factor display perinatal loss of sensory and sympathetic neurons yet develop basal forebrain cholinergic neurons. Cell *76*, 1001–1011.

Cuello, A.C. (1987). Peptides as neuromodulators in primary sensory neurons. Neuropharmacology *26*, 971–979.

Cummins, K.L., and Dorfman, L.J. (1981). Nerve fiber conduction velocity distributions: studies of normal and diabetic human nerves. Ann. Neurol. *9*, 67–74.

Cummins, T.R., Black, J.A., Dib-Hajj, S.D., and Waxman, S.G. (2000). Glial-derived neurotrophic factor upregulates expression of functional SNS and NaN sodium channels and their currents in axotomized dorsal root ganglion neurons. J. Neurosci. Off. J. Soc. Neurosci. *20*, 8754–8761.

D. Purves, Augustine, G.J., Fitzpatrick, D., Hall, W.C., LaMantia, A.S., McNamara, J.O., and White, L.E. (2009). Neuroscience.

Dallenbach, K.M. (1939). Pain: History and Present Status. Am. J. Psychol. *52*, 331.

Davis, K.D. (1998). Cold-induced pain and prickle in the glabrous and hairy skin. Pain *75*, 47–57.

Delfini, M.-C., Mantilleri, A., Gaillard, S., Hao, J., Reynders, A., Malapert, P., Alonso, S., François, A., Barrere, C., Seal, R., et al. (2013). TAFA4, a chemokine-like protein, modulates injury-induced mechanical and chemical pain hypersensitivity in mice. Cell Rep. *5*, 378–388.

Descartes, R., Clerselier, C., La Forge, L., and Schuyl, F. (1664). L'homme et un Traitté de la ormation du Foetus du Mesme Autheur (Paris).

Devor, M., and Wall, P.D. (1990). Cross-excitation in dorsal root ganglia of nerve-injured and intact rats. J. Neurophysiol. *64*, 1733–1746.

Dib-Hajj, S., Black, J.A., Cummins, T.R., and Waxman, S.G. (2002). NaN/Nav1.9: a sodium channel with unique properties. Trends Neurosci. *25*, 253–259.

Djouhri, L., Newton, R., Levinson, S.R., Berry, C.M., Carruthers, B., and Lawson, S.N. (2003a). Sensory and electrophysiological properties of guinea-pig sensory neurones expressing Nav 1.7 (PN1) Na+ channel α subunit protein. J. Physiol. *546*, 565–576.

Djouhri, L., Fang, X., Okuse, K., Wood, J.N., Berry, C.M., and Lawson, S.N. (2003b). The TTX-resistant sodium channel Nav1.8 (SNS/PN3): expression and correlation with membrane properties in rat nociceptive primary afferent neurons. J. Physiol. *550*, 739–752.

Dodd, J., and Jessell, T.M. (1985). Lactoseries carbohydrates specify subsets of dorsal root ganglion neurons projecting to the superficial dorsal horn of rat spinal cord. J. Neurosci. Off. J. Soc. Neurosci. *5*, 3278–3294.

Donnerer, J., Liebmann, I., and Schicho, R. (2005). Differential regulation of 3-beta-hydroxysteroid dehydrogenase and vanilloid receptor TRPV1 mRNA in sensory neurons by capsaicin and NGF. Pharmacology *73*, 97–101.

Doupis, J., Lyons, T.E., Wu, S., Gnardellis, C., Dinh, T., and Veves, A. (2009). Microvascular reactivity and inflammatory cytokines in painful and painless peripheral diabetic neuropathy. J. Clin. Endocrinol. Metab. *94*, 2157–2163.

Drel, V.R., Mashtalir, N., Ilnytska, O., Shin, J., Li, F., Lyzogubov, V.V., and Obrosova, I.G. (2006). The leptin-deficient (ob/ob) mouse: a new animal model of peripheral neuropathy of type 2 diabetes and obesity. Diabetes *55*, 3335–3343.

Dublin, P., and Hanani, M. (2007). Satellite glial cells in sensory ganglia: Their possible contribution to inflammatory pain. Brain. Behav. Immun. *21*, 592–598.

Elitt, C.M., McIlwrath, S.L., Lawson, J.J., Malin, S.A., Molliver, D.C., Cornuet, P.K., Koerber, H.R., Davis, B.M., and Albers, K.M. (2006). Artemin overexpression in skin enhances expression of TRPV1 and TRPA1 in cutaneous sensory neurons and leads to behavioral sensitivity to heat and cold. J. Neurosci. Off. J. Soc. Neurosci. *26*, 8578–8587.

England, S., Heblich, F., James, I.F., Robbins, J., and Docherty, R.J. (2001). Bradykinin evokes a Ca2+-activated chloride current in non-neuronal cells isolated from neonatal rat dorsal root ganglia. J. Physiol. *530*, 395–403.

Erdoğan, Ç., Cenikli, U., Değirmenci, E., and Oğuzhanoğlu, A. (2013). Effect of hyperglycemia on conduction parameters of tibial nerve's fibers to different muscles: A rat model. J. Neurosci. Rural Pract. *4*, 9–12.

Ernfors, P., Lee, K.F., Kucera, J., and Jaenisch, R. (1994). Lack of neurotrophin-3 leads to deficiencies in the peripheral nervous system and loss of limb proprioceptive afferents. Cell *77*, 503–512.

Fan, N., Sikand, P., Donnelly, D.F., Ma, C., and Lamotte, R.H. (2011). Increased Na ♀ and K ♀ currents in small mouse dorsal root ganglion neurons after ganglion compression. 211–218.

Fang, M., Wang, Y., He, Q.H., Sun, Y.X., Deng, L.B., Wang, X.M., and Han, J.S. (2003). Glial cell line-derived neurotrophic factor contributes to delayed inflammatory hyperalgesia in adjuvant rat pain model. Neuroscience *117*, 503–512.

Fang, X., Djouhri, L., Black, J.A., Dib-Hajj, S.D., Waxman, S.G., and Lawson, S.N. (2002). The presence and role of the tetrodotoxin-resistant sodium channel Na(v)1.9 (NaN) in nociceptive primary afferent neurons. J. Neurosci. Off. J. Soc. Neurosci. *22*, 7425–7433.

Fang, X., McMullan, S., Lawson, S.N., and Djouhri, L. (2005). Electrophysiological differences between nociceptive and non-nociceptive dorsal root ganglion neurones in the rat in vivo. J. Physiol. *565*, 927–943.

Fang, X., Djouhri, L., McMullan, S., Berry, C., Waxman, S.G., Okuse, K., and Lawson, S.N. (2006). Intense Isolectin-B4 Binding in Rat Dorsal Root Ganglion Neurons Distinguishes C-Fiber Nociceptors with Broad Action Potentials and High Nav1.9 Expression. J. Neurosci. *26*, 7281–7292.

Fariñas, I., Jones, K.R., Backus, C., Wang, X.Y., and Reichardt, L.F. (1994). Severe sensory and sympathetic deficits in mice lacking neurotrophin-3. Nature *369*, 658–661.

Ferrari, L.F., Lotufo, C.M., Araldi, D., Rodrigues, M.A., Macedo, L.P., Ferreira, S.H., and Parada, C.A. (2014). Inflammatory sensitization of nociceptors depends on activation of NMDA receptors in DRG satellite cells. Proc. Natl. Acad. Sci. U. S. A. *111*, 18363–18368.

Fields, H.L., Basbaum, A.I., and Heinricher, M.M. (2006). Central nervous system mechanisms of pain modulation. In Wall and Melzack's Textbook of Pain, (Elsevier), pp. 125–142.

FitzGerald, M.J.T., and Folan-Curran, J. (2002). Clinical Neuroanatomy and Related Neuroscience (W. B. Saunders).

Fjell, J., Cummins, T.R., Dib-Hajj, S.D., Fried, K., Black, J.A., and Waxman, S.G. (1999). Differential role of GDNF and NGF in the maintenance of two TTX-resistant sodium channels in adult DRG neurons. Brain Res. Mol. Brain Res. *67*, 267–282.

Gabra, B.H., and Sirois, P. (2005). Hyperalgesia in non-obese diabetic (NOD) mice: a role for the inducible bradykinin B1 receptor. Eur. J. Pharmacol. *514*, 61–67.

Gaillard, S., Lo Re, L., Mantilleri, A., Hepp, R., Urien, L., Malapert, P., Alonso, S., Deage, M., Kambrun, C., Landry, M., et al. (2014). GINIP, a Gαi-interacting protein, functions as a key modulator of peripheral GABAB receptor-mediated analgesia. Neuron *84*, 123–136.

Garcia-Bennett, A.E., Kozhevnikova, M., König, N., Zhou, C., Leao, R., Knöpfel, T., Pankratova, S., Trolle, C., Berezin, V., Bock, E., et al. (2013). Delivery of differentiation factors by mesoporous silica particles assists advanced differentiation of transplanted murine embryonic stem cells. Stem Cells Transl. Med. *2*, 906–915.

Gardell, L.R., Vanderah, T.W., Gardell, S.E., Wang, R., Ossipov, M.H., Lai, J., and Porreca, F. (2003a). Enhanced evoked excitatory transmitter release in experimental neuropathy requires descending facilitation. J. Neurosci. Off. J. Soc. Neurosci. *23*, 8370–8379.

Gardell, L.R., Wang, R., Ehrenfels, C., Ossipov, M.H., Rossomando, A.J., Miller, S., Buckley, C., Cai, A.K., Tse, A., Foley, S.F., et al. (2003b). Multiple actions of systemic artemin in experimental neuropathy. Nat. Med. *9*, 1383–1389.

Giacco, F., and Brownlee, M. (2010). Oxidative stress and diabetic complications. Circ. Res. *107*, 1058–1070.

Giesler, G.J., Jr., Menétrey, D., and Basbaum, A.I. (1979). Differential origins of spinothalamic tract projections to medial and lateral thalamus in the rat. J. Comp. Neurol. *184*, 107–125.

Gomtsyan, A., and Faltynek, C.R. (2010). Vanilloid Receptor TRPV1 in Drug Discovery: Targeting Pain and Other Pathological Disorders (John Wiley & Sons).

Gong, K., Ohara, P.T., and Jasmin, L. (2016). Patch Clamp Recordings on Intact Dorsal Root Ganglia from Adult Rats. J. Vis. Exp. JoVE.

Guimaraes, M.Z.P., and Jordt, S.-E. (2007). TRPA1 : A Sensory Channel of Many Talents. In TRP Ion Channel Function in Sensory Transduction and Cellular Signaling Cascades, W.B. Liedtke, and S. Heller, eds. (Boca Raton (FL): CRC Press/Taylor & Francis), p.

Guzman, S.J., Schlögl, A., and Schmidt-Hieber, C. (2014). Stimfit: quantifying electrophysiological data with Python. Front. Neuroinformatics *8*, 16.

Hammarberg, H., Piehl, F., Cullheim, S., Fjell, J., Hökfelt, T., and Fried, K. (1996). GDNF mRNA in Schwann cells and DRG satellite cells after chronic sciatic nerve injury. Neuroreport *7*, 857–860.

Han, H.C., Lee, D.H., and Chung, J.M. (2000). Characteristics of ectopic discharges in a rat neuropathic pain model. Pain *84*, 253–261.

Hanani, M. (2005). Satellite glial cells in sensory ganglia: from form to function. Brain Res. Brain Res. Rev. *48*, 457–476.

Hanani, M. (2012). Intercellular communication in sensory ganglia by purinergic receptors and gap junctions: implications for chronic pain. Brain Res. *1487*, 183–191.

Hanani, M. (2015). Role of satellite glial cells in gastrointestinal pain. Front. Cell. Neurosci. *9*.

Hanani, M., Huang, T.Y., Cherkas, P.S., Ledda, M., and Pannese, E. (2002). Glial cell plasticity in sensory ganglia induced by nerve damage. Neuroscience *114*, 279–283.

Hanani, M., Blum, E., Liu, S., Peng, L., and Liang, S. (2014). Satellite glial cells in dorsal root ganglia are activated in streptozotocin-treated rodents. J. Cell. Mol. Med. *18*, 2367–2371.

Hanstein, R., Zhao, J.B., Basak, R., Smith, D.N., Zuckerman, Y.Y., Hanani, M., Spray, D.C., and Gulinello, M. (2010). Focal Inflammation Causes Carbenoxolone-Sensitive Tactile Hypersensitivity in Mice. Open Pain J. *3*, 123–133.

Hanstein, R., Negoro, H., Patel, N.K., Charollais, A., Meda, P., Spray, D.C., Suadicani, S.O., and Scemes, E. (2013). Promises and pitfalls of a Pannexin1 transgenic mouse line. Front. Pharmacol. *4*, 61.

Hanstein, R., Hanani, M., Scemes, E., and Spray, D.C. (2016). Glial pannexin1 contributes to tactile hypersensitivity in a mouse model of orofacial pain. Sci. Rep. *6*, 38266.

Harper, A.A., and Lawson, S.N. (1985). Conduction velocity is related to morphological cell type in rat dorsal root ganglion neurones. J. Physiol. *359*, 31–46.

Hayar, A., Gu, C., and Al-Chaer, E.D. (2008). An improved method for patch clamp recording and calcium imaging of neurons in the intact dorsal root ganglion in rats. J. Neurosci. Methods *173*, 74–82.

Hedstrom, K.L., Murtie, J.C., Albers, K., Calcutt, N.A., and Corfas, G. (2014). Treating small fiber neuropathy by topical application of a small molecule modulator of ligand-induced GFRα/RET receptor signaling. Proc. Natl. Acad. Sci. U. S. A. *111*, 2325–2330.

Heinbecker, P., Bishop, G.H., and O'leary, J. (1933). PAIN AND TOUCH FIBERS IN PERIPHERAL NERVES. Arch. Neurol. Psychiatry *29*, 771–789.

Heinricher, M.M., Tavares, I., Leith, J.L., and Lumb, B.M. (2009). Descending control of nociception: specificity, recruitment and plasticity. Brain Res. Rev. *60*, 214–225.

Henderson, C.E., Phillips, H.S., Pollock, R.A., Davies, A.M., Lemeulle, C., Armanini, M., Simmons, L., Moffet, B., Vandlen, R.A., Simpson LC corrected to Simmons, L., et al. (1994). GDNF: a potent survival factor for motoneurons present in peripheral nerve and muscle. Science *266*, 1062–1064.

Herzog, R.I., Cummins, T.R., and Waxman, S.G. (2001). Persistent TTX-resistant Na+ current affects resting potential and response to depolarization in simulated spinal sensory neurons. J. Neurophysiol. *86*, 1351–1364.

Heuckeroth, R.O., Enomoto, H., Grider, J.R., Golden, J.P., Hanke, J.A., Jackman, A., Molliver, D.C., Bardgett, M.E., Snider, W.D., Johnson, E.M., et al. (1999). Gene Targeting Reveals a Critical Role for Neurturin in the Development and Maintenance of Enteric, Sensory, and Parasympathetic Neurons. Neuron *22*, 253–263.

Hirade, M., Yasuda, H., Omatsu-Kanbe, M., Kikkawa, R., and Kitasato, H. (1999). Tetrodotoxin-resistant sodium channels of dorsal root ganglion neurons are readily activated in diabetic rats. Neuroscience *90*, 933–939.

Ho, C., and O'Leary, M.E. (2011). Single-cell analysis of sodium channel expression in dorsal root ganglion neurons. Mol. Cell. Neurosci. *46*, 159–166.

Hofstetter, J., Suckow, M.A., and Hickman, D.L. (2006). Chapter 4 - Morphophysiology. In The Laboratory Rat (Second Edition), (Burlington: Academic Press), pp. 93–125.

Höke, A., Cheng, C., and Zochodne, D.W. (2000). Expression of glial cell line-derived neurotrophic factor family of growth factors in peripheral nerve injury in rats. Neuroreport *11*, 1651–1654.

Hong, S., Morrow, T.J., Paulson, P.E., Isom, L.L., and Wiley, J.W. (2004). Early Painful Diabetic Neuropathy Is Associated with Differential Changes in Tetrodotoxin-sensitive and -resistant Sodium Channels in Dorsal Root Ganglion Neurons in the Rat. J. Biol. Chem. *279*, 29341–29350.

Huang, T.-Y., Cherkas, P.S., Rosenthal, D.W., and Hanani, M. (2005). Dye coupling among satellite glial cells in mammalian dorsal root ganglia. Brain Res. *1036*, 42–49.

Hunt, S.P., and Rossi, J. (1985). Nociception and pain - Peptide- and non-peptide-containing unmyelinated primary afferents: the parallel processing of nociceptive information. Phil Trans R Soc Lond B *308*, 283–289.

Iggo, A., and Muir, A.R. (1969). The structure and function of a slowly adapting touch corpuscle in hairy skin. J. Physiol. *200*, 763–796.

Ingber, D.E. (1997). Tensegrity: The architectural basis of cellular mechanotransduction. Annu. Rev. Physiol. *59*, 575–599.

Iyer, S.M., Montgomery, K.L., Towne, C., Lee, S.Y., Ramakrishnan, C., Deisseroth, K., and Delp, S.L. (2014). Virally mediated optogenetic excitation and inhibition of pain in freely moving nontransgenic mice. Nat. Biotechnol. *32*, 274.

Jasmin, L., Vit, J.., Bhargava, A., and Ohara, P.T. (2010). Can satellite glial cells be therapeutic targets for pain control? Neuron Glia Biol. *6*, 63–71.

Jin, G., Omori, N., Li, F., Sato, K., Nagano, I., Manabe, Y., Shoji, M., and Abe, K. (2002). Activation of cell-survival signal Akt by GDNF in normal rat brain. Brain Res. *958*, 429–433.

Johansson, R.S., and Vallbo, A.B. (1979). Tactile sensibility in the human hand: relative and absolute densities of four types of mechanoreceptive units in glabrous skin. J. Physiol. *286*, 283–300.

Kaplan, D.R., and Stephens, R.M. (1994). Neurotrophin signal transduction by the Trk receptor. J. Neurobiol. *25*, 1404–1417.

Kestell, G.R., Anderson, R.L., Clarke, J.N., Haberberger, R.V., and Gibbins, I.L. (2015). Primary afferent neurons containing calcitonin gene-related peptide but not substance P in forepaw skin, dorsal root ganglia, and spinal cord of mice. J. Comp. Neurol. *523*, 2555–2569.

Kim, Y.S., Anderson, M., Park, K., Zheng, Q., Agarwal, A., Gong, C., Saijilafu, Young, L., He, S., LaVinka, P.C., et al. (2016). Coupled Activation of Primary Sensory Neurons Contributes to Chronic Pain. Neuron *91*, 1085–1096.

King, A.J. (2012). The use of animal models in diabetes research: Animal models of diabetes. Br. J. Pharmacol. *166*, 877–894.

Kobayashi, K., Fukuoka, T., Yamanaka, H., Dai, Y., Obata, K., Tokunaga, A., and Noguchi, K. (2005). Differential expression patterns of mRNAs for P2X receptor subunits in neurochemically characterized dorsal root ganglion neurons in the rat. J. Comp. Neurol. *481*, 377–390.

Koltzenburg, M., Bennett, D.L.H., Shelton, D.L., and McMahon, S.B. (1999). Neutralization of endogenous NGF prevents the sensitization of nociceptors supplying inflamed skin: NGF neutralization prevents nociceptor sensitization. Eur. J. Neurosci. *11*, 1698–1704.

Kotzbauer, P.T., Lampe, P.A., Heuckeroth, R.O., Golden, J.P., Creedon, D.J., Johnson, E.M., and Milbrandt, J. (1996). Neurturin, a relative of glial-cell-line-derived neurotrophic factor. Nature *384*, 467–470.

Kullander, K., and Ebendal, T. (1994). Neurotrophin-3 acquires NGF-like activity after exchange to five NGF amino acid residues: Molecular analysis of the sites in NGF mediating the specific interaction with the NGF high affinity receptor. J. Neurosci. Res. *39*, 195–210.

Landau, W., and Bishop, G.H. (1953). Pain from dermal, periosteal, and fascial endings and from inflammation; electrophysiological study employing differential nerve blocks. AMA Arch. Neurol. Psychiatry *69*, 490–504.

Latremoliere, A., and Woolf, C.J. (2009). Central sensitization: a generator of pain hypersensitivity by central neural plasticity. J. Pain Off. J. Am. Pain Soc. *10*, 895–926.

Lawson, S.N. (1979). The postnatal development of large light and small dark neurons in mouse dorsal root ganglia: a statistical analysis of cell numbers and size. J. Neurocytol. *8*, 275–294.

Lawson, E., and Backonja, M. "Misha" (2013). Painful Diabetic Polyneuropathy: A Comprehensive Guide for Clinicians (Springer Science & Business Media).

Lawson, S.N., Harper, A.A., Harper, E.I., Garson, J.A., and Anderton, B.H. (1984). A monoclonal antibody against neurofilament protein specifically labels a subpopulation of rat sensory neurones. J. Comp. Neurol. *228*, 263–272.

Lawson, S.N., Perry, M.J., Prabhakar, E., and McCarthy, P.W. (1993). Primary sensory neurones: neurofilament, neuropeptides, and conduction velocity. Brain Res. Bull. *30*, 239–243.

Le Pichon, C.E., and Chesler, A.T. (2014). The functional and anatomical dissection of somatosensory subpopulations using mouse genetics. Front. Neuroanat. *8*, 1–18.

Ledda, M., De Palo, S., and Pannese, E. (2004). Ratios between number of neuroglial cells and number and volume of nerve cells in the spinal ganglia of two species of reptiles and three species of mammals. Tissue Cell *36*, 55–62.

Leiter, E.H. (2009). Selecting the "Right" Mouse Model for Metabolic Syndrome and Type 2 Diabetes Research. In Type 2 Diabetes, C. Stocker, ed. (Totowa, NJ: Humana Press), pp. 1–17.

Levine, J.D., Fields, H.L., and Basbaum, A.I. (1993). Peptides and the primary afferent nociceptor. J. Neurosci. Off. J. Soc. Neurosci. *13*, 2273–2286.

Lewin, G.R., Ritter, A.M., and Mendell, L.M. (1993). Nerve growth factor-induced hyperalgesia in the neonatal and adult rat. J. Neurosci. Off. J. Soc. Neurosci. *13*, 2136–2148.

Lewin, G.R., Rueff, A., and Mendell, L.M. (1994). Peripheral and central mechanisms of NGF-induced hyperalgesia. Eur. J. Neurosci. *6*, 1903–1912.

Lieberman, A.R. (1976). Sensory Ganglia. Peripher. Nerve 188–278.

Light, A.R., and Perl, E.R. (1979b). Reexamination of the dorsal root projection to the spinal dorsal horn including observations on the differential termination of coarse and fine fibers. J. Comp. Neurol. *186*, 117–131.

Light, A.R., and Perl, E.R. (1979a). Spinal termination of functionally identified primary afferent neurons with slowly conducting myelinated fibers. J. Comp. Neurol. *186*, 133–150.

Lin, L.F., Doherty, D.H., Lile, J.D., Bektesh, S., and Collins, F. (1993). GDNF: a glial cell line-derived neurotrophic factor for midbrain dopaminergic neurons. Science *260*, 1130–1132.

Liu, G.-S., Shi, J.-Y., Lai, C.-L., Hong, Y.-R., Shin, S.-J., Huang, H.-T., Lam, H.-C., Wen, Z.-H., Hsu, K.-S., Chen, C.-H., et al. (2009). Peripheral Gene Transfer of Glial Cell-Derived Neurotrophic Factor Ameliorates Neuropathic Deficits in Diabetic Rats. Hum. Gene Ther. *20*, 715–727.

Ma, Q.-P., and Woolf, C.J. (1996). Progressive tactile hypersensitivity: an inflammation-induced incremental increase in the excitability of the spinal cord. PAIN *67*, 97.

Maier, C., Baron, R., Tölle, T.R., Binder, A., Birbaumer, N., Birklein, F., Gierthmühlen, J., Flor, H., Geber, C., Huge, V., et al. (2010). Quantitative sensory testing in the German Research Network on Neuropathic Pain (DFNS): somatosensory abnormalities in 1236 patients with different neuropathic pain syndromes. Pain *150*, 439–450.

Malcangio, M. (1997). Nerve growth factor treatment increases stimulus-evoked release of sensory neuropeptides in the rat spinal cord. Eur. J. Neurosci. *9*, 1101–1104.

Malcangio, M., Ramer, M.S., Boucher, T.J., and McMahon, S.B. (2000). Intrathecally injected neurotrophins and the release of substance P from the rat isolated spinal cord. Eur. J. Neurosci. *12*, 139–144.

Malcangio, M., Getting, S.J., Grist, J., Cunningham, J.R., Bradbury, E.J., Issa, P.C., Lever, I.J., Pezet, S., and Perretti, M. (2002). A novel control mechanism based on GDNF modulation of somatostatin release from sensory neurones. FASEB J. *16*, 730–732.

Malin, S.A., Molliver, D.C., Koerber, H.R., Cornuet, P., Frye, R., Albers, K.M., and Davis, B.M. (2006). Glial cell line-derived neurotrophic factor family members sensitize nociceptors in vitro and produce thermal hyperalgesia in vivo. J. Neurosci. Off. J. Soc. Neurosci. *26*, 8588–8599.

Marmigère, F., and Ernfors, P. (2007). Specification and connectivity of neuronal subtypes in the sensory lineage. Nat. Rev. Neurosci. *8*, 114–127.

Martin, R.J., Apkarian, A.V., and Hodge, C.J. (1990). Ventrolateral and dorsolateral ascending spinal cord pathway influence on thalamic nociception in cat. J. Neurophysiol. *64*, 1400–1412.

Matheson, C.R., Carnahan, J., Urich, J.L., Bocangel, D., and Zhang, T.J. (1996). Glial Cell Line-Derived Neurotrophic Factor (GDNF) Is a Neurotrophic Factor for Sensory Neurons : Comparison with the Effects of the Neurotrophins. 22–32.

Maurel, P., Einheber, S., Galinska, J., Thaker, P., Lam, I., Rubin, M.B., Scherer, S.S., Murakami, Y., Gutmann, D.H., and Salzer, J.L. (2007). Nectin-like proteins mediate axon Schwann cell interactions along the internode and are essential for myelination. J. Cell Biol. *178*, 861–874.

McCarthy, P.W., and Lawson, S.N. (1990). Cell type and conduction velocity of rat primary sensory neurons with calcitonin gene-related peptide-like immunoreactivity. Neuroscience *34*, 623–632.

McCoy, E.S., Taylor-Blake, B., Street, S.E., Pribisko, A.L., Zheng, J., and Zylka, M.J. (2013a). Peptidergic CGRPα primary sensory neurons encode heat and itch and tonically suppress sensitivity to cold. Neuron *78*, 138–151.

McCoy, E.S., Taylor-Blake, B., Street, S.E., Pribisko, A.L., Zheng, J., and Zylka, M.J. (2013b). Peptidergic CGRP+ Primary Sensory Neurons Encode Heat and Itch and Tonically Suppress Sensitivity to Cold. Neuron *78*, 138–151.

McEvoy, R.C., Andersson, J., Sandler, S., and Hellerström, C. (1984). Multiple low-dose streptozotocin-induced diabetes in the mouse. Evidence for stimulation of a cytotoxic cellular immune response against an insulin-producing beta cell line. J. Clin. Invest. *74*, 715–722.

McKemy, D.D. (2007). TRPM8: The Cold and Menthol Receptor. In TRP Ion Channel Function in Sensory Transduction and Cellular Signaling Cascades, W.B. Liedtke, and S. Heller, eds. (Boca Raton (FL): CRC Press/Taylor & Francis), p.

Melzack, R., and Casey, K. (1968). Sensory, motivational, and central control determinants of pain: a new conceptual model. In The Skin Senses, (Spriengfield, IL), p.

Melzack, R., and Wall, P.D. (1965). Pain mechanisms: a new theory. Science *150*, 971–979.

Merighi, A. (2016). Targeting the glial-derived neurotrophic factor and related molecules for controlling normal and pathologic pain. Expert Opin. Ther. Targets *20*, 193–208.

Merighi, A., Polak, J.M., and Theodosis, D.T. (1991). Ultrastructural visualization of glutamate and aspartate immunoreactivities in the rat dorsal horn, with special reference to the co-localization of glutamate, substance P and calcitonin-gene related peptide. Neuroscience *40*, 67–80.

Merighi, A., Salio, C., Ghirri, A., Lossi, L., Ferrini, F., Betelli, C., and Bardoni, R. (2008a). BDNF as a pain modulator. Prog. Neurobiol. *85*, 297–317.

Merighi, A., Bardoni, R., Salio, C., Lossi, L., Ferrini, F., Prandini, M., Zonta, M., Gustincich, S., and Carmignoto, G. (2008b). Presynaptic functional trkB receptors mediate the release of excitatory neurotransmitters from primary afferent terminals in lamina II (substantia gelatinosa) of postnatal rat spinal cord. Dev. Neurobiol. *68*, 457–475.

Meyer, R.A., and Campbell, J.N. (1981b). Myelinated nociceptive afferents account for the hyperalgesia that follows a burn to the hand. Science *213*, 1527–1529.

Meyer, R.A., and Campbell, J.N. (1981a). Evidence for two distinct classes of unmyelinated nociceptive afferents in monkey. Brain Res. *224*, 149–152.

Michael, G.J., Averill, S., Nitkunan, A., Rattray, M., Bennett, D.L.H., Yan, Q., and Priestley, J.V. (1997). Nerve Growth Factor Treatment Increases Brain-Derived Neurotrophic Factor Selectively in TrkA-Expressing Dorsal Root Ganglion Cells and in Their Central Terminations within the Spinal Cord. J. Neurosci. *17*, 8476–8490.

Middlemas, D.S., Lindberg, R.A., and Hunter, T. (1991). trkB, a neural receptor protein-tyrosine kinase: evidence for a full-length and two truncated receptors. Mol. Cell. Biol. *11*, 143–153.

Milbrandt, J., de Sauvage, F.J., Fahrner, T.J., Baloh, R.H., Leitner, M.L., Tansey, M.G., Lampe, P.A., Heuckeroth, R.O., Kotzbauer, P.T., Simburger, K.S., et al. (1998). Persephin, a Novel Neurotrophic Factor Related to GDNF and Neurturin. Neuron *20*, 245–253.

Millan, M.J. (1999). The induction of pain: An integrative review. Prog. Neurobiol. *57*, 1–164.

Miller, K.E., Richards, B.A., and Kriebel, R.M. (2002). Glutamine-, glutamine synthetase-, glutamate dehydrogenase- and pyruvate carboxylase-immunoreactivities in the rat dorsal root ganglion and peripheral nerve. Brain Res. *945*, 202–211.

Mills, C.D., Allchorne, A.J., Griffin, R.S., Woolf, C.J., and Costigan, M. (2007). GDNF selectively promotes regeneration of injury-primed sensory neurons in the lesioned spinal cord. Mol. Cell. Neurosci. *36*, 185–194.

Milosevic, N., Ristanovic, D., and Stanković, J.B. (2005). Fractal analysis of the laminar organization of spinal cord neurons. J. Neurosci. Methods *146*, 198–204.

Minichiello, L., Casagranda, F., Tatche, R.S., Stucky, C.L., Postigo, A., Lewin, G.R., Davies, A.M., and Klein, R. (1998). Point mutation in trkB causes loss of NT4-dependent neurons without major effects on diverse BDNF responses. Neuron *21*, 335–345.

Moayedi, M., and Davis, K.D. (2013). Theories of pain: from specificity to gate control. J. Neurophysiol. *109*, 5–12.

Molliver, D.C., and Snider, W.D. (1997). Nerve growth factor receptor trkA is down-regulated during postnatal development by a subset of dorsal root ganglion neurons. J. Comp. Neurol. *381*, 428–438.

Molliver, D.C., Wright, D.E., Leitner, M.L., Parsadanian, A.S., Doster, K., Wen, D., Yan, Q., and Snider, W.D. (1997a). IB4-binding DRG neurons switch from NGF to GDNF dependence in early postnatal life. Neuron *19*, 849–861.

Molliver, D.C., Wright, D.E., Leitner, M.L., Parsadanian, A.S., Doster, K., Wen, D., Yan, Q., and Snider, W.D. (1997b). IB4-binding DRG neurons switch from NGF to GDNF dependence in early postnatal life. Neuron *19*, 849–861.

Moore, M.W., Klein, R.D., Fariñas, I., Sauer, H., Armanini, M., Phillips, H., Reichardt, L.F., Ryan, A.M., Carver-Moore, K., and Rosenthal, A. (1996). Renal and neuronal abnormalities in mice lacking GDNF. Nature *382*, 76.

Müller, M., Felmy, F., Schwaller, B., and Schneggenburger, R. (2007). Parvalbumin is a mobile presynaptic Ca2+ buffer in the calyx of Held that accelerates the decay of Ca2+ and short-term facilitation. J. Neurosci. Off. J. Soc. Neurosci. *27*, 2261–2271.

Murakami, T., Iwanaga, T., Ogawa, Y., Fujita, Y., Sato, E., Yoshitomi, H., Sunada, Y., and Nakamura, A. (2013). Development of sensory neuropathy in streptozotocin-induced diabetic mice. Brain Behav. *3*, 35–41.

Nagano, M., Sakai, A., Takahashi, N., Umino, M., Yoshioka, K., and Suzuki, H. (2003). Decreased expression of glial cell line-derived neurotrophic factor signaling in rat models of neuropathic pain. Br. J. Pharmacol. *140*, 1252–1260.

Nagy, J.I., and Hunt, S.P. (1983). The termination of primary afferents within the rat dorsal horn: Evidence for rearrangement following capsaicin treatment. J. Comp. Neurol. *218*, 145–158.

Nascimento, O.J.M. do, Pupe, C.C.B., and Cavalcanti, E.B.U. (2016). Diabetic neuropathy. Rev. Dor *17*.

Nascimento, R.S., Santiago, M.F., Marques, S.A., Allodi, S., and Martinez, A.M.B. (2008). Diversity among satellite glial cells in dorsal root ganglia of the rat. Braz. J. Med. Biol. Res. Rev. Bras. Pesqui. Medicas E Biol. *41*, 1011–1017.

Neher, E., and Augustine, G.J. (1992). Calcium gradients and buffers in bovine chromaffin cells. J. Physiol. *450*, 273–301.

NIH (2009). Nerve Damage (Diabetic Neuropathies) | NIDDK.

O'Brien, P.D., Sakowski, S.A., and Feldman, E.L. (2014). Mouse models of diabetic neuropathy. ILAR J. *54*, 259–272.

Obrosova, I.G., Ilnytska, O., Lyzogubov, V.V., Pavlov, I.A., Mashtalir, N., Nadler, J.L., and Drel, V.R. (2007). High-fat diet induced neuropathy of pre-diabetes and obesity: effects of "healthy" diet and aldose reductase inhibition. Diabetes *56*, 2598–2608.

Ogun-Muyiwa, P., Helliwell, R., McIntyre, P., and Winter, J. (1999). Glial cell line derived neurotrophic factor (GDNF) regulates VR1 and substance P in cultured sensory neurons. Neuroreport *10*, 2107–2111.

Ohta, K., Inokuchi, T., Gen, E., and Chang, J. (2001). Ultrastructural study of anterograde transport of glial cell line-derived neurotrophic factor from dorsal root ganglion neurons of rats towards the nerve terminal. Cells Tissues Organs *169*, 410–421.

Orozco, O.E., Walus, L., Sah, D.W.Y., Pepinsky, R.B., and Sanicola, M. (2001). GFRalpha3 is expressed predominantly in nociceptive sensory neurons: GFRalpha3 sensory neurons are nociceptors. Eur. J. Neurosci. *13*, 2177–2182.

Otoshi, K., Kikuchi, S., Konno, S., and Sekiguchi, M. (2010). The Reactions of Glial Cells and Endoneurial Macrophages in the Dorsal Root Ganglion and Their Contribution to Pain-Related Behavior After Application of Nucleus Pulposus Onto the Nerve Root in Rats. Spine *35*, 264–271.

Pabbidi, R.M., Cao, D.-S., Parihar, A., Pauza, M.E., and Premkumar, L.S. (2008). Direct role of streptozotocin in inducing thermal hyperalgesia by enhanced expression of transient receptor potential vanilloid 1 in sensory neurons. Mol. Pharmacol. *73*, 995–1004.

Pannese, E. (1981). The satellite cells of the sensory ganglia. Adv. Anat. Embryol. Cell Biol. *65*, 1–111.

Pannese, E., Ledda, M., Arcidiacono, G., and Rigamonti, L. (1991). Clusters of nerve cell bodies enclosed within a common connective tissue envelope in the spinal ganglia of the lizard and rat. Cell Tissue Res. *264*, 209–214.

Pannese, E., Procacci, P., Ledda, M., and Conte, V. (1993). The percentage of nerve cell bodies arranged in clusters decreases with age in the spinal ganglia of adult rabbits. Anat. Embryol. (Berl.) *187*, 331–334.

Paratcha, G., Ledda, F., Baars, L., Coulpier, M., Besset, V., Anders, J., Scott, R., and Ibáñez, C.F. (2001). Released GFRalpha1 potentiates downstream signaling, neuronal survival, and differentiation via a novel mechanism of recruitment of c-Ret to lipid rafts. Neuron *29*, 171–184.

Patestas, M.A., and Gartner, L.P. (2016). A Textbook of Neuroanatomy (John Wiley & Sons).

Pearce, R.J., and Duchen, M.R. (1994). Differential expression of membrane currents in dissociated mouse primary sensory neurons. Neuroscience *63*, 1041–1056.

Pearson, J.A., Wong, F.S., and Wen, L. (2016). The importance of the Non Obese Diabetic (NOD) mouse model in autoimmune diabetes. J. Autoimmun. *66*, 76–88.

Peeraer, E., Van Lutsenborg, A., Verheyen, A., De Jongh, R., Nuydens, R., and Meert, T.F. (2011). Pharmacological evaluation of rat dorsal root ganglion neurons as an in vitro model for diabetic neuropathy. J. Pain Res. *4*, 55–65.

Pertovaara, A. (2006). Noradrenergic pain modulation. Prog. Neurobiol. *80*, 53–83.

Pezet, S., Malcangio, M., Lever, I.J., Perkinton, M.S., Thompson, S.W.N., Williams, R.J., and McMahon, S.B. (2002). Noxious stimulation induces Trk receptor and downstream ERK phosphorylation in spinal dorsal horn. Mol. Cell. Neurosci. *21*, 684–695.

Pfaller, K., and Arvidsson, J. (1988). Central distribution of trigeminal and upper cervical primary afferents in the rat studied by anterograde transport of horseradish peroxidase conjugated to wheat germ agglutinin. J. Comp. Neurol. *268*, 91–108.

Pichel, J.G., Shen, L., Sheng, H.Z., Granholm, A.C., Drago, J., Grinberg, A., Lee, E.J., Huang, S.P., Saarma, M., Hoffer, B.J., et al. (1996). Defects in enteric innervation and kidney development in mice lacking GDNF. Nature *382*, 73–76.

Piltonen, M., Bespalov, M.M., Ervasti, D., Matilainen, T., Sidorova, Y.A., Rauvala, H., Saarma, M., and Männistö, P.T. (2009). Heparin-binding determinants of GDNF reduce its tissue distribution but are beneficial for the protection of nigral dopaminergic neurons. Exp. Neurol. *219*, 499–506.

Poggio, G.F., and Mountcastle, V.B. (1960). A study of the functional contributions of the lemniscal and spinothalamic systems to somatic sensibility. Central nervous mechanisms in pain. Bull. Johns Hopkins Hosp. *106*, 266–316.

Pogorzala, L.A., Mishra, S.K., and Hoon, M.A. (2013). The cellular code for mammalian thermosensation. J. Neurosci. Off. J. Soc. Neurosci. *33*, 5533.

Pomonis, J.D., Rogers, S.D., Peters, C.M., Ghilardi, J.R., and Mantyh, P.W. (2001). Expression and localization of endothelin receptors: implications for the involvement of peripheral glia in nociception. J. Neurosci. Off. J. Soc. Neurosci. *21*, 999–1006.

Prescott, E.D., and Julius, D. (2003). A Modular PIP2 Binding Site as a Determinant of Capsaicin Receptor Sensitivity. Science *300*, 1284–1288.

Price, D.D., Hu, J.W., Dubner, R., and Gracely, R.H. (1977). Peripheral suppression of first pain and central summation of second pain evoked by noxious heat pulses. Pain *3*, 57–68.

Rajasekhar, P., Poole, D.P., Liedtke, W., Bunnett, N.W., and Veldhuis, N.A. (2015). P2Y1 Receptor Activation of the TRPV4 Ion Channel Enhances Purinergic Signaling in Satellite Glial Cells. J. Biol. Chem. *290*, 29051–29062.

Rambourg, A., Clermont, Y., and Beaudet, A. (1983). Ultrastructural features of six types of neurons in rat dorsal root ganglia. J. Neurocytol. *12*, 47–66.

Ramer, M.S., Bradbury, E.J., Michael, G.J., Lever, I.J., and McMahon, S.B. (2003). Glial cell line-derived neurotrophic factor increases calcitonin gene-related peptide immunoreactivity in sensory and motoneurons in vivo. Eur. J. Neurosci. *18*, 2713–2721.

Rateau, Y. (2006). Expression of a Functional Hyperpolarization-Activated Current (Ih) in the Mouse Nucleus Reticularis Thalami. J. Neurophysiol. *95*, 3073–3085.

Rees, D.A., and Alcolado, J.C. (2005). Animal models of diabetes mellitus. Diabet. Med. J. Br. Diabet. Assoc. *22*, 359–370.

Ren, K., and Dubner, R. (2002). Descending modulation in persistent pain: an update. Pain *100*, 1–6.

Rexed, B. (1952). The cytoarchitectonic organization of the spinal cord in the cat. J. Comp. Neurol. *96*, 415–495.

Rey, R. (1995). The History of Pain (Harvard University Press).

Richardson, D.S., Lai, A.Z., and Mulligan, L.M. (2006). RET ligand-induced internalization and its consequences for downstream signaling. Oncogene *25*, 3206–3211.

Romanovsky, D., Wang, J., Al-Chaer, E.D., Stimers, J.R., and Dobretsov, M. (2010). Comparison of metabolic and neuropathy profiles of rats with streptozotocin-induced overt and moderate insulinopenia. Neuroscience *170*, 337–347.

Rose, R.D., Koerber, H.R., Sedivec, M.J., and Mendell, L.M. (1986). Somal action potential duration differs in identified primary afferents. Neurosci. Lett. *63*, 259–264.

Rozanski, G.M., Li, Q., and Stanley, E.F. (2013). Transglial transmission at the dorsal root ganglion sandwich synapse: glial cell to postsynaptic neuron communication. Eur. J. Neurosci. *37*, 1221–1228.

Ruffini, A. (1893). Sur un nouvel organe nerveux terminal et sur la presence des corpuscules Golgi-Mazzoni dens le conjonctif souscutané de la pulpe des doigts de l'homme. Mémoires de l'Academie Royale. 249–265.

Runeberg-Roos, P., and Saarma, M. (2007). Neurotrophic factor receptor RET: structure, cell biology, and inherited diseases. Ann. Med. *39*, 572–580.

Rydén, M., Murray-Rust, J., Glass, D., Ilag, L.L., Trupp, M., Yancopoulos, G.D., McDonald, N.Q., and Ibáñez, C.F. (1995). Functional analysis of mutant neurotrophins deficient in low-affinity binding reveals a role for p75LNGFR in NT-4 signalling. EMBO J. *14*, 1979–1990.

Salio, C., and Ferrini, F. (2016). BDNF and GDNF expression in discrete populations of nociceptors. Ann. Anat. Anat. Anz. Off. Organ Anat. Ges. *207*, 55–61.

Salio, C., Lossi, L., Ferrini, F., and Merighi, A. (2005). Ultrastructural evidence for a pre- and postsynaptic localization of full-length trkB receptors in substantia gelatinosa (lamina II) of rat and mouse spinal cord. Eur. J. Neurosci. *22*, 1951–1966.

Salio, C., Ferrini, F., Muthuraju, S., and Merighi, A. (2014). Presynaptic modulation of spinal nociceptive transmission by glial cell line-derived neurotrophic factor (GDNF). J. Neurosci. Off. J. Soc. Neurosci. *34*, 13819–13833.

Sánchez, M.P., Silos-Santiago, I., Frisén, J., He, B., Lira, S.A., and Barbacid, M. (1996). Renal agenesis and the absence of enteric neurons in mice lacking GDNF. Nature *382*, 70–73.

Schmidt, R., Schmelz, M., Forster, C., Ringkamp, M., Torebjörk, E., and Handwerker, H. (1995). Novel classes of responsive and unresponsive C nociceptors in human skin. J. Neurosci. Off. J. Soc. Neurosci. *15*, 333–341.

Schmidt, R., Schmelz, M., Torebjörk, H.E., and Handwerker, H.O. (2000). Mechano-insensitive nociceptors encode pain evoked by tonic pressure to human skin. Neuroscience *98*, 793–800.

Schrader, L.A., Birnbaum, S.G., Nadin, B.M., Ren, Y., Bui, D., Anderson, A.E., and Sweatt, J.D. (2006). ERK/MAPK regulates the Kv4.2 potassium channel by direct phosphorylation of the pore-forming subunit. Am. J. Physiol. - Cell Physiol. *290*, C852–C861.

Schuchardt, A., D'Agati, V., Larsson-Blomberg, L., Costantini, F., and Pachnis, V. (1994). Defects in the kidney and enteric nervous system of mice lacking the tyrosine kinase receptor Ret. Nature *367*, 380–383.

Scroggs, R.S., and Fox, A.P. (1992). Calcium current variation between acutely isolated adult rat dorsal root ganglion neurons of different size. J. Physiol. *445*, 639–658.

Sengul, G., and Watson, C. (2012). Chapter 13 - Spinal Cord. In The Mouse Nervous System, (San Diego: Academic Press), pp. 424–458.

Shaikh, A.S., and Somani, R.S. (2010). Animal models and biomarkers of neuropathy in diabetic rodents. Indian J. Pharmacol. *42*, 129.

Sherrington, C.S. (1906). Observations on the scratch-reflex in the spinal dog. J. Physiol. *34*, 1–50.

Shi, T.-J.S., Li, J., Dahlström, A., Theodorsson, E., Ceccatelli, S., Decosterd, I., Pedrazzini, T., and Hökfelt, T. (2006). Deletion of the neuropeptide Y Y1 receptor affects pain sensitivity, neuropeptide transport and expression, and dorsal root ganglion neuron numbers. Neuroscience *140*, 293–304.

Shi, T.-J.S., Xiang, Q., Zhang, M.-D., Barde, S., Kai-Larsen, Y., Fried, K., Josephson, A., Glück, L., Deyev, S.M., Zvyagin, A.V., et al. (2014). Somatostatin and its 2A receptor in dorsal root ganglia and dorsal horn of mouse and human: expression, trafficking and possible role in pain. Mol. Pain *10*, 12.

Shu, X., and Mendell, L.M. (2001). Acute Sensitization by NGF of the Response of Small-Diameter Sensory Neurons to Capsaicin. J. Neurophysiol. *86*, 2931–2938.

Sidorova, Y.A., Bespalov, M.M., Wong, A.W., Kambur, O., Jokinen, V., Lilius, T.O., Suleymanova, I., Karelson, G., Rauhala, P.V., Karelson, M., et al. (2017). A Novel Small Molecule GDNF Receptor RET Agonist, BT13, Promotes

Neurite Growth from Sensory Neurons in Vitro and Attenuates Experimental Neuropathy in the Rat. Front. Pharmacol. *8*, 365.

Silverman, W.R., de Rivero Vaccari, J.P., Locovei, S., Qiu, F., Carlsson, S.K., Scemes, E., Keane, R.W., and Dahl, G. (2009). The pannexin 1 channel activates the inflammasome in neurons and astrocytes. J. Biol. Chem. *284*, 18143–18151.

Sinclair, D.C. (1955). Cutaneous sensation and the doctrine of specific energy. Brain J. Neurol. *78*, 584–614.

Singh, R., Kishore, L., and Kaur, N. (2014). Diabetic peripheral neuropathy: Current perspective and future directions. Pharmacol. Res. *80*, 21–35.

Smith, A.G., Russell, J., Feldman, E.L., Goldstein, J., Peltier, A., Smith, S., Hamwi, J., Pollari, D., Bixby, B., Howard, J., et al. (2006). Lifestyle intervention for pre-diabetic neuropathy. Diabetes Care *29*, 1294–1299.

Spray, D.C. (1996). Physiological Properties of Gap Junction Channels in the Nervous System. In Gap Junctions in the Nervous System, (Berlin, Heidelberg: Springer Berlin Heidelberg), pp. 39–59.

Stahnisch, F.W. (2009). François Magendie (1783–1855). J. Neurol. *256*, 1950–1952.

Stucky, C.L., and Lewin, G.R. (1999a). Isolectin B(4)-positive and -negative nociceptors are functionally distinct. J. Neurosci. Off. J. Soc. Neurosci. *19*, 6497–6505.

Stucky, C.L., and Lewin, G.R. (1999b). Isolectin B(4)-positive and -negative nociceptors are functionally distinct. J. Neurosci. *19*, 505.

Stucky, C.L., DeChiara, T., Lindsay, R.M., Yancopoulos, G.D., and Koltzenburg, M. (1998). Neurotrophin 4 Is Required for the Survival of a Subclass of Hair Follicle Receptors. J. Neurosci. *18*, 7040–7046.

Stucky, C.L., Rossi, J., Airaksinen, M.S., and Lewin, G.R. (2002). GFR alpha2/neurturin signalling regulates noxious heat transduction in isolectin B4-binding mouse sensory neurons. J. Physiol. *545*, 43–50.

Sullivan, K.A., Hayes, J.M., Wiggin, T.D., Backus, C., Oh, S.S., Lentz, S.I., Brosius, F., and Feldman, E.L. (2007). Mouse models of diabetic neuropathy. Neurobiol. Dis. *28*, 276–285.

Sullivan, K.A., Lentz, S.I., Roberts, J.L., and Feldman, E.L. (2008). Criteria for Creating and Assessing Mouse Models of Diabetic Neuropathy. Curr. Drug Targets *9*, 3–13.

Sun, W., Miao, B., Wang, X.-C., Duan, J.-H., Ye, X., Han, W.-J., Wang, W.-T., Luo, C., and Hu, S.-J. (2012). Gastrodin inhibits allodynia and hyperalgesia in painful diabetic neuropathy rats by decreasing excitability of nociceptive primary sensory neurons. PloS One *7*, e39647.

Swett, J.E., and Woolf, C.J. (1985). The somatotopic organization of primary afferent terminals in the superficial laminae of the dorsal horn of the rat spinal cord. J. Comp. Neurol. *231*, 66–77.

Takahashi, K., and Ninomiya, T. (1987). Morphological changes of dorsal root ganglion cells in the process-forming period. Prog. Neurobiol. *29*, 393–410.

Takeda, M., Kitagawa, J., Nasu, M., Takahashi, M., and Iwata, K. (2010). Glial cell line-derived neurotrophic factor acutely modulates the excitability of rat small-diameter trigeminal ganglion neurons innervating facial skin. Brain. Behav. Immun. *24*, 72–82.

Tang, M., Wu, G., Wang, Z., Yang, N., Shi, H., He, Q., Zhu, C., Yang, Y., Yu, G., Wang, C., et al. (2016). Voltage-gated potassium channels involved in regulation of physiological function in MrgprA3-specific itch neurons. Brain Res. *1636*, 161–171.

Tang, X., Schmidt, T.M., Perez-Leighton, C.E., and Kofuji, P. (2010). Kir4.1 is Responsible for the Native Inward Potassium Conductance of Satellite Glial Cells in Sensory Ganglia. Neuroscience *166*, 397–407.

Tansey, M.G., Baloh, R.H., Milbrandt, J., and Johnson, E.M. (2000). GFRalpha-mediated localization of RET to lipid rafts is required for effective downstream signaling, differentiation, and neuronal survival. Neuron *25*, 611–623.

Tate, S., Benn, S., Hick, C., Trezise, D., John, V., Mannion, R.J., Costigan, M., Plumpton, C., Grose, D., Gladwell, Z., et al. (1998). Two sodium channels contribute to the TTX-R sodium current in primary sensory neurons. Nat. Neurosci. *1*, 653–655.

Tavares, I., and Lima, D. (2002). The caudal ventrolateral medulla as an important inhibitory modulator of pain transmission in the spinal cord. J. Pain Off. J. Am. Pain Soc. *3*, 337–346.

Taylor, D.C.M., Korf, H.-W., and Pierau, F.-K. (1982). Distribution of sensory neurones of the pudendal nerve in the dorsal root ganglia and their projection to the spinal cord. Cell Tissue Res. *226*, 555–564.

Tesfaye, S., and Selvarajah, D. (2012). Advances in the epidemiology, pathogenesis and management of diabetic peripheral neuropathy. Diabetes Metab. Res. Rev. *28*, 8–14.

Themistocleous, A.C., Ramirez, J.D., Shillo, P.R., Lees, J.G., and Selvarajah, D. (2016). The Pain in Neuropathy Study (PiNS): a cross-sectional observational study determining the somatosensory phenotype of painful and painless diabetic neuropathy. *157*, 1132–1145.

Todd, A.J. (2002). Anatomy of primary afferents and projection neurones in the rat spinal dorsal horn with particular emphasis on substance P and the neurokinin 1 receptor. Exp. Physiol. *87*, 245–249.

Tokugawa, K., Yamamoto, K., Nishiguchi, M., Sekine, T., Sakai, M., Ueki, T., Chaki, S., and Okuyama, S. (2003). XIB4035, a novel nonpeptidyl small molecule agonist for GFRalpha-1. Neurochem. Int. *42*, 81–86.

Toth, C., Brussee, V., Cheng, C., and Zochodne, D.W. (2004). Diabetes Mellitus and the Sensory Neuron. J. Neuropathol. Exp. Neurol. *63*, 561–573.

Tracey, D.J., Romm, M.A., and Yao, N.N. (1995). Peripheral hyperalgesia in experimental neuropathy: exacerbation by neuropeptide Y. Brain Res. *669*, 245–254.

Treede, R.-D., Meyer, R.A., Raja, S.N., and Campbell, J.N. (1992). Peripheral and central mechanisms of cutaneous hyperalgesia. Prog. Neurobiol. *38*, 397–421.

Treede, R.D., Meyer, R.A., and Campbell, J.N. (1998). Myelinated mechanically insensitive afferents from monkey hairy skin: heat-response properties. J. Neurophysiol. *80*, 1082–1093.

Trupp, M. (1999). Ret-dependent and -independent Mechanisms of Glial Cell Line-derived Neurotrophic Factor Signaling in Neuronal Cells. J. Biol. Chem. *274*, 20885–20894.

Tsantoulas, C., and McMahon, S.B. (2014). Opening paths to novel analgesics: the role of potassium channels in chronic pain. Trends Neurosci. *37*, 146–158.

Vallbo, A.B., Hagbarth, K.E., Torebjork, H.E., and Wallin, B.G. (1979). Somatosensory, proprioceptive, and sympathetic activity in human peripheral nerves. Physiol. Rev. *59*, 919–957.

Ventura-Sobrevilla, J., Boone, D., Aguilar, C., Román-Ramos, R., Vega, E., Campos-Sepúlveda, E., and Alarcon, F. (2011). Effect of Varying Dose and Administration of Streptozotocin on Blood Sugar in Male CD1 Mice. Proc. West. Pharmacol. Soc. *54*, 5–9.

Vogalis, F., Harvey, J.R., Neylon, C.B., and Furness, J.B. (2002). Regulation of K+ channels underlying the slow afterhyperpolarization in enteric afterhyperpolarization-generating myenteric neurons: role of calcium and phosphorylation. Clin. Exp. Pharmacol. Physiol. *29*, 935–943.

Vrontou, S., Wong, A.M., Rau, K.K., Koerber, H.R., and Anderson, D.J. (2013). Genetic identification of C-fibers that detect massage-like stroking of hairy skin in vivo. Nature *493*, 669–673.

Wall, P.D., and Devor, M. (1983). Sensory afferent impulses originate from dorsal root ganglia as well as from the periphery in normal and nerve injured rats. Pain *17*, 321–339.

Wang, R., Guo, W., Ossipov, M.H., Vanderah, T.W., Porreca, F., and Lai, J. (2003). Glial cell line-derived neurotrophic factor normalizes neurochemical changes in injured dorsal root ganglion neurons and prevents the expression of experimental neuropathic pain. Neuroscience *121*, 815–824.

Wang, X., Gu, P., Chen, S., Gao, W., Tian, H., Lu, X., Zheng, W., Zhuge, Q., and Hu, W. (2015). Endogenous neurotrophin-3 promotes neuronal sprouting from dorsal root ganglia. Neural Regen. Res. *10*, 1865–1868.

Waxman, S.G., and Zamponi, G.W. (2014). Regulating excitability of peripheral afferents: emerging ion channel targets. Nat. Neurosci. *17*, 153–163.

Weddell, G. (1955). Somesthesis and the Chemical Senses. Annu. Rev. Psychol. *6*, 119–136.

Weick, M., Cherkas, P.S., Härtig, W., Pannicke, T., Uckermann, O., Bringmann, A., Tal, M., Reichenbach, A., and Hanani, M. (2003). P2 receptors in satellite glial cells in trigeminal ganglia of mice. Neuroscience *120*, 969–977.

Welker, C. (1971). Microelectrode delineation of fine grain somatotopic organization of SmI cerebral neocortex in albino rat. Brain Res. *26*, 259–275.

Wessels, W.J., and Marani, E. (1993). A rostrocaudal somatotopic organization in the brachial dorsal root ganglia of neonatal rats. Clin. Neurol. Neurosurg. *95 Suppl*, S3-11.

Wessels, W.J., Feirabend, H.K., and Marani, E. (1990). Evidence for a rostrocaudal organization in dorsal root ganglia during development as demonstrated by intra-uterine WGA-HRP injections into the hindlimb of rat fetuses. Brain Res. Dev. Brain Res. *54*, 273–281.

White, F.A., Silos-Santiago, I., Molliver, D.C., Nishimura, M., Phillips, H., Barbacid, M., and Snider, W.D. (1996). Synchronous onset of NGF and TrkA survival dependence in developing dorsal root ganglia. J. Neurosci. Off. J. Soc. Neurosci. *16*, 4662–4672.

Wilson-Gerwing, T.D., Dmyterko, M.V., Zochodne, D.W., Johnston, J.M., and Verge, V.M.K. (2005). Neurotrophin-3 suppresses thermal hyperalgesia associated with neuropathic pain and attenuates transient receptor potential vanilloid receptor-1 expression in adult sensory neurons. J. Neurosci. Off. J. Soc. Neurosci. *25*, 758–767.

Wilson-Gerwing, T.D., Stucky, C.L., McComb, G.W., and Verge, V.M.K. (2008). Neurotrophin-3 significantly reduces sodium channel expression linked to neuropathic pain states. Exp. Neurol. *213*, 303–314.

Winkelman, D.L.B., Beck, C.L., Ypey, D.L., and Leary, M.E.O. (2005a). Inhibition of the A-Type K *2* Channels of Dorsal Root Ganglion Neurons by the Long-Duration Anesthetic Butamben. *314*, 1177–1186.

Winkelman, D.L.B., Beck, C.L., Ypey, D.L., and O'Leary, M.E. (2005b). Inhibition of the A-Type K+ Channels of Dorsal Root Ganglion Neurons by the Long-Duration Anesthetic Butamben. J. Pharmacol. Exp. Ther. *314*, 1177–1186.

Woolf, C.J. (1987). Central Terminations of Cutaneous Mechanoreceptive Afferents in the Rat Lumbar Spinal Cord. J Comp Neurol *261*, 105–119.

Woolf, C.J. (1993). The Pathophysiology of Peripheral Neuropathic Pain—Abnormal Peripheral Input and Abnormal Central Processing. In Advances in Stereotactic and Functional Neurosurgery 10, (Springer, Vienna), pp. 125–130.

Wu, A., Green, C.R., Rupenthal, I.D., and Moalem-Taylor, G. (2012). Role of gap junctions in chronic pain. J. Neurosci. Res. *90*, 337–345.

Xie, J., Price, M.P., Berger, A.L., and Welsh, M.J. (2002). DRASIC contributes to pH-gated currents in large dorsal root ganglion sensory neurons by forming heteromultimeric channels. J. Neurophysiol. *87*, 2835–2843.

Xu, Q., Cheong, Y.-K., He, S.-Q., Tiwari, V., Liu, J., Wang, Y., Raja, S.N., Li, J., Guan, Y., and Li, W. (2014). Suppression of spinal connexin 43 expression attenuates mechanical hypersensitivity in rats after an L5 spinal nerve injury. Neurosci. Lett. *566*, 194–199.

Yang, F., Feng, L., Zheng, F., Johnson, S.W., Du, J., Shen, L., Wu, C.P., and Lu, B. (2001). GDNF acutely modulates excitability and A-type K(+) channels in midbrain dopaminergic neurons. Nat. Neurosci. *4*, 1071–1078.

Yoon, Y.W., Na, H.S., and Chung, J.M. (1996). Contributions of injured and intact afferents to neuropathic pain in an experimental rat model. Pain *64*, 27–36.

Yoshida, S., Matsuda, Y., and Samejima, A. (1978). Tetrodotoxin-resistant sodium and calcium components of action potentials in dorsal root ganglion cells of the adult mouse. J. Neurophysiol. *41*, 1096–1106.

Zhang, J., and Snyder, S.H. (1995). Nitric Oxide in the Nervous System. Annu. Rev. Pharmacol. Toxicol. *35*, 213–233.

Zhang, J.M., Donnelly, D.F., and LaMotte, R.H. (1998). Patch clamp recording from the intact dorsal root ganglion. J. Neurosci. Methods *79*, 97–103.

Zhang, X., Shi, T., Holmberg, K., Landry, M., Huang, W., Xiao, H., Ju, G., and Hökfelt, T. (1997). Expression and regulation of the neuropeptide Y Y2 receptor in sensory and autonomic ganglia. Proc. Natl. Acad. Sci. U. S. A. *94*, 729–734.

Zhang, X., Huang, J., and McNaughton, P.A. (2005). NGF rapidly increases membrane expression of TRPV1 heat-gated ion channels. EMBO J. *24*, 4211–4223.

Zhang, Y., Laumet, G., Chen, S.-R., Hittelman, W.N., and Pan, H.-L. (2015). Pannexin-1 Up-regulation in the Dorsal Root Ganglion Contributes to Neuropathic Pain Development. J. Biol. Chem. *290*, 14647–14655.

Zhao, J., Seereeram, A., Nassar, M.A., Levato, A., Pezet, S., Hathaway, G., Morenilla-Palao, C., Stirling, C., Fitzgerald, M., McMahon, S.B., et al. (2006). Nociceptor-derived brain-derived neurotrophic factor regulates acute and inflammatory but not neuropathic pain. Mol. Cell. Neurosci. *31*, 539–548.

Zhou, X.F., Rush, R.A., and McLachlan, E.M. (1996). Differential expression of the p75 nerve growth factor receptor in glia and neurons of the rat dorsal root ganglia after peripheral nerve transection. J. Neurosci. Off. J. Soc. Neurosci. *16*, 2901–2911.

Zhuo, M., and Gebhart, G.F. (1997). Biphasic Modulation of Spinal Nociceptive Transmission From the Medullary Raphe Nuclei in the Rat. J. Neurophysiol. *78*, 746–758.

Zwick, M., Davis, B.M., Woodbury, C.J., Burkett, J.N., Koerber, H.R., Simpson, J.F., and Albers, K.M. (2002). Glial cell line-derived neurotrophic factor is a survival factor for isolectin B4-positive, but not vanilloid receptor 1-positive, neurons in the mouse. J. Neurosci. Off. J. Soc. Neurosci. *22*, 4057–4065.